PONTIFICIA UNIVERSIDAD CATOLICA DE CHILE
SCHOOL OF ENGINEERING

# EFFECT OF A WHEY PROTEIN NETWORK FORMED BY COLD GELATION ON STARCH GELATINIZATION AND DIGESTIBILITY

**ANAÏS LAVOISIER**

Thesis submitted to the Office of Graduate Studies in partial fulfillment of the requirements for the Degree of Doctor in Engineering Sciences.

Advisor:
**JOSÉ MIGUEL AGUILERA**

Santiago de Chile, June, 2019

*à Javier*

## ACKNOWLEDGEMENTS

First of all, thank you to Prof. José Miguel Aguilera, for his trust, his time and his teaching throughout this Thesis.

Thank you to Prof. Thomas Vilgis for welcoming me in his team at the MPIP, and for his advice and interesting discussions during this last year.

Thank you to Prof. Pedro Bouchon, Prof. Denis Fuentealba and Ximena Vergés from the Pontificia Universidad Católica de Chile for their technical and scientific support.

Thank you to Rüdiger Berger, Uwe Rietzler, Kaloian Koynov, Andreas Hanewald, Andreas Best, Ingo Lieberwirth, Gunnar Glaβer, and Domenik Prozeller for their scientific and technical assistance during my stay at the MPIP.

Thank you to the Comisión Nacional de Investigación Científica y Tecnológica (CONICYT) and the Vicerrectoría de Investigación (VRI) de la Pontificia Universidad Católica de Chile for their financial support.

A special thank you to Maike for listening to my daily grumbles and feeding me with delicious food.

Thank you to my other current and former teammates from the UIG, Mariel, Rodrigo, Valentina, Claudia, Alicia, Candelaria, Leidy Victoria, Francisco, Ross, Loreto, Javiera, Gabriel, and Marcela. You all contributed to the success of this project.

Thank you to the members of the Food Group, Bhagyashri, Martha, Trivikram, Markus, Christine, Hannah, Sarah, and Steffen, for their help and cheerfulness. Herzlichen Dank an alle!

Merci à Myriam, qui m'inspire chaque semaine par son optimisme et sa force.

Merci à Aurore, Lino, Cécilia, Charlotte, Jean, J-P, Florian, Justine, Capucine, Paul, Francisca, Laura et Patricia, qui, d'une façon ou d'une autre, de près ou de loin, m'ont aidé et soutenu pendant ces quatre ans.

Merci à ma famille d'être toujours là pour moi.

Et enfin, merci à Javier, pour sa patience et son amour inconditionnel. Sans toi rien n'a de sens.

LIST OF CONTENTS

## LIST OF TABLES

### CHAPTER 1



### CHAPTER 2

## LIST OF FIGURES

### INTRODUCTION



### CHAPTER 1

**CHAPTER 2**



**CHAPTER 3**

PONTIFICIA UNIVERSIDAD CATOLICA DE CHILE
ESCUELA DE INGENIERIA

# EFFECT OF A WHEY PROTEIN NETWORK FORMED BY COLD GELATION ON STARCH GELATINIZATION AND DIGESTIBILITY

Thesis submitted to the Office of Research and Graduate Studies in partial fulfillment of the requirements for the Degree of Doctor in Engineering Sciences.

ANAIS LAVOISIER

## ABSTRACT

Diabetes is a chronic lifestyle condition that affects millions of people worldwide and it is a major health concern in modern society. Evidence has shown that nutrition, especially postprandial glycemia, plays a crucial role in the development of type 2 diabetes. Therefore, dietary approaches that slow down carbohydrate absorption are considered useful tools in lowering the risk of type 2 diabetes and improving overall health.

In this Thesis, starch-trapping protein gelled matrices were proposed as a new strategy to design starchy foods with a slow and steady postprandial release of glucose to help managing disorders of glucose metabolism. It was postulated that a protein gel can reduce starch gelatinization during heat treatment and protect partially gelatinized starch granules from enzymatic attack during digestion.

To confirm this hypothesis, native potato starch (PS) granules were trapped within a whey protein isolate (WPI) network formed by calcium-induced cold gelation. These composite gels were then subjected to heat treatment (> 80°C) and PS gelatinized inside

the protein network. First, starch gelatinization in the WPI cold-set gel was monitored *in situ* and in real time with a DSC/hot-stage system. Changes in the microstructure of the composite gels due to swelling during heating were also indirectly followed by rheological and mechanical measurements. In addition, the microstructure of the composite gels was observed before and after heating by confocal laser scanning microscopy (CLSM) and cryo-SEM. Then, starch digestibility in the WPI cold-set gel after heat treatment was investigated using the INFOGEST *in vitro* protocol. Special attention was given to the impact of gel particle size and protein concentration on glucose release from the matrix. Finally, the different steps leading to the formation of the WPI network by calcium-induced cold gelation were observed with an atomic force microscope and the fractal dimension of the gel was determined by image analysis and oscillatory rheology. The effect of heating on the properties and microstructure of the WPI cold-set gel was analyzed by DSC, infrared spectroscopy (ATR-FTIR) and rheological measurements, and examined by CLSM and cryo-SEM. The research was focused on the influence of the formation of additional disulfide bonds on the rheological properties of the gel.

Starch gelatinization was restricted by the gelled matrix of WPI. The presence of the protein network did not delay the onset of gelatinization, but it lowered the endset temperature of the transition by 3°C, reduced the gelatinization enthalpy by 42% and restricted granules swelling by 33%. The rheological and mechanical properties of the composite gels were influenced by PS swelling, depending on starch concentration. After heat treatment, the addition of 1% PS resulted in a weakening of the gel, probably because gelatinized granules created flaws in the microstructure. On the contrary, the addition of 9% PS led to a reinforcement of the gel: an interpenetrating network formed between whey proteins and the gelatinized PS granules.

Starch digestibility *in vitro* was also restricted by the presence of the WPI network. Glucose release from the matrix was reduced until the intestinal step of the simulated

digestion when gels were ground to a particle size of ~1 mm. When gels were cut to a particle size of ~5 mm glucose release was decreased until the end of the test. In this case, at the end of the digestion glucose release was reduced by 15.5 and 20.5% for composite gels with 8 and 10% WPI respectively, whereas no significant reduction was observed for the gel with 6% WPI. Therefore, the effect of the WPI network on starch digestibility depended first on particle size reduction and then on protein concentration. The latter was related to the mechanical and rheological properties of the composite gels: starch digestibility decreased while increasing hardness and elasticity of the gels.

Heat treatment of the composite gels also modified the properties and the microstructure of the WPI network. WPI cold-set gels were more rigid and brittle after heating to 90°C. Important changes occurred in the protein network structure: additional disulfide bonds and calcium bridges formed during heating, whereas new hydrophobic interactions appeared during cooling. Consequently, the viscoelastic properties of the WPI cold-set gels were significantly and irreversibly altered.

This Thesis contributes to a better understanding of starch-trapping soft protein matrices before, during and after heat treatment. Furthermore, it provides new insights on starch digestion in soft food matrices. Altogether, the results of this study show that the use of WPI cold-set gels is as an interesting strategy to formulate food products with a slow and steady postprandial release of glucose from starch. Starch-trapping protein gels could be particularly helpful to develop functional foods specially designed for overweight diabetics or the elderly.

**Members of Doctoral Thesis Committee:**

**José Miguel Aguilera R.**
**Franco Pedreschi P.**
**Wendy Franco M.**
**Rommy Zuñiga P.**
**Thomas Vilgis**
**Jorge Vásquez P.**

**Santiago, April, 2019**

PONTIFICIA UNIVERSIDAD CATOLICA DE CHILE
ESCUELA DE INGENIERIA

# EFECTO SOBRE LA GELATINIZACIÓN Y LA DIGESTIBILIDAD DEL ALMIDÓN DE UNA RED DE PROTEÍNA DE SUERO DE LECHE FORMADA POR GELIFICACIÓN EN FRÍO

Tesis enviada a la Dirección de Investigación y Postgrado en cumplimiento parcial de los requisitos para el grado de Doctor en Ciencias de la Ingeniería

ANAIS LAVOISIER

## RESUMEN

La diabetes es una enfermedad crónica que afecta a millones de personas alrededor del mundo y por ende un problema actual de salud importante en nuestra sociedad. Hoy en día, sabemos que la alimentación es un factor de riesgo para el desarrollo de la diabetes tipo 2, en particular las dietas que provocan fluctuaciones extremas de la glicemia posprandial. Por lo tanto, se recomienda consumir alimentos con un bajo índice glicémico, para evitar un desequilibrio en el metabolismo de la glucosa, mejorar la salud en general, y reducir el riesgo de padecer diabetes tipo 2.

En esta Tesis, se propone una nueva estrategia para diseñar alimentos amiláceos con una liberación de glucosa posprandial lenta y constante. Se plantea que un gel de proteína puede reducir la gelatinización del almidón durante el tratamiento térmico y, luego, proteger los gránulos de almidón del ataque enzimático durante la digestión.

Para confirmar esta hipótesis, gránulos nativos de almidón de papa (*potato starch*, PS) fueron atrapados en una red de aislado de proteína de suero (*whey protein isolate*, WPI), elaborada por gelificación en frío inducida por adición de calcio. Estos geles compuestos fueron sometidos a un tratamiento térmico (>80°C), para provocar la gelatinización del PS dentro de la red de proteínas. Primero, la gelatinización del almidón en el gel de WPI fue estudiada, *in situ* y en tiempo real, con un sistema de placa calefactora DSC para microscopio. Los cambios en la microestructura de los geles compuestos también fueron observados indirectamente por mediciones reológicas y mecánicas. Además, la microestructura de los geles, antes y después del calentamiento, fue explorada por microscopía confocal láser de barrido (CLSM) y criomicroscopía electrónica de barrido (crio-MEB). Luego, la digestibilidad del almidón en el gel de WPI, después del tratamiento térmico, fue investigada mediante el protocolo de digestión *in vitro* "INFOGEST". Se prestó especial atención al impacto del tamaño de partícula del gel y de la concentration de proteína sobre la liberación de glucosa desde la matriz. Finalmente, los diferentes pasos que conducen a la formación de la red de WPI por gelificación en frío fueron observados con un microscopio de fuerza atómica, y la dimensión fractal del gel fue determinada mediante análisis de imagen y reología oscilatoria. El efecto del calentamiento sobre las propiedades y la microestructura del gel de WPI fue analizado con DSC, espectroscopia infrarroja (ATR-FTIR) y mediciones reológicas, además de ser examinado por CLSM y crio-MEB. La investigación se centró en la influencia de la formación de nuevos enlaces disulfuro sobre las propiedades reológicas del gel.

La gelatinización del almidón fue restringida por la matriz de WPI. La presencia de la red de proteína no retrasó el inicio de la gelatinización pero redujo la temperatura final de la transición de 3°C, tambien redujo la entalpía de gelatinización en un 42% y disminuyó el hinchamiento de los gránulos de PS en un 33%. Las propiedades reológicas y mecánicas de los geles compuestos se vieron afectadas por la gelatinización del almidón, dependiendo de su concentración en el gel. Añadir 1% de PS al gel de WPI

debilitó la estructura del gel, probablemente porque los gránulos gelatinizados crean defectos en la microestructura. Al contrario, la adición de un 9% de almidón resultó en un reforzamiento del gel: una red interpenetrante se forma entre el WPI y los gránulos gelatinizados de PS.

La digestibilidad del almidón *in vitro* también se vio restringida por la presencia de la red de WPI. La liberación de glucosa desde la matriz se redujo en la etapa intestinal, cuando los geles fueron molidos a un tamaño de partícula de ~ 1 mm. Pero cuando los geles fueron cortados a un tamaño de partícula de ~ 5 mm, la liberación de glucosa disminuyo al final de la prueba. En este caso, al final de la digestión, la liberación de glucosa fue reducida en un 15.5 y un 20.5% para los geles compuestos con 8 y 10% de WPI respectivamente, mientras que no se observó una reducción significativa para el gel con 6% de WPI. Por lo tanto, el efecto de la red de WPI sobre la digestibilidad del almidón depende primero del tamaño de partícula y luego de la concentración de proteína. Esto se relaciona con las propiedades mecánicas y reológicas de los geles compuestos: la digestibilidad del almidón disminuye cuando aumenta la dureza y la elasticidad de los geles.

El tratamiento térmico también modificó las propiedades y la microestructura de la red de WPI de los geles compuestos. Los geles de WPI eran más rígidos y más quebradizos después de ser calentados a 90ºC. En efecto, se produjeron cambios importantes en la estructura de la red de proteínas: se formaron enlaces disulfuro y puentes de calcio adicionales durante el calentamiento y nuevas interacciones hidrofóbicas durante el enfriamiento. Como consecuencia, las propiedades viscoelásticas de los geles de WPI elaborados por gelificación en frío se vieron alteradas de manera significativa e irreversible.

Esta Tesis contribuye a una mejor comprensión de los cambios que ocurren durante el tratamiento térmico de matrices blandas compuestas por proteínas y almidón. Además, aporta nuevos conocimientos sobre la digestión del almidón en matrices alimentarias

suaves. En conjunto, los resultados de este estudio muestran que el uso de geles de WPI es una estrategia interesante para formular productos amiláceos con un índice glicémico bajo. Estas estructuras podrían ser particularmente útiles para desarrollar alimentos funcionales especialmente diseñados para diabéticos con sobrepeso o personas mayores.

**Miembros de la Comisión de la Tesis Doctoral:**

**José Miguel Aguilera R.**
**Franco Pedreschi P.**
**Wendy Franco M.**
**Rommy Zuñiga P.**
**Thomas Vilgis**
**Jorge Vásquez P.**

**Santiago, Abril, 2019**

## LIST OF PAPERS

This thesis is based on the following papers:

**1.** Lavoisier, A., & Aguilera, J., M. (2019). Starch gelatinization inside a whey protein gel formed by cold gelation. *Journal of Food Engineering, 256,* 18-27. https://doi.org/10.1016/j.jfoodeng.2019.03.013

**2.** Lavoisier, A., & Aguilera, J., M. (2019). Effect of a whey protein network formed by cold gelation on starch digestibility. *Food Biophysics, (in press)*. https://doi.org/10.1007/s11483-019-09573-3

**3.** Lavoisier, A., Vilgis, T. A., & Aguilera, J., M. (2019). Impact of heating on the properties of a whey protein cold-set gel. *Food Hydrocolloids.* (submitted)

## PROCEEDINGS

### Communications in international congresses

Some of this work has been presented at international scientific events, as detailed below:

"Swelling of starch granules in a protein network formed by cold gelation". Anaïs Lavoisier and José Miguel Aguilera. 18th World Congress of Food Science and Technology, IUFoST 2016. Dublin, Irland. *(Poster presentation)*

"Matriz de proteína de suero de leche reduce la gelatinization del almidón". XXI Congreso Chileno de Ciencia y Technología de Alimentos, SOCHITAL 2017. Santiago, Chile. (*Poster presentation)*

"Whey protein network restricts the *in vitro* digestibility of starch". 7th International Symposium on Delivery of Functionality in Complex Food Systems, DOF 2017. Auckland, New Zealand. (*Oral presentation)*

"Impact of heating on the properties of a whey protein cold-set gel". 32nd International Conference: Developing Innovative Food Structure & Functionalities through Process & Reformulation to Satisfy Consumer Needs & Expectations, EFFoST 2018. Nantes, France. (*Poster presentation)*

### Predoctoral stay at a foreign institution

"Study of the physical properties of gel forming starch-whey protein systems". Group of Food Science and Statistical Physics of Soft Matter, department of Polymer Theory, Max Planck Institute for Polymer Research, Mainz, Germany. From February 2018 to August 2018, under the supervision of Prof. Thomas Vilgis.

## THESIS OUTLINE

This Doctoral Thesis is organized in four main sections: **Introduction, Hypothesis & Objectives, Chapters, Conclusions** and **Future outlook**. First, the **Introduction** section discusses the state of the art concerning the structure of starch granules, starch gelatinization and digestion, with a particular focus on potato starch and the influence of the food matrix on starch digestibility. This section also addresses the relation between starch, high glycemic index diets and diabetes, and introduces the concepts that lead to the formulation of the hypothesis of this Thesis. As its name implies, the **Hypothesis & Objectives** section presents the hypothesis and the general and specific objectives of the Thesis. Then, the methodology used and the results obtained are presented in three **Chapters**, corresponding to three research papers published or submitted to international journals. Finally, the last parts of the document, called **Conclusions** and **Future outlook,** summarizes the most relevant conclusions of the Thesis and its future prospects.

Diabetes is a chronic lifestyle condition that affects millions of people worldwide and it is a major health concern in modern society. Evidence has shown that nutrition, especially postprandial glycemia, plays a crucial role in the development of type 2 diabetes. Dietary approaches that slow down carbohydrate absorption are nowadays considered useful tools in lowering the risk of type 2 diabetes and improving overall health. There is, therefore, a growing need for the development of foods and food ingredients with a slow and steady postprandial release of glucose. This is a challenging task, which calls for a better understanding of the digestion of complex carbohydrates, like starch, in solid food matrices. Starch is the first source of carbohydrate in human nutrition across the world, but its digestion in food matrices of different compositions and textures is not fully understood yet. In particular, starch gelatinization and digestion

in protein matrices with high-water content (i.e., > 80%), like gels, have not been systematically investigated despite their potential health benefits.

In this Thesis, starch-trapping protein gelled matrices were proposed as a new strategy to reduce starch gelatinization and digestion in foods.

First, it was postulated that a protein gelled network could physically restrict the swelling of starch granules. To confirm this hypothesis, model gels composed of WPI and PS were developed using the process of cold gelation with calcium. In these composite gels, native PS granules were trapped inside a WPI matrix with a high-water content (> 80%). Gelatinization was then induced by heat treatment (up to 90°C) of the composite cold-set gels, to investigate if the presence of the WPI network was able to reduce the extent of PS swelling. The properties and microstructure of the composite gels were studied both before and after heat treatment and, more importantly, PS gelatinization inside the WPI gelled network was monitored *in situ* and in real time. This study entitled "Starch gelatinization inside a whey protein gel formed by cold gelation" is presented in **Chapter 1**. It showed that native PS granules were successfully encased inside the WPI network formed by cold gelation and that starch gelatinization was actually restricted by the protein gel matrix. Furthermore, it was observed that PS swelling inside the WPI network induced important changes in the final microstructure and properties of the composite gels.

Then, it was hypothesized that the protein gelled network could also protect gelatinized starch granules from enzymatic attack during digestion. To validate this assumption, PS digestibility in the composite cold-set gels after heat treatment was investigated using the INFOGEST *in vitro* protocol. The research was particularly focused on the impact of gel particle size and protein concentration on glucose release from the matrix. This study is reported in **Chapter 2** "Effect of a whey protein network formed by cold gelation on starch digestibility". It revealed that PS susceptibility to hydrolysis was reduced when starch granules were trapped in the WPI matrix. This barrier effect

depended first on particle size reduction of the gels, and then on protein concentration in the gels. Moreover, this study showed that mechanical and rheological properties of the composite gels were related to starch digestibility: the rate of PS hydrolysis decreased by increasing hardness and elasticity of the gels.

Some results of these two studies on starch gelatinization and digestibility suggested that the WPI cold-set gel was also modified by heat treatment. It was surmised that a rearrangement of the protein network structure occurs during heating, driven by an increase in intermolecular interactions. Therefore, the effect of heating to 90°C on the properties and microstructure of the WPI cold-set gel was investigated by several techniques, with a specific focus on the influence of the formation of additional disulfide bonds on the rheological properties of the gel. This study entitled “Impact of reheating on the properties of a whey protein cold-set gel” is presented in **Chapter 3**. It confirmed that the viscoelastic properties of the WPI cold-set gel were significantly and irreversibly impacted by heat treatment. This was related to changes on the molecular level in the particle gel. Indeed, this study demonstrated that heating leads to the formation of additional disulfide bonds, calcium bridges, and H-bonding β-sheets, all contributing to the architecture of the final network structure.

This Thesis contributes to a better understanding of changes occurring in starch-trapping protein gels during and after heat treatment and increases our knowledge of starch digestion in soft food matrices. The use of WP gels appears as a promising strategy to design soft foods with a slow and steady postprandial release of glucose from starch. Further investigation is however needed to evaluate the organoleptic properties of these starch-trapping gels and to understand how to effectively incorporate them as ingredients in new food products.

# INTRODUCTION

## 1. Starch

Starch is today the main source of energy in human nutrition across the world. It is present in most traditional staple foods and widely used as a food additive. In nature, starch is mainly found in cereal grains, rhizomes, roots, tubers and pulses. The most common sources of starch are maize, potato, rice, wheat and cassava (Carvalho, 2008).

### 1.1. Multi-scale structure of starch granules

Regardless of its botanical origin, starch consists of two types of polysaccharides: amylopectin, the major component by weight (~ 70-80%), and amylose. Both polymers are chains of D-glucose residues linked by α (1,4) bonds, forming linear segments, and α (1,6) bonds forming branches. Amylose is only slightly branched and is considered as a linear macromolecule. Its long chains of glucosyl units generally form single helices (Ai & Jane, 2018). On the contrary, amylopectin molecules are extensively branched and contain many short chains, resulting in a complex molecular structure. The amylopectin internal molecular structure varies widely among different starches (Zhu, 2018), but the organization of the chains typically corresponds to the pattern represented in Figure 1, called the “cluster model” of amylopectin structure.

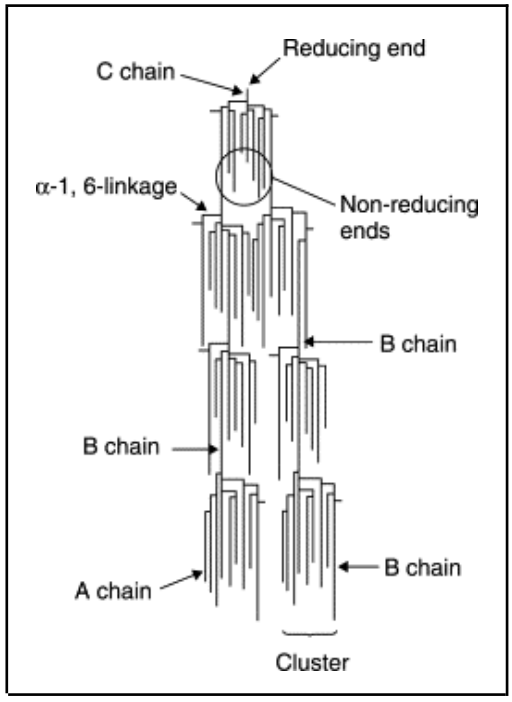


**Figure 1.** Cluster model of amylopectin structure. A- and B-chains organize from the C-chain containing the sole reducing end group of the amylopectin molecule, from Hamaker, Zhang, & Venkatachalam (2006).

The short chains of amylopectin form double-helices and crystallize. Depending on the botanical origin of the starch, different polymorphs are observed for the amylopectin crystallites: the A-type, a monoclinic crystal system; the B-type, a hexagonal crystal system; and the C-type, a mixed pattern. As illustrated by Figure 2, these regions of crystalline order alternate with amorphous layers (containing the branch points of the amylopectin molecule) and form the lamellar structure of starch. The amylose molecules are probably interspersed among the crystalline and amorphous lamellae of amylopectin molecules (Bertoft, 2017).

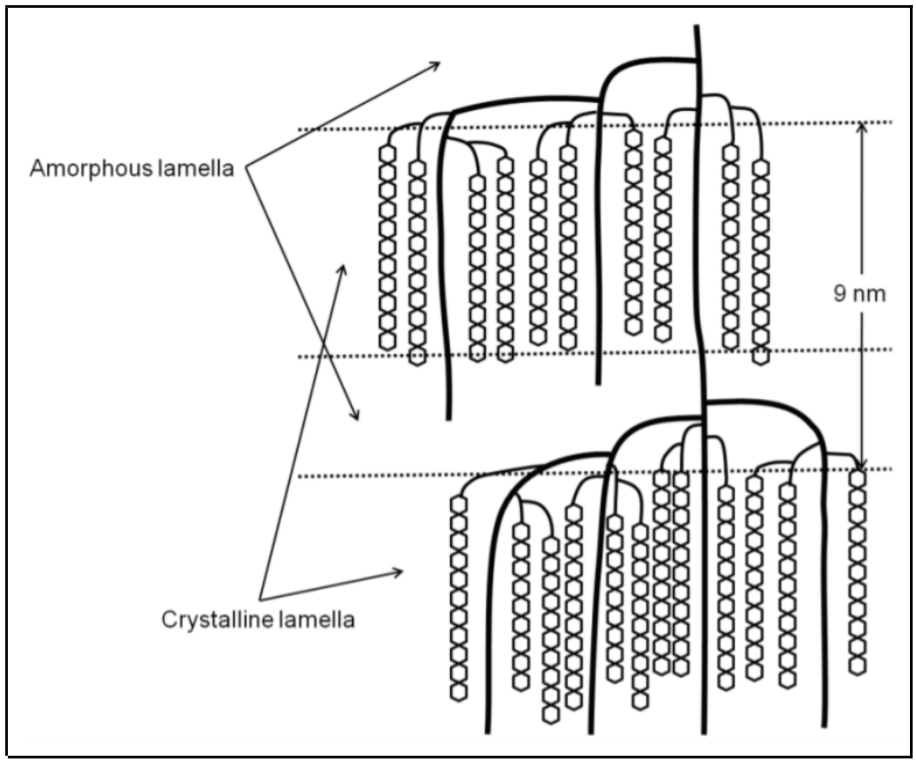


**Figure 2.** Schematic illustration of the lamellar structure of starch, from Tsubaki & Azuma (2011).

These stacks of amorphous and crystalline lamellae are arranged in rings embedded in an amorphous matrix and form structures called “blocklets” (Gallant, Bouchet, & Baldwin, 1997). Such blocklets organize in hard (i.e., crystalline) and soft shells (i.e., amorphous), which form alternate concentric rings around the hilum (Tang, Mitsunaga, & Kawamura, 2006). These “growth rings” make up granules of 1 to 100 μm in size, depending on the origin of starch (Jane et al., 1994). Because of this high degree of order inside the native starch granules, a “Maltese cross” pattern is typically observed under polarized light (Figure 3).

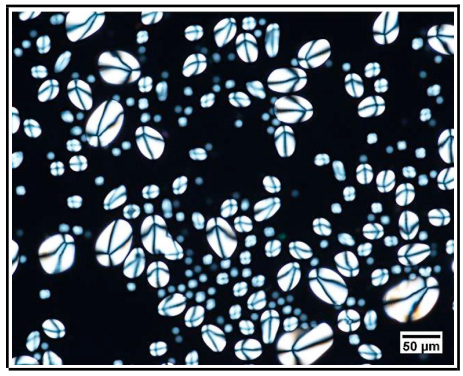


**Figure 3.** Photomicrograph of potato starch granules under polarized light, adapted from Zhao, Andersson, & Andersson (2018).

Thus, starch granules have a very complex three-dimensional structure. The exact nature of the granule architecture is still a matter of debate. For example, the actual localization of amylose inside the granules remains uncertain and it is unclear how amylose and amylopectin interact with each other (Bertoft, 2017). An overview of the multi-scale structure of starch granules is presented in Figure 4.

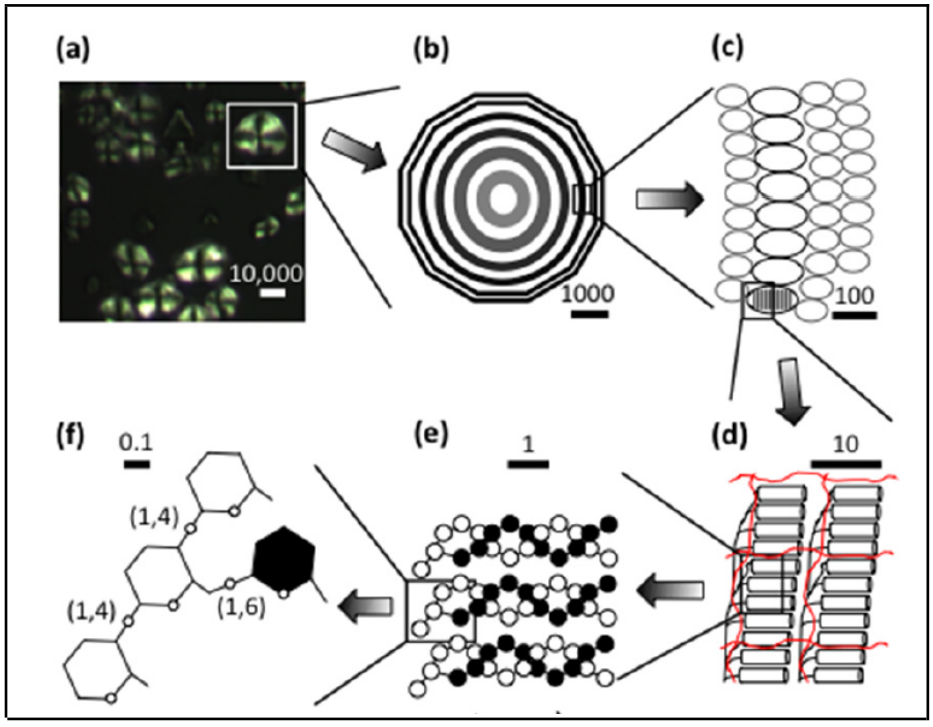


**Figure 4.** Simplified representation of the different levels of structural organization of starch: (a) granules, (b) growth rings, (c) blocklets, (d) crystalline and amorphous lamellae, (e) double-helices of amylopectin, and (f) glucosyl units. Adapted from Bertoft (2017).

### 1.2. Particular features of potato starch

Potato starch (PS) granules have a lenticular shape and are relatively large compared to other common starches (Figure 5). They measure 25 µm in average, whereas corn and wheat starch granules are around 8 µm (Alvani, Qi, Tester, & Snape, 2011; Jane et al., 1994).

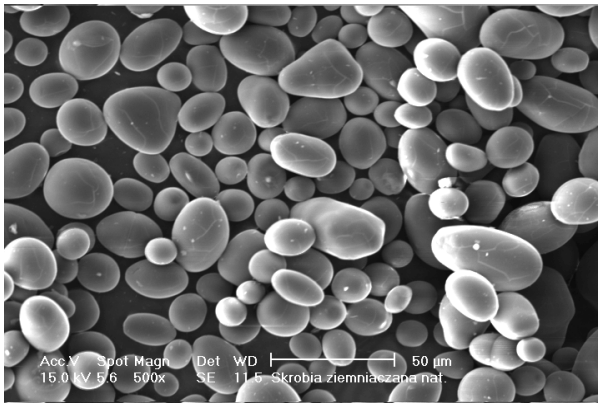


**Figure 5.** Native PS granules observed with a scanning electron microscope, from Szymónska, Targosz-Korecka, & Krok (2009).

The amylose content of potato starch is around 20%, which is lower than wheat starch (~ 29%) but slightly higher than rice starch (~ 17%) for example (Semeijin & Buwalda, 2018). Potato amylose has the highest molecular weight and the lowest degree of branching among common starches. The amylopectin of potato starch is also less densely branched and has longer chains than in other starches. These long chains of amylopectin form B-type crystals (Semeijin & Buwalda, 2018). Furthermore, one unique feature of potato starch is its high content in phosphate groups, with approximately 0.5% of glucose residues in the amylopectin amorphous fraction being phosphorylated (Xu, Huang, Visser, & Trindade, 2017). These phosphate groups generate charges on starch molecules making potato starch susceptible to electrolytes, like calcium, when dispersed in water (Jane, 1993; Zhou et al., 2014).

## 2. Gelatinization of starch granules

When heated in excess of water, starch granules undergo a series of changes known as gelatinization: they readily absorb water and swell several times their original size (Figure 6). Water enters the amorphous regions of the granules, which expand and consequently destabilize the crystallites (Wang & Copeland, 2013). The crystalline order of the granules is irreversibly lost and the Maltese cross disappears. Then, the hydrated granules collapse, amylose leach out and solubilize. Granular remnants, called "starch ghosts", which are insoluble material with high amylopectin content, are finally observed within a continuous viscous matrix (Carrillo-Navas et al., 2014; Zhang, Dhital, Flanagan, & Gidley, 2014). Upon cooling, this gelatinized starch paste may gel: amylopectin and amylose interact with each other to form a network, stabilized by long and strong junction zones attributed to the linear amylose molecules (Klucinec & Thompson, 1999). Storage for an extended period of time of gelatinized starch results in the reorganization and re-crystallization of the disrupted polymers, a complex process known as retrogradation (Matignon & Tecante, 2017).

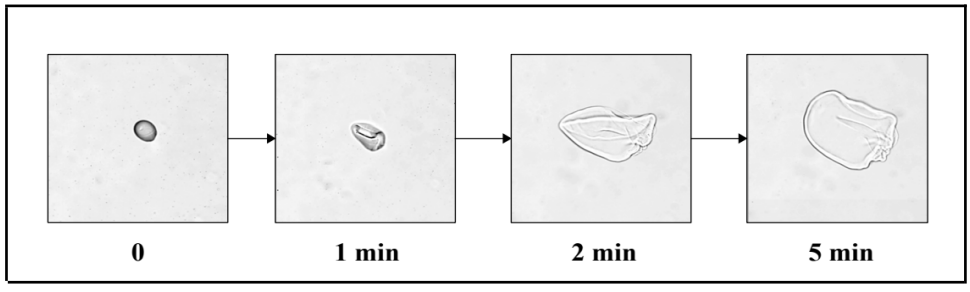


**Figure 6.** Starch heated in water at 80°C (images extracted from a video of an isolated PS granule observed by hot-stage microscopy).

Although starch gelatinization has been extensively studied since the early 1800s, no consensus has been reached on the exact nature of this transition process. Several analytical methods have been used to investigate starch gelatinization: differential scanning calorimetry (DSC), rapid visco analyzer (RVA), hot-stage microscopy, swelling power, small/wide angle X-ray scattering, among others. But each technique tends to interpret the gelatinization process differently (Schirmer, Jekle, & Becker, 2015). Therefore, various definitions of the term "gelatinization" exist in the literature, considering different end points for example, and many theories have been proposed during the past 80 years to explain gelatinization at a molecular level (Matignon & Tecante, 2017; Ratnayake & Jackson, 2009; Wang & Copeland, 2013). Recently, Matignon and Tecante proposed an enhanced definition of starch gelatinization, which describes gelatinization "*as a non-equilibrium process dependent on high energy input that leads to the collapse of native semi-crystalline orders of lamellae in starch granules*". They consider swelling as a separated event and a consequence of gelatinization (Matignon & Tecante, 2017).

### 2.1. Particular features of the gelatinization of potato starch

PS gelatinization occurs between 60 and 70°C in high amounts of water (> 60%). With DSC, an endothermic peak centered at 64°C is generally observed and the enthalpy change attributed to potato starch gelatinization is usually between 10 and 15 J/g (Alvani, Qi, & Tester, 2012; Alvani et al., 2011; Cai, Cai, Zhao, & Wei, 2014; Li & Yeh, 2001; Muñoz, Pedreschi, Leiva, & Aguilera, 2015; Parada & Aguilera, 2012; Ratnayake, Otani, & Jackson, 2009). The swelling power of PS is the highest among most common starches (Hoover, 2001; Li & Yeh, 2001) and potato starch granules may swell up to 100 times their original volume before disintegration (Singh, Singh, Kaur, Singh Sodhi, & Singh Gill, 2003). This is probably due to the high amount of phosphate

groups on potato amylopectin, which increase the hydration capacity of the starch granule (Han et al., 2019). However, because of this specificity, PS is also strongly dependent on the presence of salts in solution and gelatinization may be delayed or inhibited by bivalent cations (Semeijin & Buwalda, 2018). Upon cooling, PS form clear pastes with high viscosity and tend to form strong gels after retrogradation. They are therefore extensively used as texturing agents in foods like soups, meat products, Asian style noodles, bakery fillings, confections, cheese analogs, potato-based extruded snacks, etc. (Semeijin & Buwalda, 2018).

**3. Digestion of starch granules**

Starch is hydrolyzed into glucose by amylolytic enzymes during the human digestion. First, starch molecules are digested by α-amylases from saliva in the mouth and from the pancreatic fluid in the duodenum. α-amylases (1,4 α-D-glucanohydrolase, EC 3.2.1.1.) are endohydrolases that randomly cleave large molecules into two smaller ones. They catalyze the hydrolysis of any accessible α (1,4) glycosidic bond in amylose and amylopectin (Lehmann & Robin, 2007). So, the final hydrolysis products from α-amylase digestion are oligosaccharides, mainly maltose, maltotriose and branched dextrins (Singh, Dartois, & Kaur, 2010). These oligosaccharides are further digested into single glucose units by several enzymes from the brush border of the small intestine (i.e., enterocytes). These enzymes are exohydrolases that release a monomer or dimer from the non-reducing end of the glucose oligomers, by catalyzing the hydrolysis of the α (1,4) bonds and the α (1,6) branch bonds, ensuring further degradation of nonlinear oligosaccharides (Dona, Pages, Gilbert, & Kuchel, 2010). The resulting glucose is then transported through the intestinal epithelium and enter the blood-stream. Finally, undigested portions of starch are fermented into short-chain fatty acids by the microbiota of the large intestine (Chassard & Lacroix, 2013).

In order to degrade the starch molecules, the enzymes first need to diffuse into the granule and adsorb to the starchy material, before hydrolyzing the glycosidic bonds. The diffusion of the α-amylase into the granule is therefore a critical step for digestion. Different modes of enzymes attack have been identified depending on the morphology and the crystalline organization of the starch variety. Enzymes can erode the entire granules surface (exo-corrosion) or penetrate into the structure through channels and digest the granule inside-out (endo-corrosion) (Lehmann & Robin, 2007). Then, at the molecular level, the crystallite structure and the packing of the amorphous phase influence the enzymatic susceptibility.

### 3.1. Particular features of the digestion of potato starch

Native PS is particularly resistant to enzymatic breakdown. PS granules have a smooth surface and are therefore mainly digested by exo-corrosion. In addition, PS granules are relatively large, so their specific surface is small, which limit enzyme binding and result in low hydrolysis (Wang & Copeland, 2013). Finally, B-type crystallites can not be digested easily by α-amylase (Lehmann & Robin, 2007).

### 3.2. Digestion of gelatinized starch granules

Gelatinized starch granules are more susceptible to degradation by α-amylase than native granules (Dona et al., 2010). For example, in the case of potato starch, gelatinization increases enzymatic digestibility by about 20-fold (Wang & Copeland, 2013). Indeed, after gelatinization the granule structure is disrupted and the semi-crystalline order is lost. Consequently, it is easier for enzymes to access the glycosidic bonds of starch polymers and gelatinized granules are rapidly hydrolyzed into glucose.

Most of our food is cooked and therefore most of the starch we consume is at least partially gelatinized. Actually, cooked starch probably played an important role in human evolution by improving the digestibility and palatability of key carbohydrates (Hardy, 2015).

From a nutritional point of view, starch can be classified into three different fractions based on its susceptibility to enzymatic attack in the small intestine: the rapidly digestible starch (RDS, converted to glucose within 20 min), the slowly digestible starch (SDS, converted to glucose between 20 and 120 min) and the resistant starch (RS, undigested by enzymes after 120 min) (Englyst, Kingman, & Cummings, 1992). The ingestion of RDS leads to a rapid and sharp increase of blood glucose levels (Figure 7), which triggers the secretion of insulin from the pancreas beta cells and promotes glucose uptake by muscle and adipose tissues to maintain the blood glucose homeostasis. The amount of glucose in the blood then decrease very quickly and may drop below baseline inducing hypoglycemia (Hamaker et al., 2006). This in turn stimulates the release of glucagon and provokes glycogenolysis and gluconeogenesis in the liver to increase again blood glucose levels and reach back equilibrium. Such large fluctuations generate high stress on the blood glucose regulatory system that can further lead to cell, tissue and organ damages (Zhang & Hamaker, 2009). In contrast, the ingestion of SDS results in a slow and prolonged release of glucose into the blood stream (Figure 7). This induces a low insulin response and a moderate postprandial glycemic response sustained over time. This fraction of starch is considered beneficial for health and has been related to a stable glucose metabolism, diabetes management, mental performance and satiety (Lehmann & Robin, 2007). RS does not influence blood glucose levels after ingestion because it is not digested in the small intestine. Like other dietary fibers, it is metabolized into short chain fatty acids (acetate, butyrate and propionate) by the colonic microbiota. especially by *Ruminococcus bromii* (Ze, Duncan, Louis, & Flint, 2012). Such bacterial metabolites can impact the host and gut health by

modulating inflammation, as well as glucose and lipid metabolisms (Chassard & Lacroix, 2013).

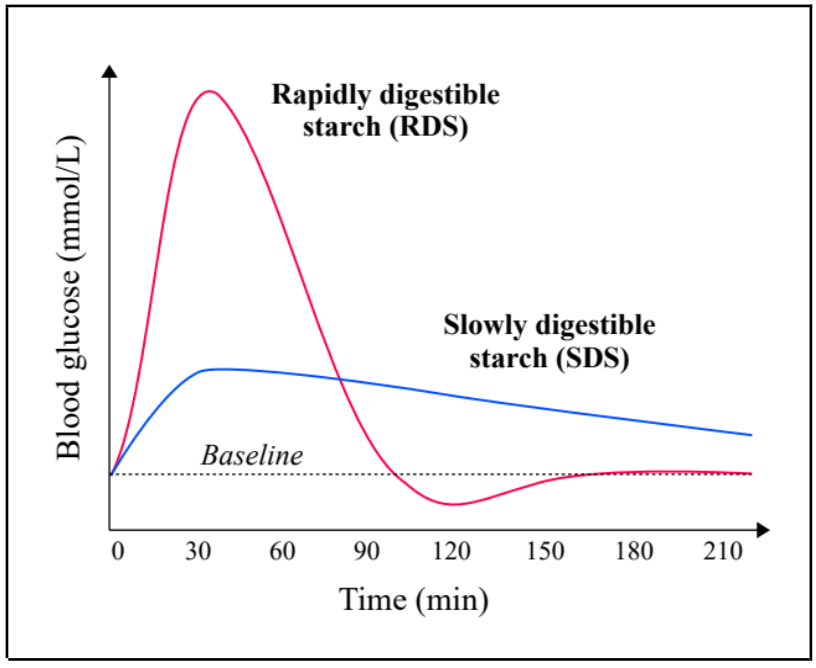


**Figure 7.** Schematic diagram of the effect of rapidly and slowly digestible starch on the blood glucose levels.

**4. Glycemic index**

The physiological effect of dietary carbohydrates in foods is typically represented by the Glycemic Index (GI). This concept was introduced by Jenkins et al. (1982) to classify foods from 0 to 100 on the basis of their postprandial blood glucose response. The GI is defined as the postprandial incremental glycemic area after a test meal, expressed as the percentage of the corresponding area after an equi-carbohydrate portion (50g) of a

reference food (glucose solution or white wheat bread) (Goñi, Garcia-Alonso, & Saura-Calixto, 1997). Based on their GI values, products are generally divided in three groups: high (GI > 70), intermediate (70 > GI > 55) and low (GI < 55) GI foods. The concept of Glycemic Load (GL = GI x available carbohydrate/given amount of food) is also increasingly used.

### 4.1. Risks related to high glycemic index diets

High GI/GL diets are associated with increased risks for obesity, type 2 diabetes and coronary heart disease (Augustin et al., 2015; Bhupathiraju et al., 2014). Indeed, high GI/GL meals produce an initial period of high blood glucose and insulin levels, followed by reactive hypoglycemia, counter-regulatory hormone secretion and elevated serum free fatty acid concentrations. These events may promote excessive food intake, beta cell dysfunction, dyslipidemia and endothelial dysfunction, leading to the development of such chronic diseases, as illustrated in Figure 8 (Ludwig, 2002).

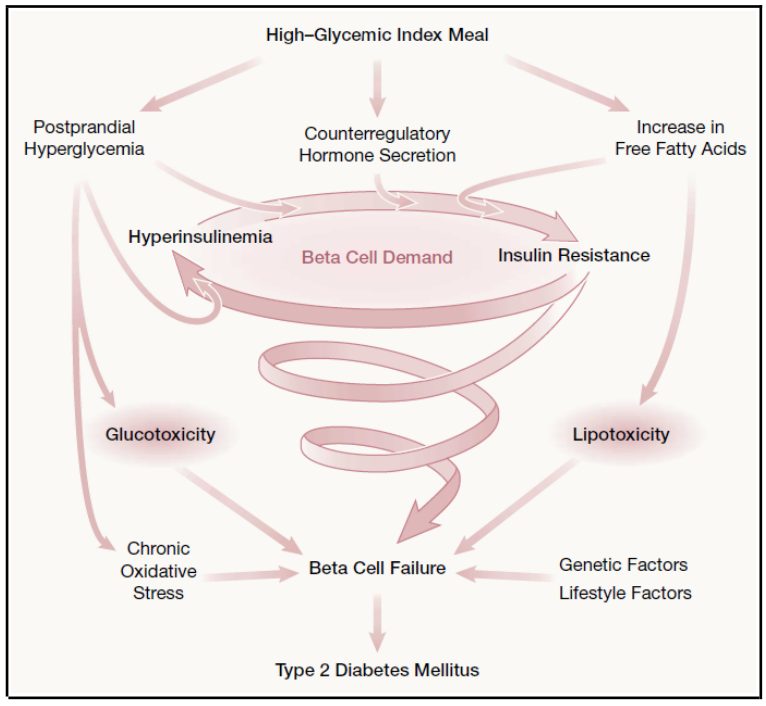


**Figure 8.** Hypothetical model of the relation between high-GI diets and increased risks for type 2 diabetes, from Ludwig (2002).

Recently, a panel of international experts on carbohydrate research recognized postprandial glycemia as a relevant factor in overall health. Dietary approaches that slow down carbohydrate absorption are considered useful tools in lowering the risk of type 2 diabetes and coronary heart disease, by improving related modifiable risk factors (Augustin et al., 2015; Bansal, 2015).

### 4.2. Diabetes

Diabetes mellitus is a chronic disease in which the body is unable to regulate sugar levels in the blood, because the pancreas does not produce enough insulin or because the body cannot effectively use the insulin it produces, or both. The diagnostic criteria for diabetes is a fasting venous plasma glucose ≥ 7.0 mmol/L (126 mg/dL) or a venous plasma glucose 2 h after ingestion of a 75 g oral glucose load ≥ 11.1 mmol/L (200 mg/dL) (World Health Organization, 2006). Raised blood glucose, over time, lead to serious damage to the heart, blood vessels, eyes, kidneys and nerves, that can result in disability and premature death.

There are two main type of diabetes, called type 1 and type 2 diabetes. Type 1, formerly known as insulin-dependent or childhood-onset diabetes, is characterized by deficient insulin production in the body. People with type 1 diabetes requires the daily administration of insulin to survive. The cause of type 1 diabetes is not known and it is currently not preventable. Type 2 diabetes, also known as non-insulin-dependent or adult-onset diabetes, results from the body's ineffective use of insulin. It is by far the most common and accounts for approx. 95% of diabetes figures around the world. Symptoms may be absent and the disease may go undiagnosed for several years, until the development of complications. The risk of type 2 diabetes is determined by an interplay of genetic and metabolic factors, overweight and obesity being the strongest risk factors. Nowadays, this type of diabetes also occurs in children.

Diabetes killed 1.6 million people in 2016 and is ranked within the top 10 of the global causes of death before road injuries (World Health Organization, 2018). The World Health Organization (WHO) estimated that approximately 422 million adults were suffering from diabetes in 2014 (World Health Organization, 2016). The prevalence of the disease nearly doubled across the globe since 1980 and according to the

International Diabetes Federation (IDF) over 600 million people will be diagnosed with diabetes by 2045 (International Diabetes Federation, 2017).

In addition, million of people live with Impaired Glucose Tolerance (IGT) or Impaired Fasting Glycemia (IFG), better known as “prediabetes”. These are intermediate conditions in the transition between normal blood glucose levels and diabetes: 2 h plasma glucose between 7.8 and 11.1 mmol/L (140 mg/dL to 200 mg/dL) for IGT and, fasting plasma glucose between 6.1 and 6.9 mmol/L (110 mg/dL to 125 mg/dL) for IFG (World Health Organization, 2006). The transition from this asymptomatic state of hyperglycemia to type 2 diabetes is no inevitable, but chances of developing the disease are highly increased, and people with IGT or IFG are at increased risk of heart attacks and strokes (World Health Organization, 2016; Bansal, 2015). In 2010, the worldwide prevalence of prediabetes was estimated to 343 million and the IDF projects an increase to 471 million people by 2035.

In Chile, 12.3% of the adult population currently live with diabetes, which is the highest figure in South America (Ministerio de Salud de Chile, 2017). Furthermore, 75% of Chileans are overweight and therefore at high risk.

Evidence has shown that nutrition plays a crucial role in the self-management of diabetes and the prevention of long-term complications (Boles, Kandimalla, & Reddy, 2017). The adoption of a low GI diet, as part of an overall healthy eating lifestyle, has been shown to significantly improve glycemic control, cardiovascular risk factors (blood lipids and inflammatory markers), insulin sensitivity and beta cells function, decreasing the need for anti-hyperglycemic agents in diabetics (Augustin et al., 2015; Janghorbani, Salamat, Amini, & Aminorroaya, 2017). Moreover, reducing the GI and/or GL of ingested foods together with reducing nutrient density and increasing physical activity, may delay type 2 diabetes for people with IGT by targeting obesity and overweight (Bansal, 2015). There is therefore a growing need for the development of foods and food ingredients with a slow and steady postprandial release of glucose.

## 5. Factors affecting starch digestibility in foods

### 5.1. Degree of gelatinization

As addressed before, starch granules are more susceptible to amylolytic enzymes after gelatinization. So, the degree of starch gelatinization in a food directly influences the glycemic response to this product (Holm, Lundquist, Björck, Eliasson, & Asp, 1988). The degree of gelatinization depends mainly on the type of starch (amylose/amylopectin ratio, crystalline polymorph, etc.), the composition of the food (water availability, sugar content, etc.) and the processing conditions used (temperature, heating rate, shear, etc.). Thus, starches are usually present in our diet as a combination of fully, partially and not gelatinized granules (Chung, Lim, & Lim, 2006; Delcour et al., 2010). For example, the percentage of totally gelatinized starch granules will be almost 100% in mashed potatoes, while it will be close to 0% in sugar-snap cookies. The degree of gelatinization may also vary between different parts of a same product, like in white wheat bread, where the amount of starch granules fully gelatinized is not the same in the crumb and in the crust (~100% and ~60%, respectively) (Primo-Martín, van Nieuwenhuijzen, Hamer, & van Vliet, 2007).

### 5.2. Food matrix

The food matrix in which starch granules are encased may also affect the degree of gelatinization. In dense food microstructures (e.g., pasta products), gelatinization is restricted during cooking because water transfer inside the structure is limited and swelling is constrained by the compact matrix surrounding starch granules (Aguilera 2018; Cuq, Abecassis, & Morel, 2014). On the other hand, non-starch hydrocolloid gums, like xanthan gum, may also influence starch gelatinization and swelling during

processing. Indeed, these polysaccharides have high water binding capacity and reduce water availability and mobility in the system (Mahmood et al., 2017).

The food matrix may also reduce the digestion of starch and the absorption of hydrolysis products in the gastrointestinal tract (Singh et al., 2010). For example, in foods like legumes and minimally processed cereal grains, starch granules are trapped within the plan cell wall, which hinder their degradation by α-amylases (Do, Singh, Oey, & Singh, 2018). This barrier effect is also observed in some processed products such as cooked pasta. The tortuous gluten network formed around starch protects the gelatinized granules from enzymatic attack and delay their hydrolysis into glucose (Cuq et al., 2014; Fardet, Hoebler, Baldwin, et al., 1998; Heneen & Brismar, 2003; Kim et al., 2008; Petitot, Abecassis, & Micard, 2009; Zou, Sissons, Gidley, Gilbert, & Warren, 2015; Zou, Sissons, Warren, Gidley, & Gilbert, 2016). The presence of soluble fibers in foods influences starch digestibility as well. Guar gum, for example, increases the viscosity of digesta within the gastrointestinal tract, which slow the rate of starch digestion and the transport of amylolytic products (Singh et al., 2010; Mahmood et al., 2017). Finally, minor components of the food matrix may affect the rate of starch digestion, such as phytates, phenolic compounds, saponins, lectins and several enzyme inhibitors (i.e., anti-nutrients). These components interfere with he catalytic activity of the glucosidase enzymes, thereby limiting their action (Singh et al., 2010; Hamaker et al., 2006).

Furthermore, it is important to note that starch is normally ingested with other food components, like proteins and lipids, in whole meals. The intake of these other macronutrients along with starch tends to reduce the postprandial glucose response, probably by decreasing the rate of gastric emptying (Bellissimo & Akhavan, 2015). New structures like emulsions and protein gels may also be formed in the stomach, promoted by the acidic pH and the peristaltic movements (Floury et al., 2018; Mulet-Cabero, Rigby, Brodkorb, & Mackie, 2017; Singh, Ye, & Ferrua, 2015).

To sum up, factors acting on starch digestibility in foods are multiple and often related among themselves (Singh et al., 2010). Digestion of starch in solid food matrices of different compositions and textures is not fully understood yet (Hamaker et al., 2006; Mackie, 2017). In particular, starch gelatinization and digestion in protein matrices with high-water content (i.e., > 80%), like hydrogels, have not been systematically investigated despite their potential health benefits.

## 6. A strategy to reduce gelatinization and slow down starch digestion

Protein-based hydrogels have been used successfully to modulate lipids digestion (Guo, Ye, Bellissimo, Singh, & Rousseau, 2017). Hence, they naturally appear as interesting matrices to encase starch and modulate its digestibility. In addition, such gels may help reducing overeating by increasing satiation and satiety (Bellissimo & Akhavan, 2015; Benelam, 2009; Campbell, Wagoner, & Foegeding, 2017) and mimic some of the organoleptic attributes of fat and carbohydrates (Chung, Degner, & McClements, 2013). Protein hydrogels therefore offer interesting prospects for the creation of low-calorie and/or satiety-inducing foods and ingredients, targeting overeating. Such matrices are also attractive for the development of soft foods specially designed for the elderly: the texture of protein hydrogels can be modulated to ease mastication and swallowing (Aguilera & Park, 2016).

Hydrogels are three-dimensional solid networks fabricated by physically or chemically cross-linked hydrophilic polymeric structures that can entangle a lot of liquid water inside their network (Abaee, Mohammadian, & Jafari, 2017). Two other types of gels exist: the oleogels, where the liquid phase is oil; and the bi-gels, which are a combination of an oleogel with a hydrogel. In this Thesis only hydrogels will be discussed, hereafter referred simply as “gels”.

Globular proteins are able to produce gels formed either by heat-induced gelation (i.e., heat-set gels) or by cold gelation (i.e., cold-set gels) (Zhang, Zhang, Chen, Tong, & McClements, 2015). Heat-induced gelation is a one-step process: globular proteins unfold and aggregate until a network is formed. Gelation rate and gel strength depend on protein composition, protein concentration, heating temperature, heating time, pH, salt concentration and salt type, among others (Brodkorb, Croguennec, Bouhallab, & Kehoein, 2016). On the contrary, cold gelation is a two-step process. First, the protein solution is heated under conditions where unfolding is encouraged but aggregation is limited (low ionic strength, pH away from pI, low protein concentration, optimized heating time and temperature). A stable solution of protein aggregates is formed (step 1). Then, gelation is induced by addition of salt (e.g. $CaCl_2$ or NaCl), by decreasing the pH (e.g. addition of glucono-δ-lactone) or by the action of enzymes (e.g. transglutaminase) at ambient temperature (step 2). The structure and the properties of the cold-set gels depend mainly on the choice of agent used to induce gelation (Brodkorb et al., 2016). Cold-set gels have been used as delivery systems to protect and enhance the bioavailability of heat-sensitive components like bioactive molecules (e.g. probiotics) or micronutrients (hydrophobic vitamins and minerals, for example α-tocopherol or iron) (Abaee, Mohammadian, et al., 2017; Livney, 2010; Tavares, Croguennec, & Carvalho, 2014). Similarly, native starch could be entrapped in a protein gel through cold gelation, avoiding gelatinization until further processing.

Different types of globular proteins can form cold-set gels. In food the most common are β-lactoglobulin and bovine serum albumin from whey, ovalbumin from egg white, β-conglycinin and glycinin from soybean. Whey proteins (WP) have been extensively used to prepare gels protecting sensitive components (Abaee et al., 2017), mainly because of their outstanding functional, biological and nutritional properties (Smithers, 2015). Furthermore, WP supplementation has been proposed to reduce postprandial glycemia in patients with type 2 diabetes. WP intake before meals may indeed stimulate

the secretion of insulin and incretins and delay gastric emptying (Almario, Buchan, Rocke, & Karakas, 2017; Mignone, Wu, Horowitz, & Rayner, 2015).

Considering all the above, using WP cold-set gels to develop low-calorie soft starchy foods with a slow and steady postprandial release of glucose seem promising.

## 7. Whey proteins

WP are by-products of cheese manufacture used as functional foods in sports nutrition, as dietary supplements for the elderly and as functional ingredients for the food industry (in emulsions, foams, gels and fat reduced products for example) (Smithers, 2015). Compared to other protein sources, WP are rich in branched-chain amino acids (leucine, isoleucine and valine) known for their protein anabolic properties. WP are also rapidly absorbed and readily bioavailable (Ha & Zemel, 2003).

The main components of WP in bovine milk are the globular proteins β-lactoglobulin (β-lg), which represents more than 50% of the total proteins, and α-lactalbumin (α-la) constituting approx. 20% of the WP. Then comes the immunoglobulins, serum albumin and proteose peptone (Cheison & Kulozik, 2017).

The gelling properties of whey proteins are mainly related to the β-lg (Havea, Singh, & Creamer, 2001). Native β-lg is made of a sequence of 178 amino acids, including a signal peptide of 16 residues, and contains seven cysteines (Figure 9). Two of them are on the signal peptide, four others form disulfide bridges, between $Cys^{82}$ and $Cys^{176}$ (near the C-terminus) and between $Cys^{122}$ and $Cys^{135}$ (in the interior of the molecule), while the last one, $Cys^{137}$, is a free thiol group (The UniProt Consortium, 2019). The secondary structure of β-lg consists of about 8% α-helix, 45% β-sheet and 47% random coil (Figure 10). This structure organizes in strands of anti-parallel β-sheet and forms a hydrophobic barrel (The UniProt Consortium, 2019). At room temperature and neutral

pH, native β-lg exists as a dimer of two non-covalently linked monomeric molecules. The isoelectric point (pI) of β-lg is 5.2.

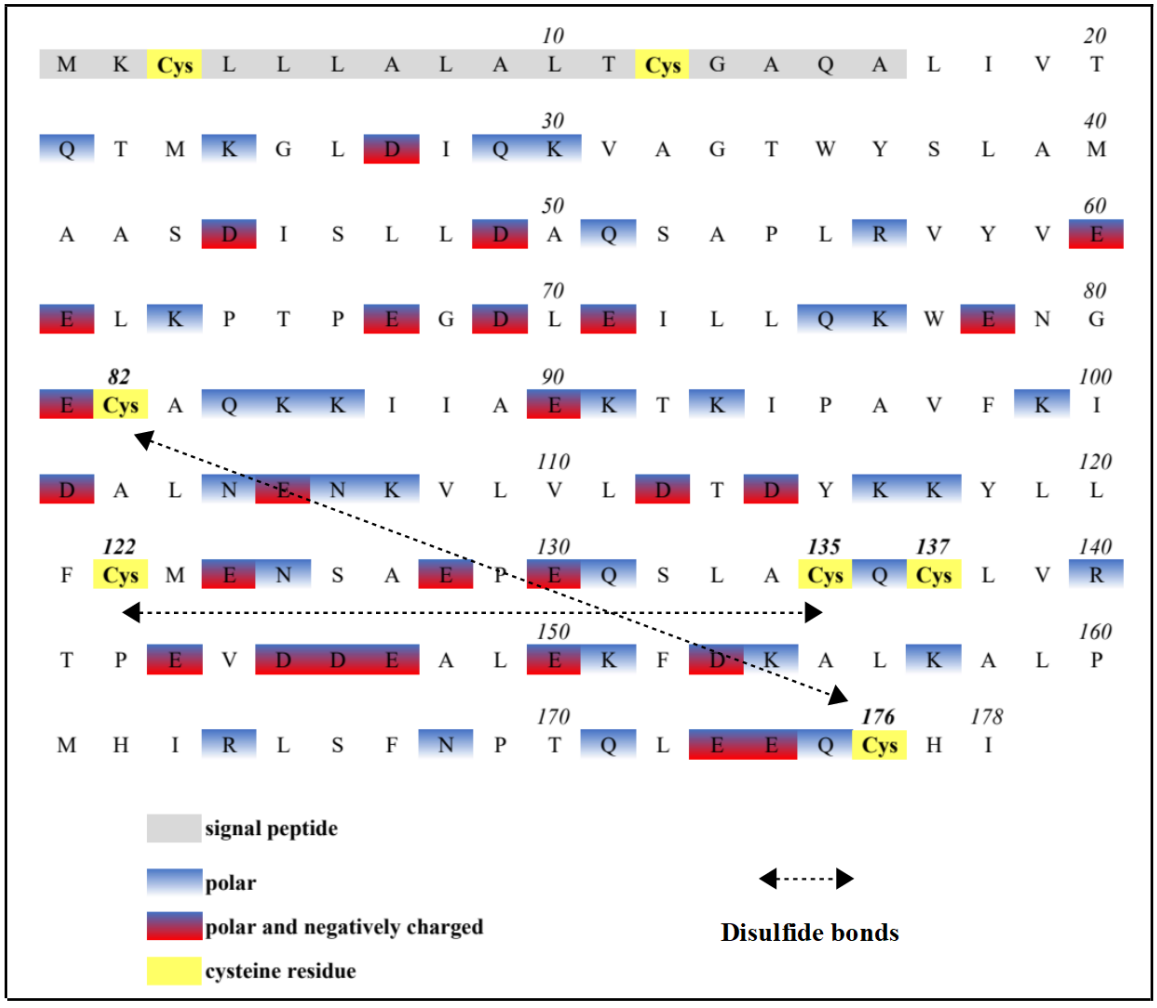


**Figure 9.** Detailed sequence of β-lg, adapted from The UniProt Consortium (2019).

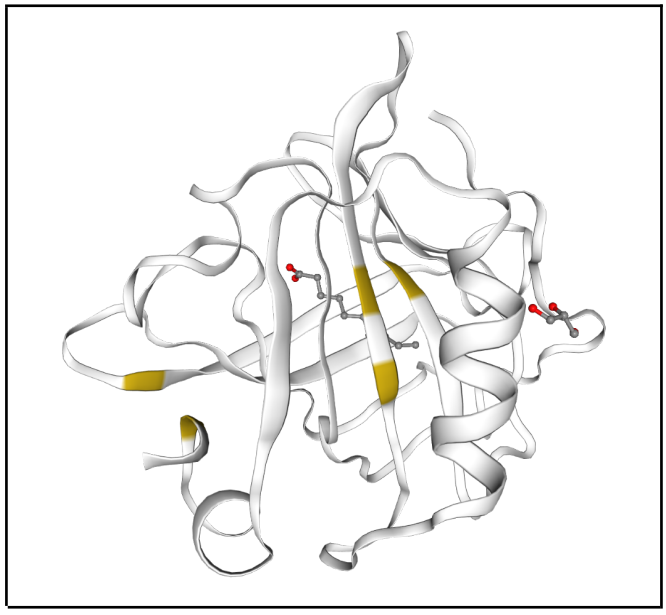

**Figure 10.** Globular structure of a monomer of β-lg, from the SWISS-MODEL repository (Bienert et al., 2017). Cysteine residues are marked in yellow.

## 8. *In vitro* study of starch digestibility in solid food matrices

Although human nutritional studies are still considered the "gold standard" for addressing diet-related questions, *in vitro* gastrointestinal digestion systems are widely used for understanding the behavior of food and food components during human digestion (Lucas-González, Viuda-Martos, Pérez-Alvarez, & Fernández-López, 2018). Compared to *in vivo* feeding methods, *in vitro* protocols are more rapid, less expensive, easier to implement, to control and to reproduce, and most importantly, do not have ethical restrictions (Minekus et al., 2014).

*In vitro* methods are therefore valuable tools for testing the efficacy of newly developed food-based delivery systems, since they allow a rapid screening of different

compositions and structures (Hur, Lim, Decker, & Mcclements, 2011). Moreover, the current detailed understanding of digestion biochemistry has allowed *in vitro* models to become a relatively good predictor of *in vivo* behavior for macronutrients, especially when considering simple systems (Bohn et al., 2018). Regarding the digestion of starch, numerous studies have demonstrated an excellent correlation between *in vitro* and *in vivo* data (Bohn et al., 2018). Overall, *in vitro* protocols do appear to be reliable indicators of *in vivo* glucose response (Araya, Contreras, Alviña, Vera, & Pak, 2002; Englyst, Englyst, Hudson, Cole, & Cummings, 1999; Goñi et al., 1997; Jenkins et al., 1982; Monro & Mishra, 2010; Seal et al., 2003), and thus are very suitable for mechanistic studies and hypothesis building in early stages of product development.

Among the multitude of *in vitro* protocols available to study starch digestion in food matrices (Dona et al., 2010; Woolnough, Monro, Brennan, & Bird, 2008), one of the most popular methods is an enzymatic assay developed by Englyst et al. (1999). This approach evaluates the amounts of glucose that are likely to be available for rapid and slow absorption in the human small intestine, and classifies it into rapidly available glucose (RAG), slowly available glucose (SAG) and unavailable glucose (UG). This methodology has been extensively used to estimate the glycemic response of starch-based foods (Singh et al., 2010; Dona et al., 2010; Woolnough et al., 2008) and a recent inter-laboratory trial confirmed that this method provides repeatable and reproducible results (Englyst et al., 2018). However, this protocol does not specify the enzyme activities, and most importantly, it omits the oral phase. This first step of the human digestion is still often neglected in studies on starch digestibility, even if it is known that mastication and salivation substantially influence the hydrolysis of starch in solid foods (Bornhorst & Singh, 2013; Freitas, Le Feunteun, Panouillé, & Souchon, 2018; Daniela Freitas & Feunteun, 2019; Hoebler et al., 1998a; Mathieu et al., 2016; Minekus et al., 2014; Tamura, Okazaki, Kumagai, & Ogawa, 2017).

More recently, a standardized *in vitro* digestion method was developed by the European INFOGEST network, comprised of more than 200 scientists from 32 countries working in the field of digestion (Minekus et al., 2014). This group of experts described in great detail a static model, easy to set up and apply, aiming at harmonizing the protocols simulating human digestion so that results among studies could be compared worldwide. Since its publication, the standardized INFOGEST *in vitro* method has been used to study starch digestibility in various food matrices, in particular in cereal-based products like pasta, bread, cookies and extruded snacks (Azzollini, Derossi, Fogliano, Lakemond, & Severini, 2018; Bustos, Vignola, Pérez, & León, 2017; Gao et al., 2019; T. Liu et al., 2016), bean paste (Sęczyk, Świeca, & Gawlik-Dziki, 2015), black rice (An, Bae, Han, Lee, & Lee, 2016) and chickpeas (Ercan & El, 2016), among others. However, there is still no consensus on how to stimulates the multiple actions occurring during mastication (Gao et al., 2019).

## HYPOTHESIS & OBJECTIVES

The hypothesis of this Thesis is that a protein gel can reduce starch gelatinization during heat treatment and protect partially gelatinized starch granules from enzymatic attack during digestion.

The main objective of this Thesis was to reach a better understanding of the changes occurring in starch-trapping protein gelled matrices during and after heat treatment and to investigate the effect of the protein gelled network on starch digestibility.

The specific objectives were the following:

1. Develop composite gels of WPI and PS formed by $CaCl_2$ induced cold gelation, as model microstructures with a high-water content (> 80%) where native starch granules are encased in a protein network.

2. Study starch gelatinization inside the WPI network and analyze the impact of starch gelatinization on the mechanical and rheological properties of the composite gels.

3. Evaluate if the WPI network is able to protect gelatinized PS granules from enzymatic attack during digestion *in vitro*, and analyze the effect of particle size and texture of the composite gels on PS digestibility.

4. Investigate the impact of heating up to 90°C on the properties and the microstructure of the cold-set WPI gel and identify changes occurring on the molecular level.

# CHAPTER 1: Starch gelatinization inside a whey protein gel formed by cold gelation

## 1. Introduction

Starch is the main carbohydrate of our diet and the major source of energy in human nutrition (Lehmann & Robin, 2007; Singh, Dartois, & Kaur, 2010). Native starch granules occur as semi-crystalline structures, 5-100 µm in size, where amorphous and crystalline domains are arranged in alternating concentric rings (Parker & Ring, 2001; Tester, Karkalas, & Qi, 2004). When heated in excess of water, starch granules undergo a series of changes known as gelatinization. During this process, starch granules readily absorb water and swell several times their original size until they collapse and leach their polymeric content. Several analytical methods have been used to investigate starch gelatinization: differential scanning calorimetry (DSC), rapid visco analyzer (RVA), hot-stage microscopy, swelling power, small/wide-angle X-ray scattering, etc. Each technique tends to reflect the gelatinization event differently, in particular by considering different end points (Schirmer, Jekle, & Becker, 2015). Gelatinized starch granules are more sensitive to *in vitro* and *in vivo* enzymatic attack than native ones. Consequently, fully gelatinized granules are rapidly hydrolyzed into glucose in the gastrointestinal tract, resulting in a significant rise of the postprandial blood glucose level (Englyst, Englyst, Hudson, Cole, & Cummings, 1999; Parada & Aguilera, 2012).

Diets inducing sharp variations of blood glucose and insulin levels are associated with increased risks for obesity, type 2 diabetes and coronary heart disease (Augustin et al., 2015). Ischemic heart disease was the first global cause of death in 2016 and around 422 million people in the world were suffering from diabetes in 2014 (World Health Organization, 2016, 2018). In this context of worldwide health concerns, predicting and

controlling the glycemic response due to the ingestion of starchy foods is of great interest (Kovatchev & Cobelli, 2016; Singh et al., 2010).

Not all starchy foods are digested to the same extent. First, starch is usually present in processed foods as a combination of fully and partially gelatinized granules (Delcour et al., 2010; Primo-Martín, van Nieuwenhuijzen, Hamer, & van Vliet, 2007). Secondly, in some foods starch granules are encased in a matrix that will deter their breakdown by the digestive enzymes during transit in the gut (Singh et al., 2010; Singh, Kaur, & Singh, 2013). For example, in pasta products the compact gluten microstructure around starch granules restricts their swelling during cooking. This dense matrix also acts as a barrier against enzymatic attack during digestion (Cuq, Abecassis, & Morel, 2014; Heneen & Brismar, 2003; Zou, Sissons, Gidley, Gilbert, & Warren, 2015). Both phenomena eventually lead to a reduction of starch digestibility and low glycemic responses (Fardet, Hoebler, Baldwin, et al., 1998; Kim et al., 2008; Petitot, Abecassis, & Micard, 2009; Zou, Sissons, Warren, Gidley, & Gilbert, 2016).

As opposed to compact gluten-starch microstructures, gelatinization of starch inside other protein matrices with high water content (i.e., > 80%) like gels, has not been systematically investigated despite their potential applications as low-calorie soft foods (Chung, Degner, & McClements, 2013; Pogaku, Eng Seng, Boonbeng, & Kallu, 2007).

Some hydrocolloids in solution, like xanthan gum, are capable of limiting gelatinization and swelling of starch granules (Silva, Birkenhake, Scholten, Sagis, & van der Linden, 2013). These polysaccharides with high water binding capacity lead to changes in gelatinization patterns of starches via reducing the volume fraction of water in the system and restricting water availability/mobility (Tester & Sommerville, 2003). Non-starch hydrocolloid gums have been used to modify starch properties and functionalities, particularly to delay starch retrogradation and improve freeze-thaw stability, but also to develop reduced-calorie and colon friendly starchy foods (Mahmood et al., 2017).

Whey proteins are known to form gels by different mechanisms, including cold gelation (Brodkorb, Croguennec, Bouhallab, & Kehoein, 2016). Through cold gelation, starch can be entrapped in a whey protein gel while in its native state, avoiding gelatinization until further processing. This is different from thermal gelation where the formation of the protein network occurs at about 80°C after starch gelatinization around 65°C (Aguilera & Baffico, 1997; Aguilera & Rojas, 1997; Chung, Degner, & McClements, 2013; Yang, Ashton, & Kasapis, 2015; Yang, Luan, Ashton, Gorczyca, & Kasapis, 2014). In addition to cold gelling properties, whey proteins have demonstrated a positive effect in reducing the glycemic response *in vivo* by stimulating the secretion of metabolic hormones and by delaying gastric emptying (Almario, Buchan, Rocke, & Karakas, 2017; Mignone, Wu, Horowitz, & Rayner, 2015).

The aim of this investigation was to study the gelatinization of native potato starch (PS) within a model gel of whey protein isolate (WPI) formed by cold gelation. The hypothesis of this study is that a protein gel can reduce the extent of starch gelatinization during heat treatment. PS gelatinization inside the WPI gel was investigated with a DSC/hot-stage system and confocal laser scanning microscopy (CLSM), and indirectly followed by mechanical and rheological measurements before and after heat treatment. A better understanding of starch-trapping mechanisms in protein gels could be useful for the future design of starchy soft foods with tailored postprandial glycemic responses.

## 2. Materials and methods

### 2.1. Materials

BiPro® WPI with a moisture content of 4.6% and a protein content of 97,7% (d.b.) was purchased from Davisco (Davisco Foods Intl., MN, USA) and native PS was from Roquette (Blumos S.A., Santiago, Chile). All other chemicals were standard analytical grade and distilled water was used for the preparation of all mixtures.

### 2.2. Sample preparation

The composite gels of WPI and PS were prepared by cold gelation of proteins induced by $CaCl_2$, hence, the structure contained native starch granules. PS was used because the large granule size made microscopy observation easier compared to other starches like cereal starches. Therefore gelatinization and related events could be measured more accurately. Additionally, the swelling power of potato starch is the highest among most common starches (Hoover, 2001; Li & Yeh, 2001). This feature was interesting in the context of this investigation where it is postulated that swelling of granules could be physically restricted by the protein network. A solution of 11% (w/w) WPI in distilled water (pH of the solution = 6.8) was heated in a water bath at 80°C for 30 min in order to obtain a dispersion of protein aggregates. After cooling for 30 min in a water bath at ~20°C, this dispersion was used immediately in the subsequent step of gelation. PS was added to the dispersion and the mixture was stirred for 15 min. An aqueous $CaCl_2$ solution was then added under continuous stirring in order to obtain a final mixture of 10% (w/v) WPI with 1, 3, 5, 7 or 9% (w/v) PS and 10 mM $CaCl_2$. This formulation was

chosen to avoid starch sedimentation during gelation and produce a homogeneous, soft and self-standing cold-set gel. Depending on the requirements of the method used to characterize the samples, the mixture of WPI, PS and $CaCl_2$ was cast in different types of containers (glass crucibles, tubes or disposable rheometer plates) and finally stored overnight at 4°C. Controls were dispersions of PS in the $CaCl_2$ solution at 10 mM and a pure WPI gel (10% (w/v) WPI and 10 mM $CaCl_2$). The composite gel WPI (10%) + PS (5%) and the dispersion of PS (5%), both containing 10 mM $CaCl_2$, were used as models for microscope observations.

### 2.3. DSC/hot-stage microscopy

For DSC/hot-stage microscopy, 15 µL of the mixture of WPI, PS and $CaCl_2$ was transferred into 7 mm diameter glass crucibles (Mettler-Toledo Inc., Columbus, OH, USA, catalog number 17780), covered with a glass coverslip and sealed with nail polish to prevent moisture loss. Samples in sealed crucibles were equilibrated at ambient temperature for one hour prior to measuring with a HS84 DSC/hot-stage system (Mettler-Toledo Inc., Columbus, OH, USA) positioned under an Olympus BX50 optical microscope (Olympus Optical Co., Ltd. Tokyo, Japan). Indium was used to calibrate the DSC/hot-stage system and an empty sealed glass crucible was used as reference. The microscope was equipped with a polarized filter and analyzer as well as a 5.0 MP digital USB microscope camera (OMAX Co., Ltd, Gyeonggi-do, Korea). Samples were heated at 10°C/min from 30°C to 85°C and observed under normal or polarized light. This temperature range was imposed by the DSC/hot-stage system, first because it does not include a cooling system and then, because the glass crucible may break with the increase in pressure due to water evaporation. The heating rate of 10°C/min was chosen as it is appropriate to mimic cooking conditions (i.e., high heat transfer rate) while obtaining accurate results within the technical limitations of the DSC/hot-stage system.

This relatively high heating rate may increase gelatinization temperatures and enthalpy, and reduce granules swelling. Images and videos with a resolution of 2592×1944 pixels were recorded in real time with the AmScope software (United Scope LLC, Irvine, CA, USA). Each DSC/hot-stage run was done at least in triplicate.

### 2.3.1. Thermal properties

The onset temperature, peak temperature, endset temperature and heat of gelatinization (ΔH) were determined with the STARe Thermal Analysis Evaluation software, version 14.0 (Mettler-Toledo Inc., Columbus, OH, USA). Measurements were done in triplicate.

### 2.3.2. Swelling

Swelling was associated to the increase in projected area of a starch granule as observed by microscopy. The onset temperature of swelling was determined from visual analysis of videos. As not all starch granules swelled simultaneously, the onset temperature was defined as the temperature at which the first granule of the observed group began to swell.

Images corresponding to specific temperatures of interest (between 30 and 85°C) were extracted from videos, processed and analyzed using Matlab R2012b software, version 8.0 (The MathWorks, Inc., Natick, MA, USA). Isolated starch granules were selected from raw images and the increase in area of each selected granule during heat treatment was followed individually. Starch granules were segmented from the background in order to determine their projected area using a binary mask, threshold segmentation and morphological image operations (e.g., elimination of small isolated groups of pixels and

suppression of objects at image borders). The projected area was quantified at the beginning of the heating treatment and at each selected temperature.

Granule swelling was calculated at any temperature Ti according to the following equation:

$$Granule\ swelling = \left(\frac{Projected\ area\ at\ Ti}{Initial\ projected\ area}\right) - 1 \quad (1)$$

Variations in size of at least 30 starch granules from five replicates were compiled for each experimental condition.

**2.4. Confocal laser scanning microscopy**

After heating in the DSC/hot-stage system (at 10°C/min, from 30 to 70°C or from 30 to 85°C), glass crucibles were cooled and carefully opened to extract samples for further observation under a confocal microscope Spectral Nikon Eclipse C2 (Nikon Corporation, Tokyo, Japan) with dual excitation. Gelled samples were stained with an aqueous solution of fluorescein isothiocyanate (FITC) (in DMSO, 0.05% w/v) and rhodamine B (0.05% w/v). PS samples dispersed in water were stained only with FITC. Rhodamine B stained proteins and FITC stained both proteins and starch granules. Samples were placed on a large coverslip with a 5 µl droplet of the staining solution. The excess of staining solution was removed with absorbent paper and the sample was immediately observed under the confocal microscope. A FITC and a tetramethyl rhodamine isothiocyanate filter block were used for the excitation of the two dyes under wavelengths of 488 and 561 nm, respectively. A 20x magnification objective lens was used to scan fields and generate stacks of images of 2048×2048 pixels every 1 µm along the z axis. Each focal plane of the observed samples consisted of two individual images, one representing the rhodamine B stained parts (in red) and the other representing the

FITC stained portions (in green). Both images were processed individually in order to remove noise (with a median filter 4×4 pixels) and adjust contrast. Then, an overlay image was obtained for each focal plane. The open source ImageJ software and the image processing package Fiji were used to visualize and process confocal images (Schindelin, Arganda-Carreras, & Frise, 2012). Two replicates of the composite gel and of the control were prepared and observed for each experimental condition.

### 2.5. Mechanical properties

The mechanical properties of gels were analyzed by uniaxial compression using a TA.XT2 Texture Analyzer (Texture Technology Corp., Scarsdale, NJ, USA). The mixture of WPI, PS and $CaCl_2$ was transferred into glass tubes (15 cm long x 2 cm in diameter). After gelation, samples were equilibrated at ambient temperature for one hour and cylinders of gels (10 mm height x 20 mm diameter) were cut from the gel samples cast in the glass tubes. These gel cylinders were compressed with a 75 mm diameter plate at a constant deformation speed of 0.1 mm/s up to fracture or a final compression strain of 80%. Measurements were conducted at room temperature (ca. 20°C). Gel samples were assayed after cold gelation (i.e., before heat treatment) and after reheating at 90°C for 30 min followed by cooling in iced water for 5 min. Results are reported as stress (kPa) – strain (%) curves. Measurements were done in triplicate.

### 2.6. Rheological properties

For rheological studies, samples were cast onto disposable plates of 25 mm in diameter and 1 mm of height. For all rheological measurements, a Discovery Hybrid Rheometer HR-3 equipped with an advanced Peltier plate and a solvent trap and evaporation

blocker (TA Instruments Corp., New Castle, DE, USA) was used. The bottom disposable parallel plate (25 mm) where the gel sample was previously cast was carefully installed on the Peltier plate. A top parallel plate (40 mm) with a solvent trap filled with distilled water was used. Gap size between plates was 1 ±0.2 mm. Amplitude sweeps were performed at 20°C at a constant frequency of 1 Hz, between 0.02 and 2000% shear strain (γ), measuring 10 points per decade. Temperature sweeps were carried out from 20 to 90°C and from 90 to 20°C with a heating/cooling rate of 1°C/min, at a constant frequency of 1 Hz and a constant strain of 1.0%, which was in the linear viscoelastic region (LVR) for all samples. An axial force of compression of 0.5 N ±0.1 N was used as conditioning to avoid loosing contact between the plates and the sample during the test. After this oscillatory temperature ramp, gels were equilibrated for 15 min at 20°C and subjected to an amplitude sweep test in order to measure the rheological properties of the gels after heat treatment. Each measurement was performed in triplicate. From amplitude sweep curves, the plateau value of G' ($G'_0$) and tan δ were both evaluated at $\gamma = 0.1\%$. These parameters were evaluated for both amplitude sweeps before and after heat treatment. Finally, values of G' at 55, 75 and 90°C were extracted from the final temperature sweep curves with the objective of evaluating the effect of PS gelatinization on the rheological properties of the composite gels. Measurements were done in triplicate.

### 2.7. Statistical analysis

Reported results correspond to the mean ± the standard deviation. Statistical significance of the results was tested using one-way analysis of variance (ANOVA) and differences between group means were analyzed by LSD multiple-range test with a probability level of 0.05 ($p < 0.05$). Statistical analysis was carried out with Statgraphics

Centurion software, version 17.1.12 (Statpoint Technologies, Inc. Warrenton, VA, USA).

## 3. Results and discussion

### 3.1. Cold gelation of the composite gels

#### 3.1.1. Microstructure

After cold gelation and before heat treatment, PS granules were homogeneously embedded in the WPI gel (Figure 1a). Moreover, Maltese cross patterns were observed under polarized light (Figure 1b), meaning that the encased PS granules were still in their native form. Fu & Nakamura (2017) also observed intact PS granules inserted in a continuous protein network of WPI cold-set gels at pH 6.8.

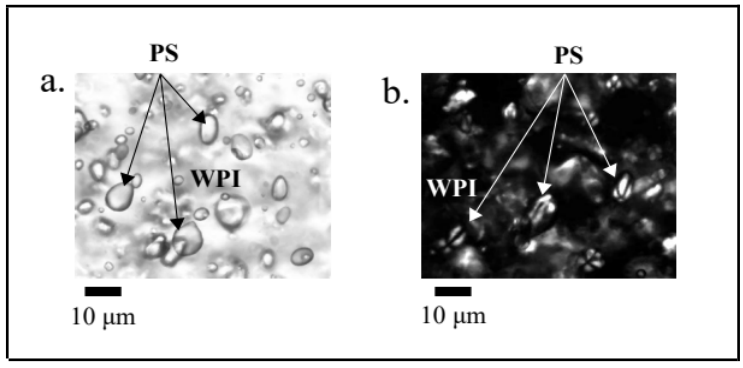


**Figure 1.** Microstructure of the PS granules (5%) inside the WPI gel (10%), before heat treatment; (a) observed with light microscopy, and; (b) observed with polarized light microscopy. The arrows point to the PS granules inside the background of WPI gel.

### 3.1.2. Mechanical and rheological properties

Self-standing, soft gels were obtained after cold gelation. Addition of PS may result in a weakening of the whey protein gel structure favoring fracture at the interface between PS granules and the continuous phase of WPI (Fu & Nakamura, 2017). However, in this study mechanical and rheological properties were not significantly modified by the addition of PS to the protein matrix.

No statistically significant differences were observed between hardness under compression (i.e., the maximum force divided by the original cross-sectional area) of the pure WPI gel, which was 65.1 ±6 kPa, and hardness of the composite gels (all PS contents pulled together), which was ~ 61 kPa. Neither of the two types of gels was fractured after 80% of deformation (Figure 2).

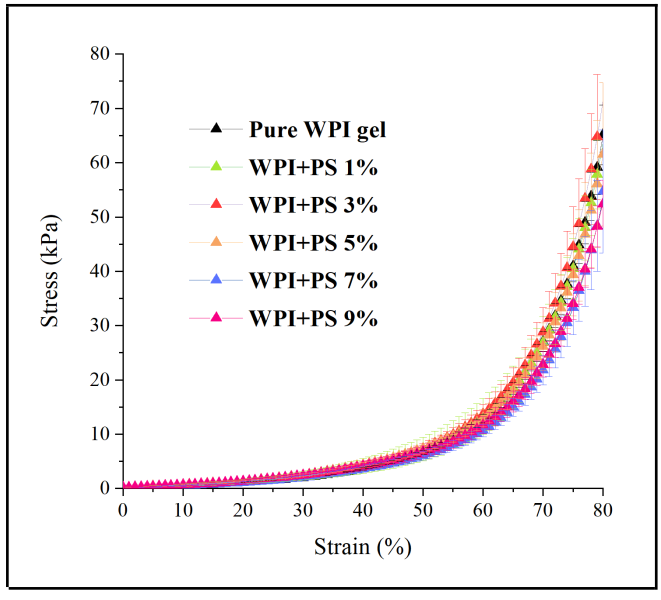


**Figure 2.** Stress-strain curves of the pure WPI gel (10%) and the composite gels (WPI 10% + PS 1, 3, 5, 7 or 9%), before heat treatment.

Amplitude sweep rheological measurements showed that all samples behaved as viscoelastic gels with dominating elastic properties, i.e., the storage modulus G' was higher than the loss modulus G'' ($\tan \delta < 1$) in the LVR (Figure 3). Under increasing strain amplitude, all samples showed a shear thinning behavior due to the successive breakdown of the structure of the WPI gel. In the LVR, $G'_0$ was 2.3 ±0.4 kPa for the pure WPI gel and between 1.5 and 2.2 kPa for the composite gels (differences not statistically significant), while $G''_0$ was 0.31 ±0.07 kPa for the pure WPI gel and between 0.19 and 0.33 kPa for the composite gels (differences not statistically significant). All gels were completely destroyed at ~ 350% oscillation strain (ie., cross point between G' and G'' curves). Regarding the methodology employed for the amplitude sweep measurements, the use of parallel plates with sandpaper could be a better option for the rheological study of this kind of gels at room temperature. Indeed, the shape of the curves in the non-LVR part of the graph (Fig. 3) suggests that the samples slid slightly between the smooth parallel plates of the rheometer when the gels started to soften under the increasing strain amplitude.

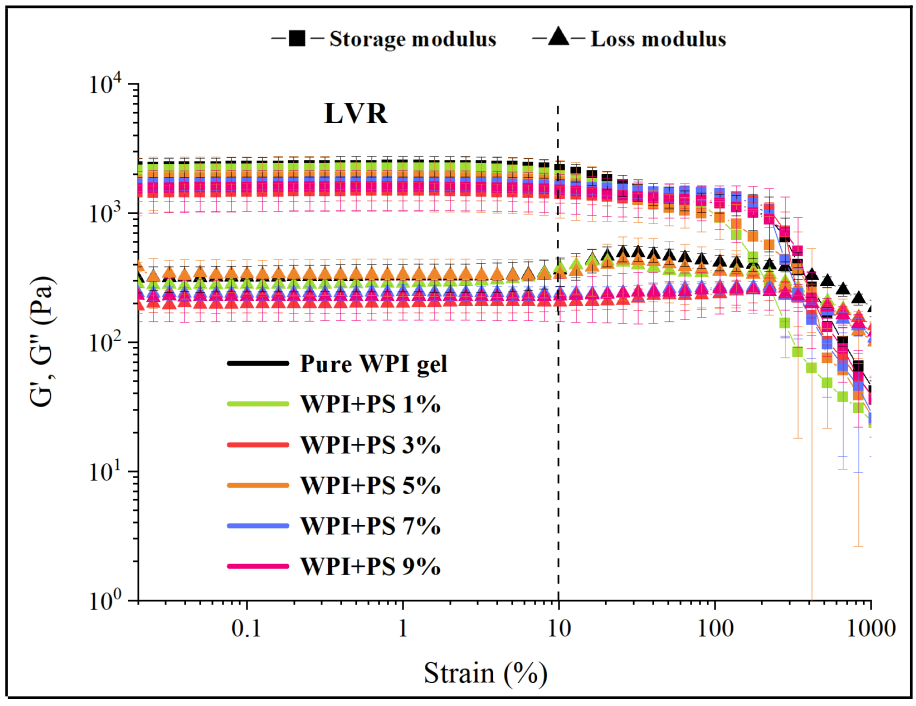


**Figure 3.** Amplitude sweep curves of the pure WPI gel (10%) and the composite gels (WPI 10% + PS 1, 3, 5, 7 or 9%), before heat treatment (20°C, gap 1 mm, constant frequency of 1 Hz). G' is the storage modulus, G'' the loss modulus and the linear viscoelastic region (LVR) is delimited by the discontinuous line.

Based on these results, the addition of PS to the WPI cold-set gel did not modified its mechanical and rheological properties. Before heat treatment, native PS granules behaved as inactive filler particles dispersed in the viscoelastic protein network.

### 3.2. Heat treatment of the composite cold-set gels

The DSC/hot-stage system allowed measuring of the thermal properties while observing the sample transformation in real time, either by light or polarized light microscopy. To

our knowledge, such system has never been used to study starch gelatinization. Li, Xie, Yu, & Gao (2013) investigated starch gelatinization by a combination of hot-stage light microscopy and DSC but the two techniques were implemented in separated instruments. Most investigations on starch gelatinization have used different starch-to-water ratios and/or different heating rates in the hot-stage and the DSC, thus complicating the interpretation of results (Cai, Cai, Zhao, & Wei, 2014; Molina, Leiva, & Bouchon, 2016). Even if the starch-to-water ratios and heating programs were the same in both experiments, heat transfer rates to the actual sample would still be different. Indeed, sample holder shape and material, volume of sample as well as the contact between heat source and geometry of the system, for example, are necessarily different and may influence heat transfer. These factors may explain differences between results from independent hot-stage and DSC experiments as highlighted by Muñoz, Pedreschi, Leiva, & Aguilera (2015)

### 3.2.1. Thermal properties

Figure 4 shows typical DSC thermograms obtained for the PS dispersions and the composite gels during heating. Mean values for the onset, peak, endset temperatures and the enthalpy change (ΔH) attributed to PS gelatinization, are summarized in Table 1. Gelatinization of PS in the $CaCl_2$ solution occurred between 60 and 70°C with an endothermic peak at 65°C and ΔH around 8.2 J/g.

PS gelatinization is generally reported to have a peak temperature at 64°C with a gelatinization enthalpy between 10 and 15 J/g (Alvani, Qi, & Tester, 2012; Alvani, Qi, Tester, & Snape, 2011; Cai et al., 2014; Li & Yeh, 2001; Muñoz et al., 2015; Parada & Aguilera, 2012; Ratnayake & Jackson, 2009). The presence of $CaCl_2$ in the system slightly delayed PS gelatinization and reduced ΔH. This was probably due to the high content of phosphate groups in PS. These phosphate groups generate charges on starch

molecules making PS susceptible to electrolytes, especially bivalent cations like calcium (Jane, 1993; Zhou et al., 2014), which may delay or inhibit PS gelatinization (Semeijin & Buwalda, 2018).

PS gelatinization within the WPI gel happened between 60 and 67°C with a peak temperature at 63°C and ΔH around 4.8 J/g, except for the composite gel containing 9% of PS. In the latter case, gelatinization of PS was measured between 60 and 70°C, with an endothermic peak at 65.5°C and a ΔH of 6.0 J/g. Therefore, for PS contents < 9%, the presence of the protein network shortened the gelatinization process by ~3°C and reduced ΔH by 41.5%. A decrease in gelatinization intensity was also observed by Li, Yeh, & Fan (2007) in starch-soy protein gels and by Jekle, Mühlberger, & Becker (2016) in starch-gluten dough-like systems. In both studies, this effect was attributed to a reduction in water availability for gelatinization. However, the reduction of gelatinization is also probably due to the presence of the protein network around starch granules directly constraining their swelling. When the PS content of the composite gel was increased to 9%, gelatinization was not shortened by the protein network and ΔH was only reduced by 26.8%. It is surmised that the WPI gelled microstructure was partly ruptured by starch granules swelling and was then unable to fully restrict PS gelatinization.

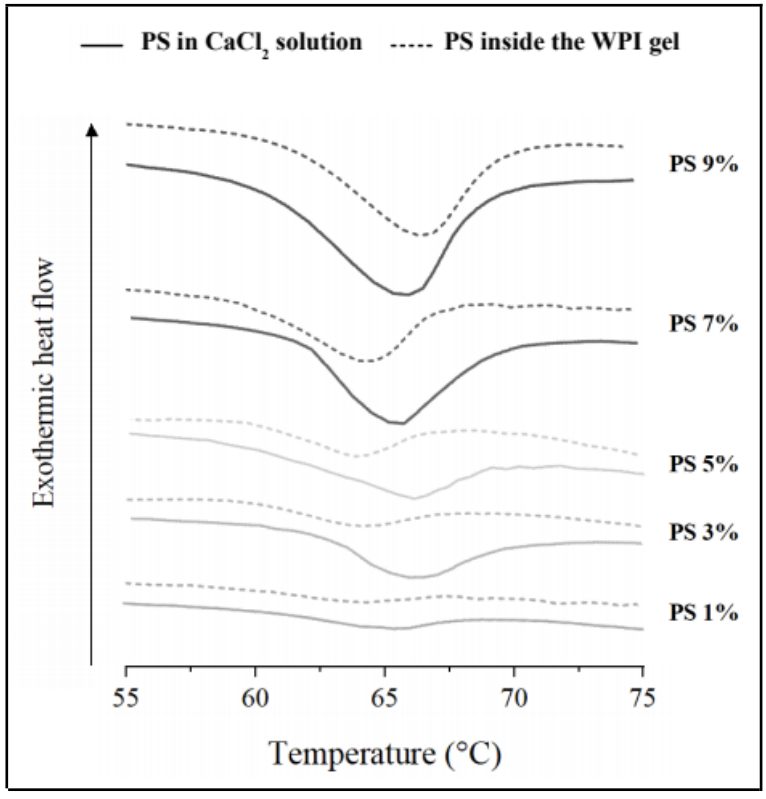


**Figure 4.** DSC thermograms for PS (1,3,5,7 or 9%) in the $CaCl_2$ solution and inside the WPI gel (10%), scan rate 10°C/min. To facilitate comparison, the individual traces have been displaced vertically by arbitrary amounts.

| Sample | PS (%) | T onset (°C) | T peak (°C) | T endset (°C) | ΔH (J/g) |
|---|---|---|---|---|---|
| PS in $CaCl_2$ solution | 1 | 59.9 ±1.0 [b] | 64.7 ±0.4 [a,b] | 69.1 ±0.1 [a] | 7.9 ±0.3 [a] |
| | 3 | 60.2 ± 0.2 [b] | 65.4 ± 0.1 [b,c] | 69.3 ±0.4 [a,b] | 8.1 ±0.1 [a] |
| | 5 | 59.8 ±0.3 [a,b] | 64.8 ±0.3 [a,b,c] | 69.6 ±0.7 [a,b] | 8.0 ±0.8 [a] |
| | 7 | 59.8 ±0.9 [b] | 64.3 ±0.2 [a] | 70.1 ±0.2 [b] | 8.6 ±0.5 [a] |
| | 9 | 60.0 ±0.2 [b] | 64.8 ±0.4 [a,b] | 69.9 ±0.4 [a,b] | 8.4 ±0.2 [a] |
| PS inside the WPI gel | 1 | 59.8 ±0.6 [b] | 63.4 ±0.4 [d] | 67.2 ±0.6 [c] | 4.5 ±0.2 [b] |
| | 3 | 59.6 ±0.4 [a,b] | 63.1 ±0.5 [d] | 67.0 ±0.2 [c] | 4.8 ±1.0 [b] |
| | 5 | 60.1 ±0.5 [b] | 63.4 ±0.3 [d] | 67.1 ±0.3 [c] | 4.4 ±0.5 [b] |
| | 7 | 59.6 ±0.1 [b] | 63.2 ±0.6 [d] | 67.2 ±0.8 [c] | 5.5 ±0.6 [b,c] |
| | 9 | 60.4 ±0.9 [b] | 65.6 ±0.3 [c] | 70.1 ±0.1 [b] | 6.0 ±0.7 [c] |

**Table 1.** PS gelatinization (PS content 1, 3, 5, 7 or 9%) in the $CaCl_2$ solution and inside the WPI gel (10%) assessed by DSC. The onset, peak, endset temperatures and the enthalpy of gelatinization were obtained from the DSC thermograms. Same letter as superscript in a column indicates that differences are not statistically significant (one-way ANOVA, $p < 0.05$).

### 3.2.2. Swelling

According to the videos recorded during heating in the DSC/hot-stage system, swelling of PS granules began at ~ 58°C in the $CaCl_2$ solution and inside the WPI gel. So, the presence of the protein network did not influence the onset of swelling.

Figure 5 shows light microscopy images extracted from videos during DSC heating, allowing the qualitative evaluation of changes in the microstructure of the samples. At 30ºC, a larger amount of native PS granules was noticeable in the $CaCl_2$ solution (Fig. 5a) compared to the gelled sample (Fig. 5d), revealing one of the major drawbacks when dealing with starch suspensions: the settling of granules on the bottom of the sample holder. However, at 70ºC all PS granules in solution were swollen into a packed condition (Fig. 5b), so settling appeared not to be an impediment for gelatinization. When the composite gel was heated to 70ºC, some PS granules had swollen into a more or less rounded shape, while others remained largely unchanged (Fig. 5e) After further heating to 85ºC, no additional changes were observed for PS in solution. Packed granules appeared to have irregular borders and a wrinkled surface (Fig. 5c). For the composite gel, heating to 85ºC had resulted in the swelling of some new granules and apparently no further changes in size of those previously swollen. The final microstructure was that of a continuous gel matrix having PS granules swollen to different extents as a discontinuous phase (Fig. 5f).

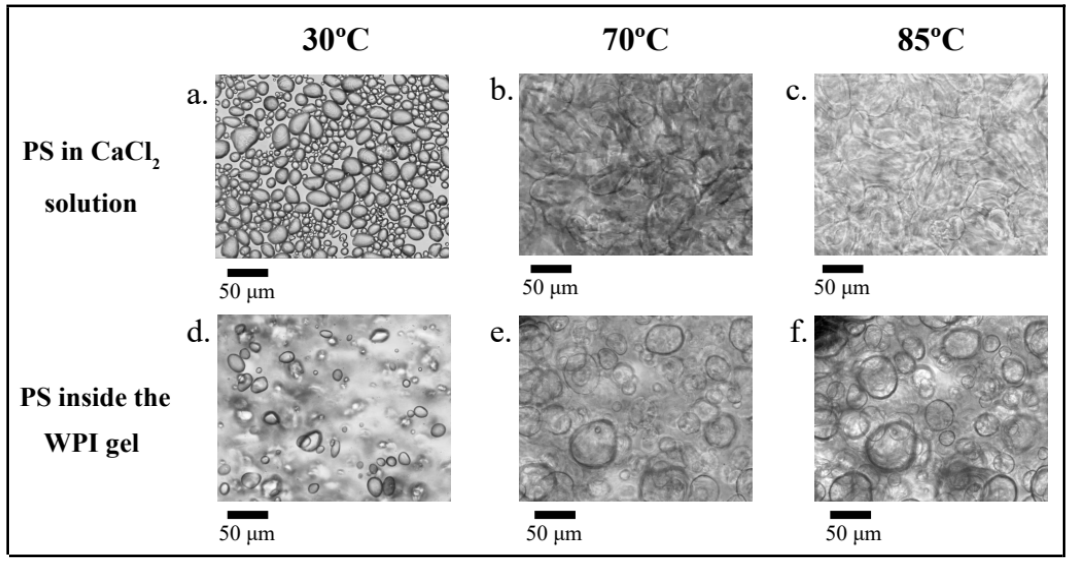


**Figure 5.** Microstructural changes of PS granules (5%) during heat treatment (DSC/hot-stage light microscopy); (a, b, c) in the $CaCl_2$ solution, and; (d, e, f) inside the WPI gel (10%). Images were extracted from representative videos at 30, 70 and 85°C.

To better understand the effect of the gelled matrix on PS gelatinization, samples with a lower starch concentration (0.05%) were prepared in order to accurately quantify the swelling of starch granules. Swelling of PS measured as the increase of projected area of granules reported in literature vary between 2.6 (Liu, Charlet, Yelle, & Arul, 2002) to up to 10 times (Singh, Singh, Kaur, Singh Sodhi, & Singh Gill, 2003) depending on variety, cultivar and experimental conditions (e.g. heating rate, temperature ranges, starch-to-water ratio, salts, etc.). In this study, when heated up to 85°C, PS granules dispersed in the $CaCl_2$ solution swelled up to 6.4 times their initial size, whereas PS granules inside the protein gel only swelled 4.3 times their initial size (Figure 6). In both cases, swelling was fast between 60 and 70°C, and then slowed down between 71 and 85°C. Beyond this last temperature swelling will probably reach an asymptotic value.

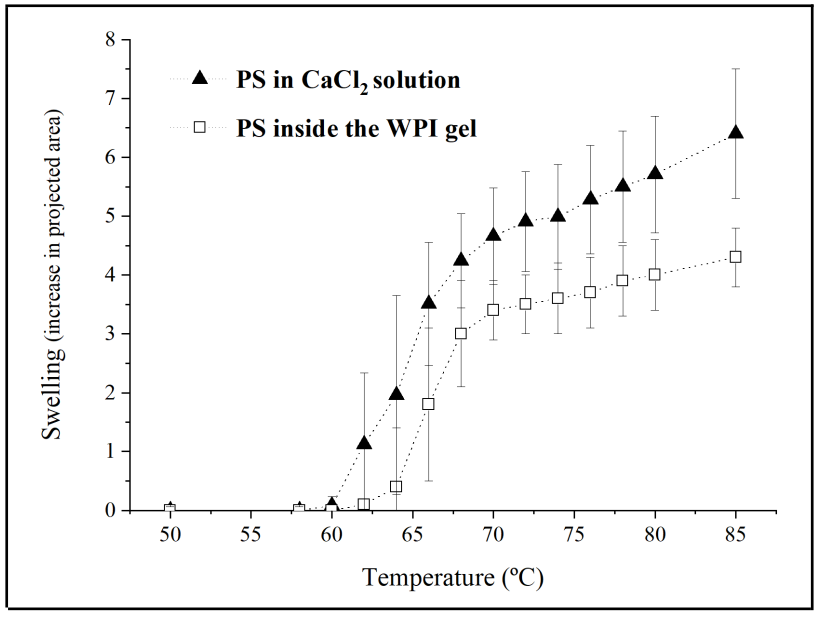


**Figure 6.** Swelling of PS granules (0.05%) during heat treatment in the $CaCl_2$ solution and inside the WPI gel (10%).

These findings are in line with the DSC results presented before (cf. Section 3.2.1) and support the hypothesis that swelling is constrained by the WPI network wrapped around PS granules.

### 3.2.3. Rheological properties

Figure 7 presents the storage modulus G' of gels as a function of their PS content at 20°C before heat treatment, at 90°C and at 20°C after heat treatment. The rheological properties of the pure WPI gel and the composite gels were modified by the heat treatment. G' increased with temperature in both cases, but a jump in G' between 55 and 75°C during heating was observed only for the composite gels. This jump in G',

attributed to starch gelatinization inside the protein network, depended on the PS content of the gel (Figure 8).

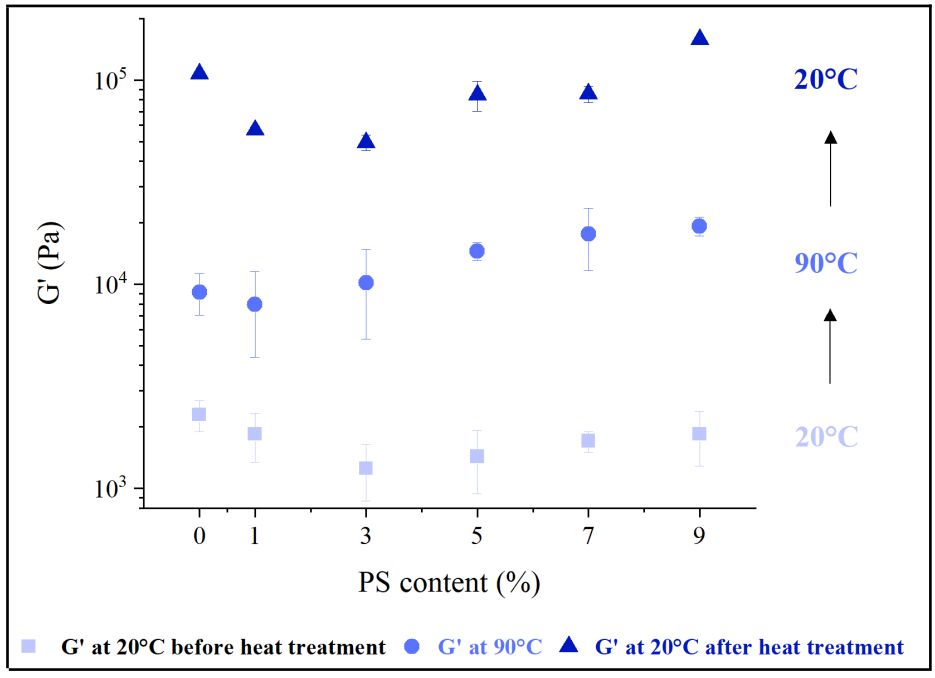


**Figure 7.** Storage modulus (G') of gels as a function of PS content (pure WPI gel, composite gels WPI 10% + PS 1, 3, 5, 7 or 9%), at 20°C before heat treatment, at 90°C, and at 20°C after heat treatment up to 90°C. Values were extracted from temperature sweep measurements.

Before heat treatment, the addition of PS to the protein network did not have a significant effect on G', regardless of the percentage of starch added (Fig. 7). According to Dille, Draget, & Hattrem (2015), this is typical of inactive filler particles dispersed in a viscoelastic network.

During heating, gelatinization occurred and G' increased rapidly for all samples. Starch granules embedded in the WPI gel began to absorb water, swell and exert pressure on

the protein network, leading to a raise in G' as observed in starch-containing surimi (Kong et al., 2016). The reinforcement effect measured between 55 and 75°C increased with the PS content of the gels. When 1% PS was added G' increased by ~0.3 kPa while G' increased by ~9.4 kPa for PS 9%, compared to the pure WPI gel (Fig. 8).

At 90°C, a similar trend was observed. G' also increased with PS content, but this rise was significant only for composite gels containing at least 5% PS (Fig. 7). It is then surmised that the gel reinforcement is not only due to the increase of volume of starch granules. According to section 3.2.2, PS granules embedded in the WPI gel may swell up to 4 times their initial size and therefore they are likely to touch each other and interact after gelatinization, when PS concentration is increased. The contribution of starch-starch interactions to the modulus of the gluten matrix at high volume fraction of starch has also been observed in model dough systems (Schiedt, Baumann, Conde-Petit, & Vilgis, 2013).

Starch swelling during gelatinization removes water from the cold-set protein gel. This water transfer is likely to induce important changes in the microstructure and the mechanical properties of the gelled protein phase, as observed by Baffico & Aguilera (1997) and Yang Liu, Ashton, Gorczyca, & Kasapis (2013).

After cooling, G' was almost halved by the addition of 1 and 3 % of PS and reduced by ~20% by the addition of 5 and 7% of PS (Fig. 7). An antagonistic effect of the addition of starch was also observed by Li et al. (2007) in composite gels of corn starch and soy protein concentrate and by Ravindra, Genovese, Foegeding, & Rao (2004) in heat-set gels of WPI and cosslinked waxy maize starch. Gelatinized PS granules may have ruptured the protein network, creating flaws in the microstructure and resulting in a global weakening of the gel. Furthermore, at low starch fractions, gelatinized starch granules probably act as weak inactive filler particles. This could also explain the decrease in modulus of the composite gels compared to the pure WPI gel, as proposed by Aguilera & Rojas (1996) and Dille et al. (2015). On the contrary, G' was

significantly increased when PS content reached 9% (158.0 ±3.9 kPa against 107.1 ±3.5 kPa for the pure WPI gel). Fan et al. (2017) also reported a strong reinforcement effect of cassava starch on a fish myofibrillar protein gel at starch fractions 0.5 and 0.6. This synergistic effect on modulus was attributed by the authors to the formation of an interpenetrating network. Interpenetrating networks are formed when two components, thermodynamically incompatibles, gel separately and form independent networks, both continuous through the sample (Turgeon & Beaulieu, 2001). At this concentration a PS gel may have formed upon cooling, creating an interpenetrating network with the existing WPI gel, resulting in the strengthening of the composite.

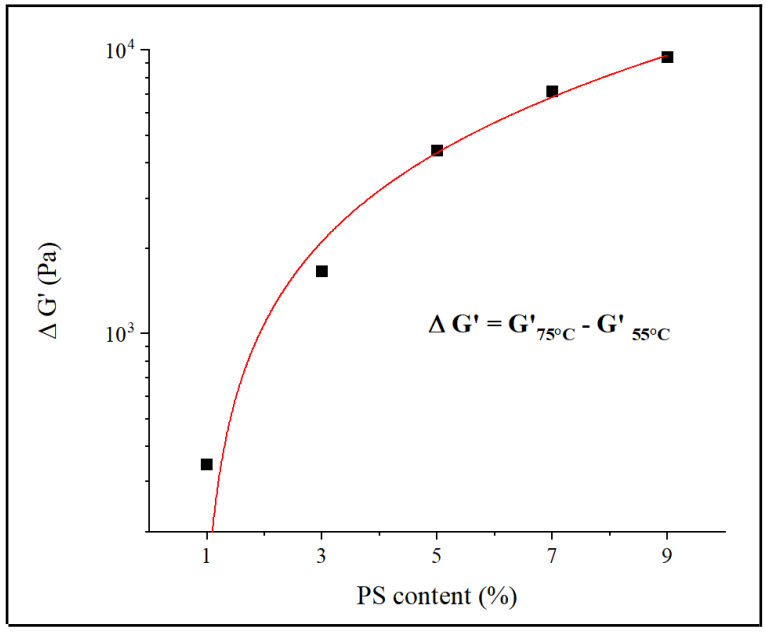


**Figure 8.** Effect of PS gelatinization inside the WPI gel (10%) on the storage modulus (G') of the composite gels as function of PS content (1, 3, 5, 7 or 9%). ΔG' was calculated with values extracted from temperature sweep measurements.

After heat treatment, critical strain was measured at ~5% for pure WPI gels and at ~8% for the composite gels, regardless of the PS% (data not shown). Nevertheless, at this stage data acquired in the non-LVR were very variable, probably because some parts of the gels stuck between the rheometer plates while the rest of the structure was already destroyed.

### 3.2.4. Mechanical properties

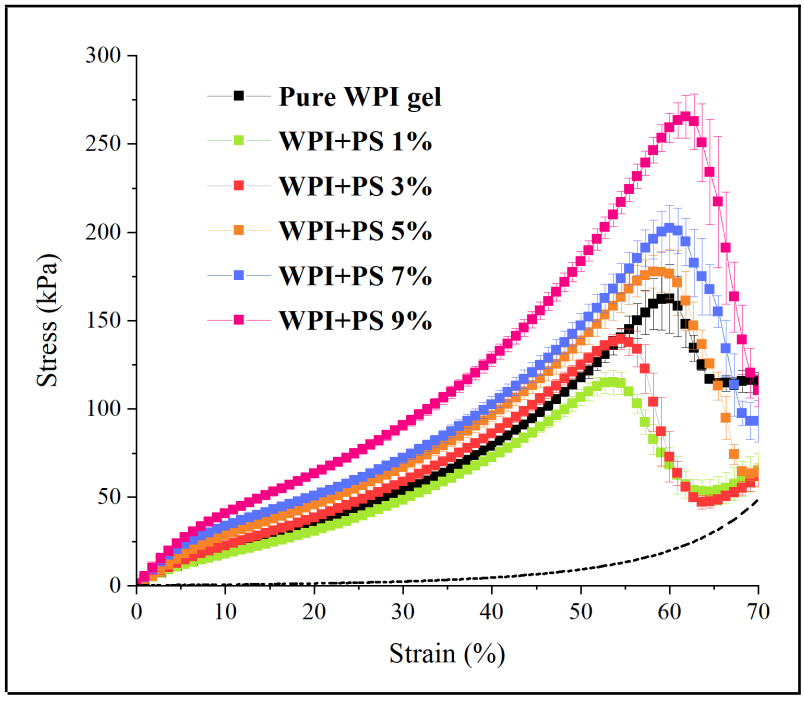


**Figure 9.** Stress-strain curves of gels as a function of PS content (pure WPI gel, composite gels WPI 10% + PS 1, 3, 5, 7 or 9%), after heat treatment to 90°C. The dashed line at the bottom represents the average values of stress-strain curves of gels before heat treatment.

As shown in Figure 9, the pure WPI gel was more brittle after heat treatment and fractured at ~60% of compression strain. Hardness also increased significantly compared to the same sample before heating (cf. Fig. 2) and reached 118 ±2 kPa at 50% of deformation. These results are in line with the observations of Hongsprabhas & Barbut (1997a), who reported that re-heating improved the Young's modulus and the shear stress but reduced the shear strain of $Ca^{2+}$-induced cold-set WPI gels. Authors suggested that re-heating may increase interactions (hydrophobic and disulfide bonds) between the protein aggregates of the gels and modify their microstructure.

Overall, the same trend was observed for the composite gels (ie., harder and more brittle structures), but the addition of PS also influenced the mechanical properties of the protein gel. When small amounts of starch were added (1 and 3% of PS), rupture of the gels occurred at ~54% of compression strain, meaning that the microstructure was weakened by the presence of the swollen PS granules. For the composite gels containing 5, 7 and 9% of PS, no effect of starch addition was observed on the elasticity of the gels as they broke at ~60% of compression strain, similar to the control of pure WPI gel. However, hardness increased to 138.4 ±6, 147.1 ±7 and 183.4 ±6 kPa, respectively, at 50% of compression strain. The hardness of the protein gel was therefore enhanced when higher amounts of PS were added to the system. Thus, heat treatment and starch addition modified the breakdown properties of the protein gel, which may have a significant effect on texture and mouthfeel (van den Berg, van Vliet, van der Linden, van Boekel, & van de Velde, 2007) and must be considered when designing food products based on this composite matrix.

These results confirm that PS gelatinization inside the WPI gel influenced the final properties of the protein matrix. This effect depended on starch concentration in the composite gel, as illustrated by Figure 10. At low starch volume fraction, the addition of PS resulted in a significant weakening of the gel (ie., antagonist effect), whereas at

higher volume fraction of starch, the addition of PS led to an actual reinforcement of the gel (ie., synergistic effect).

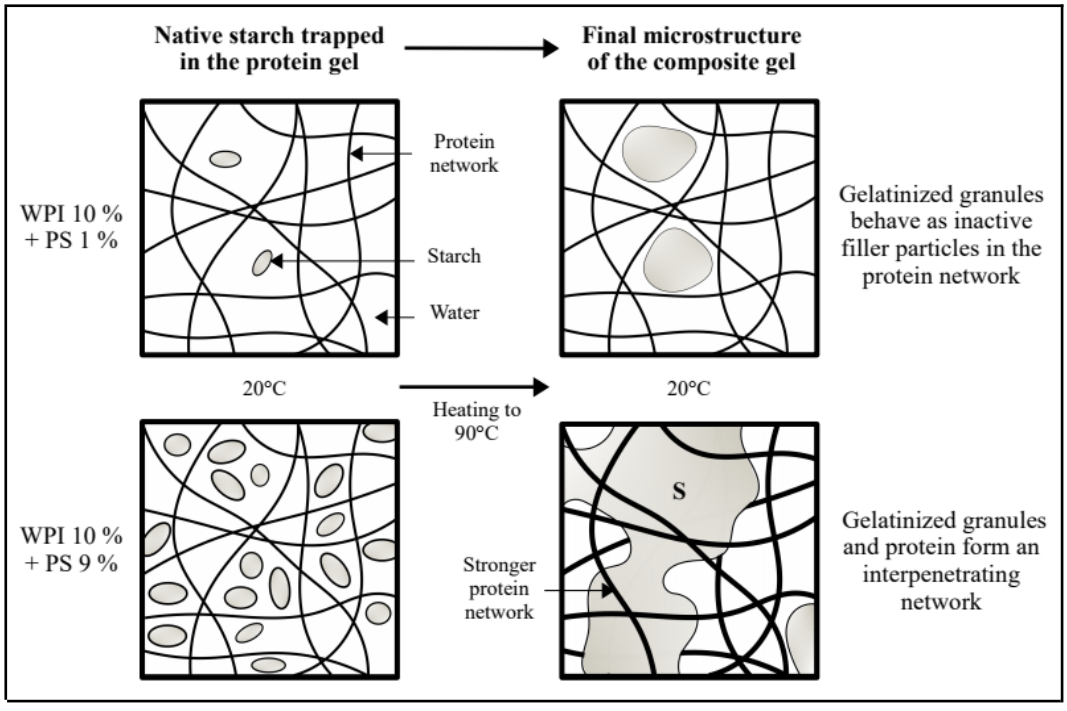


**Figure 10.** Scheme representing the changes in the microstructure of the composite gels after heat treatment.

### 3.2.5. Microstructure

To corroborate observations made with optical microscopy (cf. section 3.2.2), gel samples stained with Rhodamine B and FITC were examined with CLSM. A high level of superposition was observed between the fluorescent probes as they were not covalently fixed. Nevertheless, CLSM allowed to clearly visualize the WPI matrix

(yellow in images) which was not possible with light microscopy. Figure 11 shows representative focal planes of samples acquired by CLSM before and after heat treatment in the DSC/hot-stage.

In the $CaCl_2$ solution, native PS granules settled at the bottom of the sample holder (Fig. 11a), as noted previously with light microscopy (cf. Section 3.2.2 and Fig. 5a). Heating to 70°C resulted in PS gelatinization. Swollen hydrated PS granules of different sizes and shapes were observed (Fig. 11b). After heating to 85°C, most PS granules appeared to have collapsed into a shapeless mass (Fig. 11c). Gelatinized PS granules' integrity was lost, resulting in a featureless matrix of solubilized starch polymers and granular remnants.

In the composite gel, native PS granules were homogeneously embedded in the WPI network (Fig. 11d), as observed before with light microscopy (cf. Section 3.1.2 and Fig. 1). Heating to 70°C led to partial gelatinization of PS inside the WPI gel. Swollen PS granules surrounded by the continuous WPI gel were clearly visualized (Fig. 11e and 11f, PS in green and WPI in yellow). In this case, granules´ integrity was largely preserved after heating to 70°C and up to 85°C (Fig 11e and 11f, respectively). Partially swollen starch granules dispersed in a continuous gluten matrix were also observed by Kim et al. (2008) in cooked fettuccini and Zou et al. (2015) in the central region of cooked pasta.

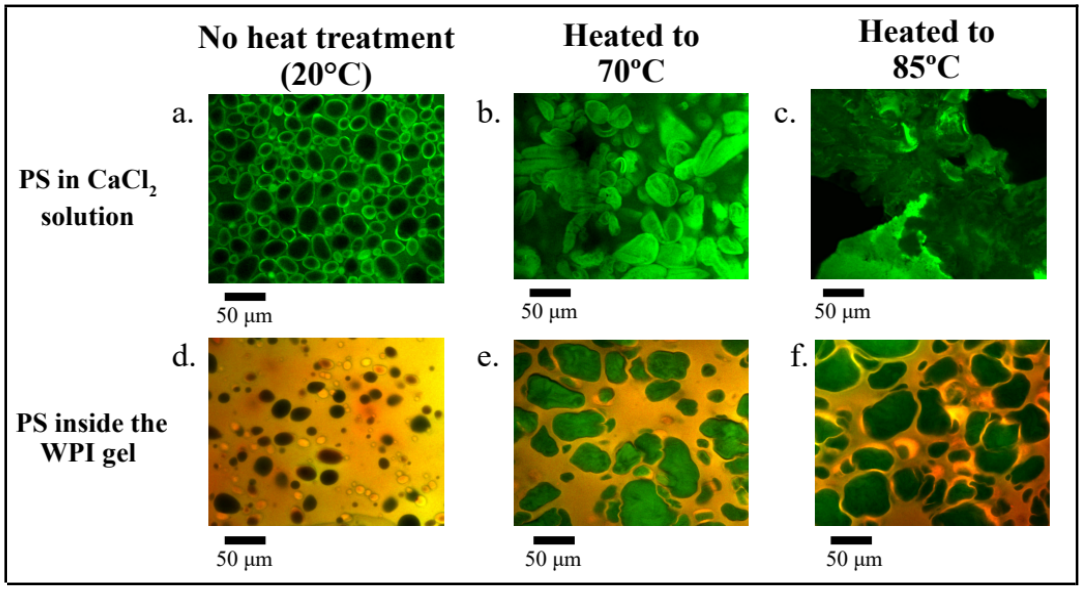


**Figure 11.** Microstructural changes of the PS granules (5%) after heat treatment (confocal laser scanning microscopy); (a, b, c) in the $CaCl_2$ solution, and; (d, e, f) inside the WPI gel (10%). The WPI appears in yellow and the PS in green.

These observations confirmed that before and after heat treatment, the composite gels' microstructure was made of a discontinuous phase of, raw or gelatinized, PS in a continuous phase of WPI and support the model presented in Figure 10 (at low PS content).

## 4. Conclusions

PS gelatinization restricted by a preformed cold-set gel matrix of WPI was characterized by several techniques. After cold gelation, the native starch granules were

homogeneously encased in the whey protein matrix. Heat treatment of the composite gels (i.e., heating above 80°C) led to partial gelatinization of PS inside the protein network. The gelatinization event was shortened, the gelatinization enthalpy was reduced and swelling was constrained when PS granules were embedded in the protein gel.

The model WPI gel was self-standing, soft and elastic after cold gelation and the addition of PS did not significantly modified its mechanical and rheological properties. Native PS granules behaved as inactive filler particles dispersed in the viscoelastic protein network. However, upon heating the addition of PS influenced the properties of the gel. For small amounts of PS, a weakening of the WPI gel was observed, probably because gelatinized granules created flaws in the microstructure. On the contrary, higher amounts of PS led to an actual reinforcement of the gel. It seems that in this case an interpenetrating network between WPI and the gelatinized PS was formed.

This work contributes to a better understanding of changes occurring in starch-trapping soft protein gelled matrices during and after heat treatment. Composite gels of WPI and native starch could be used as a structural basis for the development of low-calorie soft foods with a slow and steady postprandial release of glucose. Such microstructures could help design functional foods for the elderly or new biomimetic plant foods, for example. Further investigation is needed to evaluate the organoleptic properties of these starch-trapping gels and to understand how to effectively incorporate them as ingredients in new food products.

# CHAPTER 2: Effect of a whey protein network formed by cold gelation on starch digestibility

## 1. Introduction

The World Health Organization (WHO) estimated that approximately 422 million adults suffered diabetes in 2014 (World Health Organization, 2016). The prevalence of the disease has nearly doubled across the globe since 1980 and according to the International Diabetes Federation (IDF) over 600 million people will be diagnosed with diabetes by 2045 (International Diabetes Federation, 2017).

Evidence has shown that nutrition plays a crucial role in the self-management of diabetes and the prevention of long-term complications (Boles, Kandimalla, & Reddy, 2017). The adoption of a low glycemic index (GI) diet as part of an overall healthy eating lifestyle has been shown to significantly improve glycemic control, cardiovascular risk factors (e.g. total cholesterol, HDL), beta cell function and to decrease the need for anti-hyperglycemic agents among individuals with diabetes (Janghorbani, Salamat, Amini, & Aminorroaya, 2017). Moreover, reducing the GI and/or glycemic load (GL) of ingested foods together with reducing nutrient density and increasing physical activity, may delay type 2 diabetes for people with an impaired glucose tolerance by targeting obesity and overweight (Bansal, 2015). There is therefore a growing need for the development of specific foods with a slow and steady postprandial release of glucose to help managing disorders of glucose metabolism.

This calls for a better understanding of the digestion of complex carbohydrates, like starch, in solid food matrices. Indeed, other constituents of the food matrix may affect the final digestibility of the ingested starch (Singh, Dartois, & Kaur, 2010). In particular, the presence of a protein barrier surrounding the starch granules in processed products such as pasta has been related to a reduction of *in vitro* starch digestibility (Cuq,

Abecassis, & Morel, 2014; Fardet, Hoebler, Bouchet, Gallant, & Barry, 1998; Heneen & Brismar, 2003; Kim et al., 2008; Petitot, Abecassis, & Micard, 2009; Zou, Sissons, Gidley, Gilbert, & Warren, 2015; Zou, Sissons, Warren, Gidley, & Gilbert, 2016). A lower rate and degree of *in vitro* starch hydrolysis in thermogels of whey protein/wheat starch (Yang, Luan, Ashton, Gorczyca, & Kasapis, 2014) and whey protein/chitosan/wheat starch (Yang, Ashton, & Kasapis, 2015) has also been observed. Hence, protein gels appear as interesting matrices to encase starch and modulate its digestibility. In addition, they may help reducing overeating by increasing satiation and satiety (Bellissimo & Akhavan, 2015; Benelam, 2009; Campbell, Wagoner, & Foegeding, 2017) and mimic some of the organoleptic attributes of fat and carbohydrates (Chung, Degner, & McClements, 2013).

Whey proteins are known to form gels by different mechanisms, among them, cold gelation (Brodkorb, Croguennec, Bouhallab, & Kehoein, 2016). Currently, cold-set whey protein gels have been used to enhance the bioavailability of heat-sensitive bioactive molecules and micronutrients (Abaee, Madadlou, & Saboury, 2017), to modulate lipid digestion (Guo, Bellissimo, & Rousseau, 2017; Guo, Ye, Lad, Dalgleish, & Singh, 2014, 2016) and to create new food textures (Chung, Degner, & McClements, 2013). In cold gelation, native starch can be embedded in a whey protein network while avoiding starch gelatinization until further processing. Additionally, whey proteins have been shown to reduce postprandial glycemia in patients with type 2 diabetes by stimulating secretion of insulin and incretins as well as by delaying gastric emptying (Almario, Buchan, Rocke, & Karakas, 2017; Mignone, Wu, Horowitz, & Rayner, 2015). Starch digestibility in food matrices has been traditionally assessed by an *in vitro* enzymatic method developed by Englyst, Englyst, Hudson, Cole, & Cummings (1999). This approach evaluates the amounts of glucose likely to be available for rapid and slow absorption in the human small intestine and is useful to estimate the future glycemic response of a food. However, a standardized *in vitro* digestion method for food was recently developed by the European INFOGEST network (Minekus et al., 2014). This

group of experts described a static model, easy to set up and apply, aiming at harmonizing the protocols simulating human digestion so that results among studies could be compared worldwide. Since its publication, the harmonized INFOGEST *in vitro* method has been used to study starch digestibility in various food matrices like pasta (Liu et al., 2016), bean paste (Sęczyk, Świeca, & Gawlik-Dziki, 2015), black rice (Bae, Jun, Lee, & Lee, 2016) and chickpeas (Ercan & El, 2016), among others.

The objective of this study was to evaluate if whey protein isolate (WPI) networks formed by cold gelation were able to restrict the *in vitro* digestibility of potato starch (PS) after heat treatment. Indeed, through cold gelation native starch can be entrapped in a whey protein gel while avoiding gelatinization until further processing, different from thermal gelation where the formation of the protein network occurs after starch gelatinization (Aguilera & Baffico, 1997; Aguilera & Rojas, 1997; Chung, Degner, & McClements, 2013b; Yang et al., 2014). The hypothesis of this study is that a protein gel can protect gelatinized starch granules from enzymatic attack during digestion. *In vitro* starch digestibility was investigated using the harmonized INFOGEST protocol (Minekus et al., 2014) and the impact of particle size and protein concentration on PS digestibility were assessed. A better understanding of starch digestion in soft protein gels will be helpful for the design of low-calorie and/or satiety-inducing foods with controlled postprandial glycemic responses.

## 2. Materials and methods

### 2.1. Materials

BiPro® whey protein isolate (WPI) with a moisture content of 4.6% and a protein content of 97.7% (d.b.) was purchased from Davisco (Davisco Foods Intl., MN, USA) and native potato starch (PS), composed of approx. 20% amylose and 80% amylopectin,

with a moisture content of approx. 20% and a carbohydrate content of 99.6% (d.b.) was from a local supermarket (Santiago, Chile).

The enzymes α-amylase (A9857, activity ≥ 150 units/mg) from *Aspergillus oryzae*, pepsin (P7000, activity ≥ 250 units/mg) from porcine gastric mucosa, pancreatine (P1750, activity 4 x USP) from porcine pancreas, invertase (I4504, activity ≥ 300 units/ mg) from baker's yeast and bile porcine extract (B8631) were obtained from Sigma-Aldrich (Sigma Chemical Co., St. Louis, MO, USA), as well as the glucose oxidase/peroxidase enzymatic glucose assay kits (GAGO20). Amyloglucosidase (E-AMGDF, activity 3260 U/mL) from *Aspergillus niger* was purchased from Megazyme International (Megazyme International Co., Wicklow, Ireland). All other chemicals were standard analytical grade and distilled water was used for the preparation of all mixtures.

**2.2. Sample preparation**

Composite gels of WPI and PS were prepared by cold gelation. A solution of 11% (w/w) native WPI in distilled water (pH of the solution = 6.8) was heated in a water bath at 80°C for 30 min, in order to obtain a dispersion of protein aggregates. After cooling for 30 min in a water bath at 20°C, the solution was diluted with distilled water to reach the protein concentration needed. PS was added to the cold dispersion of WPI aggregates and stirred for 15 min, before the addition of the $CaCl_2$ solution under continuous stirring, in order to obtain a final mixture of 6, 8 or 10% (w/v) WPI, 5% (w/v) PS and $CaCl_2$ 10 mM. These formulations were chosen to avoid starch sedimentation and to produce soft and elastic cold-set gels. For *in vitro* digestion, mechanical properties and cryo-SEM studies, samples were transferred to stoppered glass tubes (cylinders of 15 cm long x 2 cm of diameter). For the measure of thermal properties, 50 mg of each sample was sealed in a 100 μL aluminum pan and for rheological measurement, samples

were cast onto disposable plates of 25 mm in diameter and 1 mm of height. All samples were finally stored overnight at 4°C. Controls were: (1) a 5% (w/v) dispersion of PS in a $CaCl_2$ solution (10 mM); (2) a gel of pure WPI (10%, w/v) with 10 mM $CaCl_2$ and, (3) a blend of ground WPI gel (10% w/v, $CaCl_2$ 10 mM) and a dispersion of PS (5% w/v), having the same final total solids content as the composite gel of WPI 10% w/v and PS 5% w/v.

### 2.3. Heat treatment

In order to maximize PS gelatinization, gel samples and controls (in glass tubes) were heated in distilled water at 90°C for 30 min and immediately cooled in iced water for 5 min. To obtain the mixture of WPI gel and PS dispersion (control (3)), both preparations were heated separately under the above conditions and mixed after cooling.

### 2.4. *In vitro* digestion

According to Chen, Khandelwal, Liu, & Funami (2013), the projected area of particles in the bolus of a soft food after chewing may vary between ~1 and 6 $mm^2$. Samples with a small particle size (~1 mm or less) were obtained by grinding the gel with a domestic kitchen hand blender as recommend by the INFOGEST network (Minekus et al., 2014) (Braun MultiQuick 5 MQ505, 30 s at velocity no. 1) and sieving (U.S.A. Standard Test Sieve No. 18, 1 mm stainless steel wire mesh, W.S. Tyler, Mentor, OH, USA). Samples with a large particle size were obtained by cutting the gel into cubes (~5 mm sides), according to Guo et al. (2017).

*In vitro* starch digestibility was assessed according to the guidelines of the INFOGEST *in vitro* digestion method (Minekus et al., 2014). This standardized *in vitro* static

protocol comprises three digestion stages: oral, gastric and intestinal phases. For each stage, the composition and pH of the simulated digestive fluids and enzymes activities were carefully reproduced according to Minekus et al. (2014) recommendations.

### 2.4.1. Oral phase (pH 7)

The Simulated Salivary Fluid (SSF) was pre-incubated for 10 min at 37°C. Five grams of the ground or cut samples were mixed in a 50 mL conical falcon tube with 3.5 mL of SSF stock solution, 25 µL of 0.3 M $CaCl_2$ solution, 975 µL of distilled water and 0.5 mL of amylase solution 1500 U/mL (dissolved in SSF) and adjusted to a final volume of 10 mL. The mixture was incubated at 37°C for 2 min in a shaking water bath at 100 rpm. Then the pH of the solution was lowered by adding 0.15 mL of 1 M HCl solution to inactivate the amylase activity.

### 2.4.2. Gastric phase (pH 3)

7.5 mL of Simulated Gastric Fluid (SGF) stock solution, 5 µL of 0.3 M $CaCl_2$ solution, 845 µL of distilled water and 1.6 mL of pepsin solution 25000 U/mL (dissolved in SGF) were added to the oral phase mixture, to a final volume of 20 mL. The mixture was incubated at 37°C for 2 h in a shaking water bath (100 rpm). After this period, the pH of the solution was increased with 0.14 mL of 1 M NaOH solution to inactivate the pepsin activity.

### 2.4.3. Intestinal phase (pH 7)

10 mL of Simulated Intestinal Fluid (SIF) stock solution, 40 µL of 0.3 M $CaCl_2$ solution, 1.32 mL of distilled water, 2.5 mL of 160 mM bile extract, 5 mL of pancreatin solution and 1 mL of invertase solution (both dissolved in SIF) and 65 µL of amyloglucosidase, were added to the previous mixture (after the oral and gastric phase) to a final volume of 40 mL. In this digestion step, the protocol was modified according to Dartois, Singh, Kaur, & Singh (2010) to adjust the enzymatic composition to the specificity of the study of starch digestibility. The pancreatin enzyme/starch (dry weight basis) ratio was 1.3:100 (w/w), the invertase enzyme/starch (dry weight basis) ratio was 1:1000 (w/w) and the amyloglucosidase enzyme/starch (dry weight basis) ratio was 0.26:1 (v/w). The resulting mixture was incubated at 37°C for 1 h in the shaking water bath (100 rpm).

### 2.4.4. Glucose content analysis

For each sample, five different falcon tubes were prepared and withdrawn one by one at different steps and times of the *in vitro* digestion assay: after the oral phase, the gastric phase, and after 15, 30 and 60 min of intestinal digestion. Previous work showed that no further changes occurred after 60 min of intestinal digestion.

The mixture contained in the falcon tube and at the specific digestion step needed, was mixed with four times its volume of absolute ethanol in order to stop the enzymatic hydrolysis and filtered to remove the remaining solid particles. After 30 min, 0.1 mL of the filtered and stirred mixture was incubated with 0.5 mL of amyloglucosidase/invertase in acetate buffer (10 mg invertase, 0.1 mL amyloglucosidase per 10 mL of acetate buffer at pH 5.2) during 30 min at ambient

temperature[33]. This allows the conversion of oligosaccharides to glucose. The resulting aliquot was finally filtered with a Ministart® NML cellulose acetate hydrophilic syringe filter (Sartorius Stedim Biotech GmbH, Goettigen, Germany) and glucose content was analyzed using the glucose oxidase/peroxidase assay kit GAGO20. The results are expressed as milligrams of glucose released per gram of PS. Each measurement was performed in duplicate.

### 2.5. Thermal properties

Samples in hermetically sealed pans were first equilibrated at ambient temperature for one hour. Then, they were heated from 20 to 90°C at 10°C/min, kept at 90°C for 30 min, cooled back to 20°C at 10°C/min and finally heated from 20 to 90°C at 1°C/min with a Mettler Toledo DSC 822 (Mettler-Toledo Inc., Columbus, OH, USA). The equipment was calibrated using indium and a pan containing 50 mg of distilled water was used as a reference. Indeed, previous work (data not shown) showed that when using an empty pan as a reference part of the transitions occurring in this range of temperature was overlaid by the exothermic peak of water evaporation. Resulting thermograms were analyzed with the STARe Thermal Analysis Evaluation software, version 14.0 (Mettler-Toledo Inc., Columbus, OH, USA). Each measurement was performed in triplicate.

### 2.6. Mechanical properties

The mechanical properties of gels after the heat treatment were analyzed by uniaxial compression using a TA.XT2 Texture Analyzer (Texture Technology Corp., Scarsdale, NJ, USA). Cylinders (20 mm diameter x 10 mm height) of gels were compressed with a 75 mm diameter plate at a constant deformation speed of 0.1 mm/s up to fracture or a

final compression strain of 80%. Measurements were conducted at room temperature (ca. 20°C). Two sections of each gel sample were measured and three replications of each treatment were performed. The presented results are the compressive hardness in kPa (i.e., the maximum force divided by the original cross-sectional area) and the fracture strain in %, for each experimental condition.

### 2.7. Rheological properties

For all rheological measurements, a TA Instruments Discovery Hybrid Rheometer HR-3 equipped with an advanced Peltier plate and a solvent trap and evaporation blocker (TA Instruments Corp., New Castle, DE, USA) was used. The solvent trap of the 40 mm top parallel plate was filled with distilled water and the gap size was 1 mm. Temperature sweeps were carried out from 20 to 90°C and from 90 to 20°C with a heating/cooling rate of 1°C/min, at a constant frequency of 1 Hz and a constant strain of 1.0%, which was in the linear viscoelastic region (LVR) for all samples. An axial force of compression of 0.5 N ±0.1 N was used as conditioning to avoid losing contact between the plates and the sample during the test. After this oscillatory temperature ramp, gels were equilibrated for 15 min at 20°C and submitted to an amplitude sweep test in order to measure the rheological properties of the gels after heat treatment. Amplitude sweeps were performed at 20°C at a constant frequency of 1 Hz, between 0.02 and 2000 % strain (γ), measuring 10 points per decade. Each measurement was performed in triplicate. From amplitude sweep curves, the plateau value of G' ($G'_0$) and tan δ were both evaluated at $\gamma = 0.01\%$. The critical strain, corresponding to the LVR of the gels was defined as the value of γ for which G' has dropped to 90% of $G'_0$.

### 2.8. Cryo-SEM

The microstructure of composite gels before and after heat treatment were investigated with cryo-SEM, according to Ong, Dagastine, Kentish, & Gras (2011) with modifications. Composite gels of WPI 10% and PS 5% were selected. A Hitachi SU8000 scanning electron microscope, equipped with a cryo-preparation system and a vacuum transfer device, was used (Hitachi, Ltd, Tokyo, Japan). A piece of the gel was mounted on a copper holder and immersed into a freshly prepared nitrogen slush for 15 s. The frozen sample was then immediately transferred into the cryo-preparation chamber using the vacuum transfer device. The sample was fractured using a chilled scalpel blade in the chamber which was maintained at -120ºC under a high vacuum condition. The sample was then etched at -90ºC for 30 min. No coating was used. Finally, the sample was transferred under vacuum onto a nitrogen gas cooled module, maintained at -110ºC and observed at 2.0 kV.

### 2.9. Statistical analysis

Results correspond to the mean ± standard deviation. Statistical significance of the results was tested using analysis of variance (ANOVA) and differences between group means were analyzed by LSD multiple-range test with a probability level of 0.05 ($p<0.05$). Statistical analysis was carried out with Statgraphics Centurion software, version 17.1.12 (Statpoint Technologies, Inc. Warrenton, VA, USA).

## 3. Results and discussion

### 3.1. Microstructure of the composite gels

After the cold gelation process, native starch granules were homogeneously distributed and embedded in the WPI network (Fig. 1a). The dense structure of native PS was clearly identifiable inside the gel microstructure (Fig. 1b). After heating at 90ºC for 30 min, the microstructure of the composite gel was extensively modified by the gelatinization of PS (Fig. 1c). Swollen starch granules remained encased in the continuous protein matrix and were clearly detached from the network (Fig. 1d). Since no interpenetration of the protein phase and the gelatinized starch was observed by cryo-SEM, mechanical interactions that may exist between the two phases should be limited to the surface of the PS granules. Similar separated microstructures were observed by Yang, Liu, Ashton, Gorczyca, & Kasapis (2013) for wheat starch and Fu & Nakamura (2017) for potato starch, in WPI gels produced by thermal gelation.

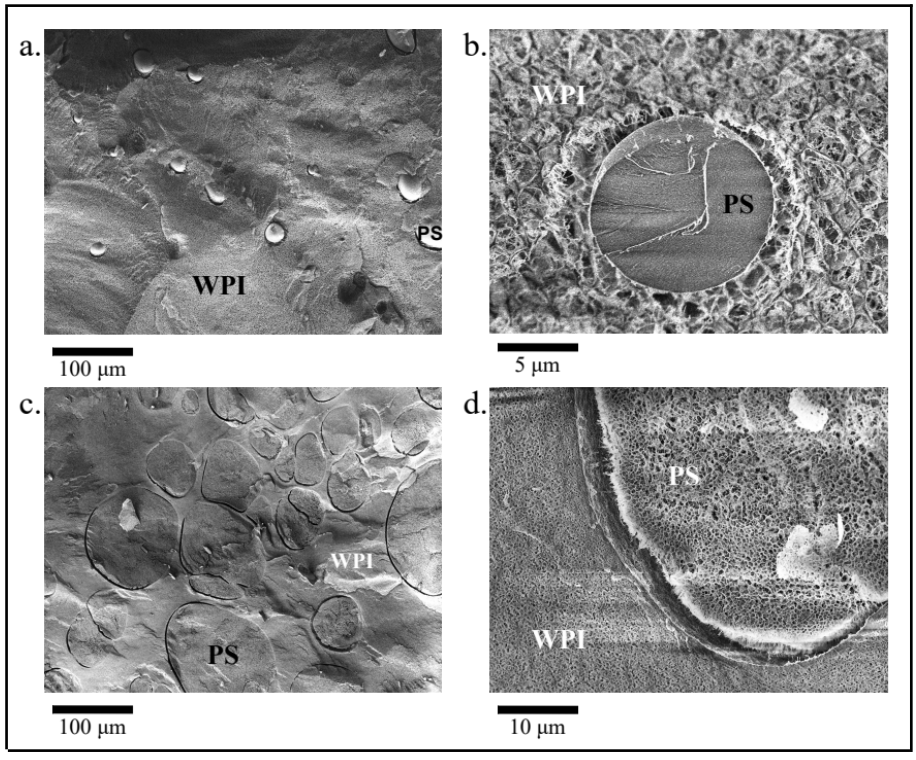


**Figure 1.** Cryo-SEM images of the composite gels before (a, b) and after heat treatment (c, d). On the images, "WPI" indicates the whey protein isolate network and "PS" highlights potato starch granules.

### 3.2. Starch gelatinization inside the protein matrix

Figure 2 shows typical DSC thermograms obtained for the PS dispersion and the composite gels during the first step of the heating program. Mean values for the onset, peak, endset temperatures and the enthalpy change, attributed to PS gelatinization, are summarized in Table 1.

| | T onset (°C) | T peak (°C) | T endset (°C) | ΔH (J/g) |
|---|---|---|---|---|
| 6% composite gel | 62.8 ±0.6 [a] | 68.8 ±0.4 [a] | 74.1 ±0.1 [a] | 13.7 ±1.8 [a] |
| 8% composite gel | 62.1 ±1.1 [a] | 68.3 ±0.5 [a] | 74.3 ±0.4 [a] | 13.2 ±0.2 [a] |
| 10% composite gel | 63.5 ±0.6 [a] | 69.1 ±0.5 [a] | 74.5 ±0.6 [a] | 16.2 ±4.5 [a] |
| PS dispersion | 59.1 ±0.1 [b] | 63.9 ±0.2 [b] | 68.9 ±1.3 [b] | 13.5 ±1.0 [a] |

**Table 1.** Potato starch (PS) gelatinization inside the whey protein isolate (WPI) matrix assessed by DSC. Same letter as superscript indicates that differences are not statistically significant in the same column.

Gelatinization of the PS dispersion occurred between 59 and 69°C, with an endothermic peak at 64°C. The enthalpy of gelatinization (ΔH) was 13.5 ± 1 J/g. These results are consistent with thermal properties reported in the literature for native PS (Alvani, Qi, & Tester, 2012; Alvani, Qi, Tester, & Snape, 2011; Cai, Cai, Zhao, & Wei, 2014; Li & Yeh, 2001; Muñoz, Pedreschi, Leiva, & Aguilera, 2015; Parada & Aguilera, 2012; Ratnayake & Jackson, 2009). In the three composite gels, PS gelatinization was delayed by ~ 4°C under the same experimental conditions. This delay may be due to a strong interaction between the hydroxyl groups of whey protein molecules and water, which may lead to higher energy requirements for the transition to take place, as was observed in starch-water-carregeenan systems (Matignon et al., 2014; Molina, Leiva, & Bouchon, 2016). However, ΔH of starch gelatinization was not modified by the presence of the protein network, regardless of the protein concentration. After the isothermic step at 90°C for 30 min, no transition was measured when samples were reheated from 20 to 90°C at 1°C/min, meaning that no further gelatinization occurred. Thus, it appears that the presence of the whey protein network did not influence the extent of starch

gelatinization. The reduction in starch hydrolysis *in vitro* was probably not related to differences in PS gelatinization.

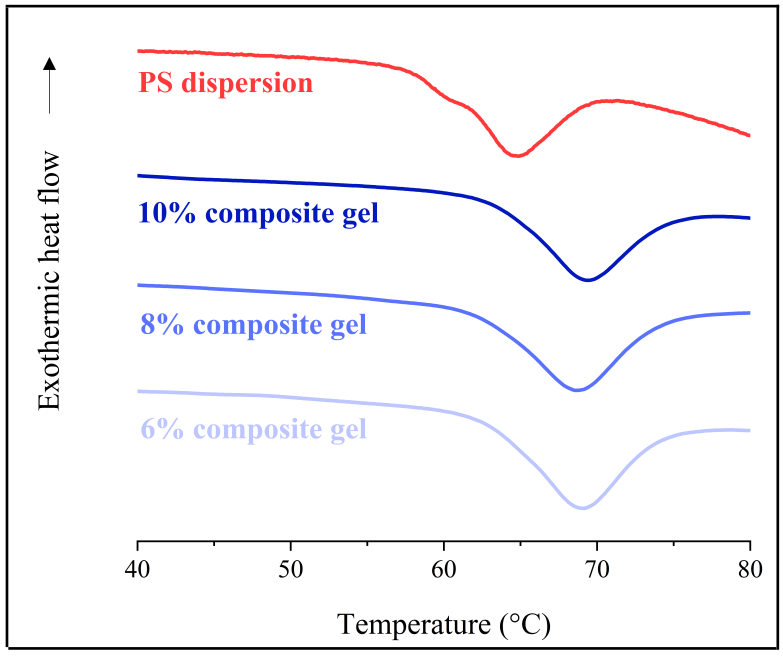


**Figure 2.** DSC thermograms for the composite gels during the first step of heating (scan rate: 10°C/min). To facilitate comparison, the individual traces have been displaced vertically by arbitrary amounts.

### 3.3. *In vitro* digestibility of starch inside the protein matrix

Results obtained at each step of the *in vitro* procedure (oral, gastric and intestinal), for each particle size and protein concentration, are detailed below.

### 3.3.1. Oral step

After the oral step, the glucose released from the PS paste was 19.4 mg/g of PS and significantly different from all samples containing WPI, except for the composite gel 10% WPI, 1 mm (Fig. 3). In the case of the composite gels, glucose released averaged 16.8 mg/g of PS for particle size 1 mm, and 14.6 mg/g of PS for size 5 mm (Fig. 3). When no matrix was formed (i.e., the mixture of the WPI gel and the PS paste), glucose released was 17.4 mg/g of PS. Thus, during the oral step, the digestibility of PS is slightly reduced when protein is present, which may be related to a lower enzyme to total solids ratio.

As shown in Figure 1d, the dense structure of native PS granules was lost after heat treatment, making them porous and more susceptible to enzymatic attack. Size reduction of the gels, either by grinding (particle size 1 mm) or cutting (particle size 5 mm) ruptured the gel structure. The high shear during grinding certainly resulted in a greater release of PS from the matrix compared to the gentle cutting of the gel into cubes, which retained most of the starch within the gel matrix. In addition, possible cracks in the microstructure may have fostered the accessibility of α-amylase to the interior of the particles.

Numerous *in vitro* carbohydrate digestion methods exist for analyzing the glycemic properties of foods and complicate comparisons between studies. As a matter of fact, differences in the time of simulated gastric digestion, in the method used to mimic chewing, in the choice of amylolytic enzyme, in pH or in stirring mode, have a substantial influence on the results obtained (Woolnough, Monro, Brennan, & Bird, 2008). Most importantly, the oral digestion step is often neglected in studies on starch digestibility. After 2 min of oral digestion *in vitro*, a significant amount of glucose was released from all samples (Fig. 3), supporting that this first step of the human digestion process should not be omitted in simulated *in vitro* studies. Hoebler et al. (1998) also

reported that even during only 20 to 30 s of oral food processing, approximately 25% of the starch in spaghetti and 50% of the starch in bread were already hydrolyzed. Similarly, it was demonstrated that α-amylase from saliva played an important role in the breakdown kinetics of bread boluses in *in vitro* models (Bornhorst & Singh, 2013) and that between 25 and 50% of the starch in bread and pasta boluses were hydrolyzed by salivary α-amylase *in vivo* (Jourdren et al., 2016). Moreover, Tamura, Okazaki, Kumagai, & Ogawa (2017) pointed out that the digestion rate of starch in cooked rice grains during the intestinal phase was influenced by changes which occurred during the previous oral digestion step.

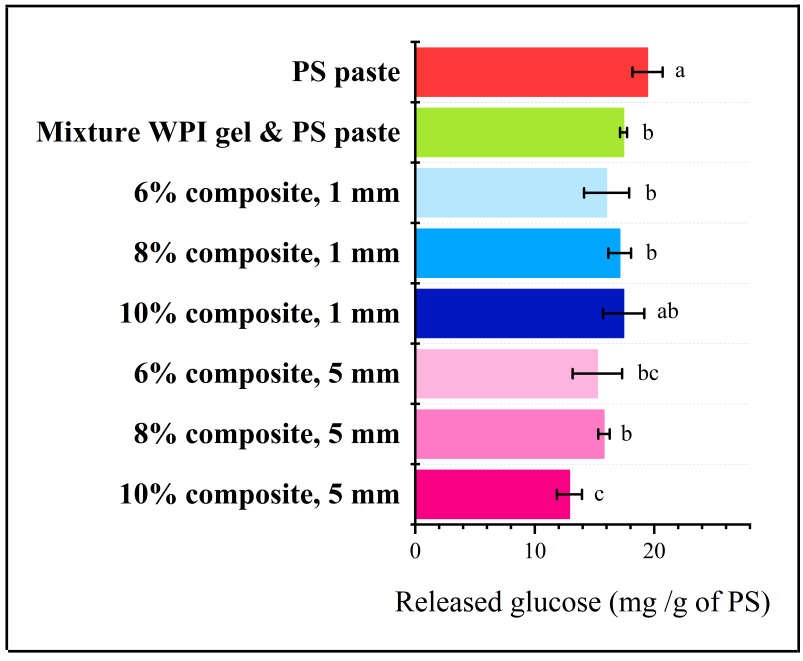


**Figure 3.** Starch digestibility after the oral step of digestion in vitro. Same letter on the graph indicates that differences are not statistically significant.

### 3.3.2. Gastric step

Glucose released after the gastric step of the *in vitro* digestion was lower when the protein matrix was present as compared to the control PS paste (Fig. 4). The amount of glucose released was reduced between 29.2% and 38.6% for all WPI concentrations and particle sizes. But when no matrix was formed around PS granules no significant difference in glucose release was observed with the control sample of PS paste. So, at this step, the protein network prevented the release of the gelatinized PS trapped inside the matrix, regardless of particle size or protein concentration. Even after 2 h under simulated gastric conditions, the WPI gel was not significantly affected and the barrier effect of the protein matrix was effective.

Besides gluten, other proteins (exogenous or not) may form a matrix around starch granules during thermal processing of foods. Recently, Oñate Narciso & Brennan (2018) showed, with an enzymatic assay including pepsin and pancreatin, that fortification of glutinous rice starch with whey protein concentrate or with pea protein modified starch digestibility *in vitro* after cooking. Using the enzymatic method developed by Englyst et al. (1999), López-Barón, Gu, Vasanthan, & Hoover (2017) also observed that the addition of denatured and/or hydrolyzed plant proteins (pea, rice and soybean) significantly delayed starch hydrolysis in cooked wheat starch-protein mixtures. Similarly, Chen et al. (2017) reported that the addition of soy protein delayed the *in vitro* digestion of gelatinized corn starch in the stomach. With regard to PS, Lu, Donner, Yada, & Liu (2016) observed a reduction in starch digestibility in PS/potato protein processed blends, using the Englyst method (Englyst et al., 1999).

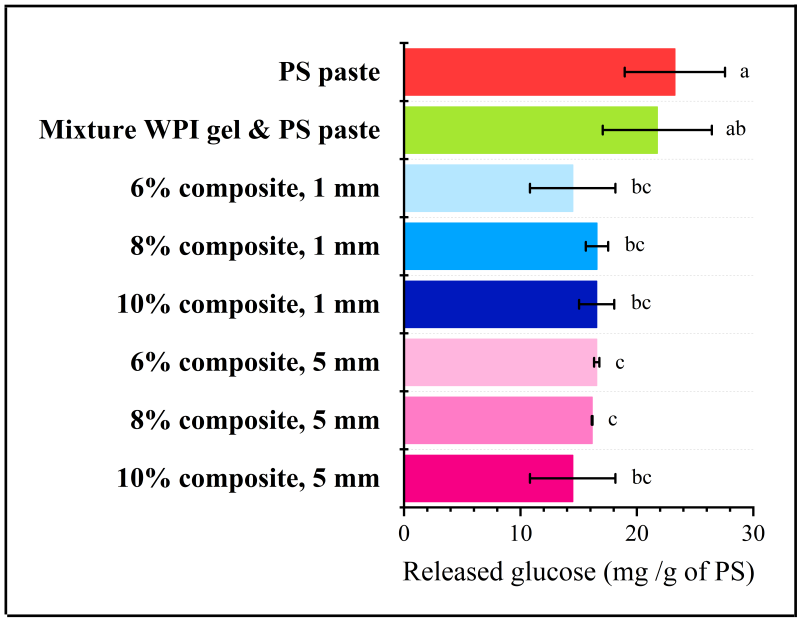


**Figure 4.** Starch digestibility after the gastric step of the digestion *in vitro*. Same letter on the graph indicates that differences are not statistically significant.

### 3.3.3. Intestinal step

After 15 min of intestinal digestion *in vitro,* glucose release was significantly reduced for composite gels with a particle size of 5 mm, compared to the PS paste (Fig. 5). Regarding the other experimental conditions, no significant differences were observed with the control sample. Furthermore, as for the PS paste, glucose release from the system already reached a maximum, that is, no further significant changes were measured after 30 and 60 min of intestinal digestion.

For composite gels with a particle size of 5 mm, glucose release was inversely related to the protein concentration of the gel, i.e., glucose values increased when protein concentration decreased. The same trend was observed after 30 and 60 min of intestinal digestion *in vitro* (Fig. 5). Hence, enzymatic attack to starch granules hidden inside the gel pieces was hindered by the protein network. As stated by Aguilera (2018), the digestion of solid matrices in the gut depends largely on their breakdown into small particles, the particle size and surface area, and the nature of these surfaces. A clear negative correlation between particle size and starch digestibility has been observed in cereals (Al-Rabadi, Gilbert, & Gidley, 2009; Farooq et al., 2018; Heaton, Marcus, Emmett, & Bolton, 1988; Mahasukhonthachat, Sopade, & Gidley, 2010; Mandalari et al., 2018; Ranawana, Monro, Mishra, & Henry, 2010), peas (Nguyen, Gidley, & Sopade, 2015; Tinus, Damour, Van Riel, & Sopade, 2012) and sweet potato (G. Chen & Sopade, 2013). However, the effect of particle size on starch digestibility in starch-based products is not well understood yet. On one hand, Colona et al. (1990) reported that grinding cooked spaghetti increases enzyme susceptibility of starch granules compared to intact spaghetti and Granfeldt & Björck (1991) confirmed that grinding increases significantly the glycemic index (from 61 to 73). On the other hand, Ranawana, Henry, & Pratt (2010) concluded that the degree of mechanical breakdown during mastication does not influence starch digestibility in spaghetti. Alam et al. (2017) reached the same

conclusion about brittle cereal foams and Nordlund, Katina, Mykkänen, & Poutanen (2016) observed a relation between particle size of masticated breads and the insulin response but not with the postprandial glucose. It should be noted that there are major differences between most of these works and our study: the protein network is generally gluten, foods have a lower moisture content than the gels, and they have a higher ratio of starch to protein. Starch digestibility in model composite gels formed by cold gelation of proteins have not been systematically investigated despite their potential application as soft food matrices (Chung et al., 2013).

After 30 min of intestinal digestion, starch hydrolysis was still reduced compared to the control sample for composite gels made with 8 and 10% WPI (particle size 5 mm). At this point, the maximum glucose release had been reached for all experimental conditions and similar results were observed after 60 min of intestinal digestion (Fig. 5).

So, at the end of the digestion protocol, starch digestibility *in vitro* was significantly reduced in composite gels with 10 and 8% WPI (-20.5% and -15.5%, respectively) when particle size was 5 mm (Fig. 5). Therefore, upon further intestinal digestion, protection of starch against enzymatic attack by the WPI network depended on the protein concentration. This means that the microstructure of the network has to be carefully considered in order to efficiently reduce starch digestibility. Microstructural differences in the matrix induced by the protein concentration (Luo, Boom, & Janssen, 2015) or salt levels (Yang et al., 2014) may have a significant effect on the disintegration of the WPI gelled structure. Also, in low cross-linked networks, the matrix might be too loose to reduce starch hydrolysis by a barrier effect, while in highly aggregated networks large pores might form, making the system more susceptible to α-amylase attack (Yang et al., 2014).

Molecular diffusion in polymer gels depends strongly on the network structure (Tokita, 2016). As may be deducted from Fig. 1d, the tortuosity of the WPI network around PS granules may lengthen the path for enzymes, leading to a barrier effect of the protein

matrix (Fardet et al., 1998). It is therefore expected that enzyme diffusion, and consequently glucose release from the matrix, should be negatively correlated with the protein network density.

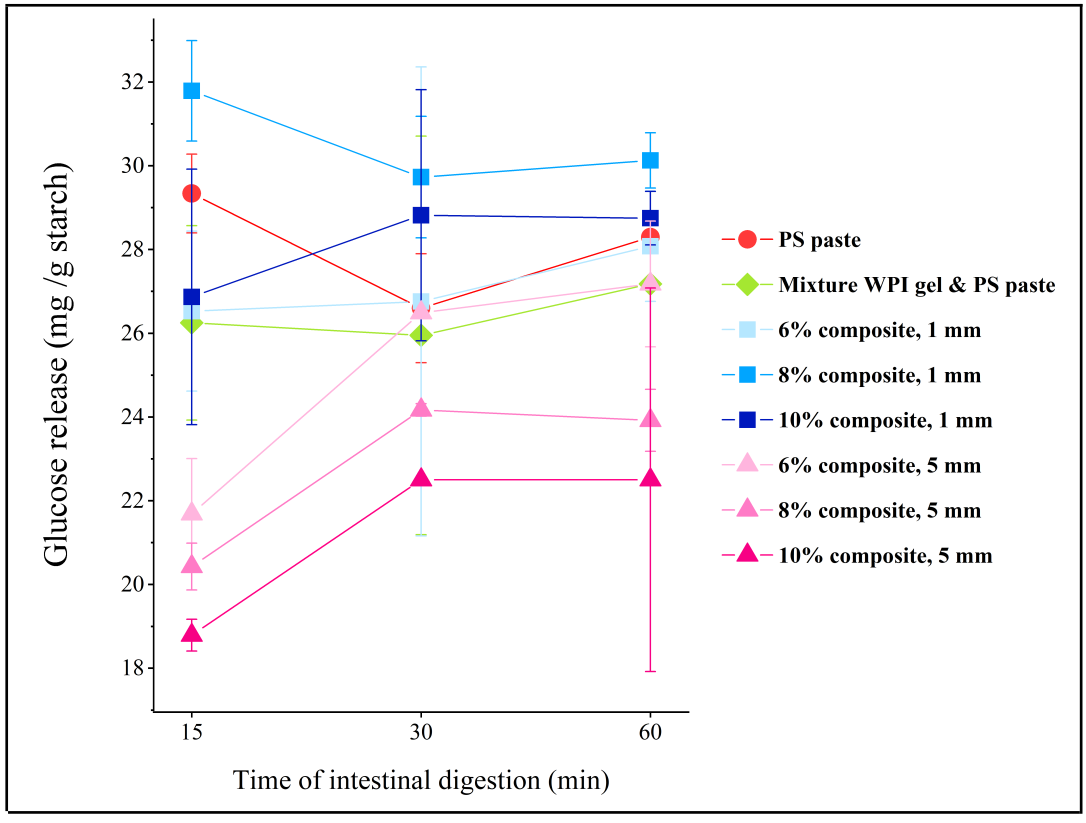


**Figure 5.** Starch digestibility during the intestinal step of the digestion *in vitro* (after 15 min, 30 min and 60 min).

### 3.4. Mechanical and rheological properties related to *in vitro* digestion

The study of the microstructure of the composite gels after heat treatment, through the study of their rheological and mechanical properties, may also give us some clue as to

their susceptibility to α-amylase attack. Guo et al. (2017) observed that the manipulation of gel strength and microstructure modified the extent and rate of lipid digestion in WPI emulsion gels. In this case, harder gels better retained their structure during *in vitro* digestion and were more efficient in delaying lipolysis (Guo et al., 2016).

No significant difference in gel hardness was observed between a pure 10% WPI gel and the 10% WPI composite gel (hardness of 154 ±16 kPa and 174 ±11 kPa, respectively, Table 2) after heat treatment. So, in this case the hardness of the protein gel was not significantly modified by the addition of PS (5% w/v). This is in accordance with the microstructure exhibited in Figure 1d. which shows that the continuous protein matrix was detached from the gelatinized starch granules, hence, responsible for taking the load in the compression test.

Regarding WPI concentrations in the composite gels, no significant difference in gel hardness was measured between composite gels made of 8 and 10% WPI (187 ±11 kPa and 174 ±11 kPa, respectively). However, the composite gel made of 6% WPI was significantly softer (hardness of 125 ± 13 kPa). Fracture strain was ~ 58% for all samples, so, failure was not significantly influenced by the composition of the gels.

| | Hardness (kPa) | Fracture strain (%) |
|---|---|---|
| 6% composite gel | 125 ± 13 [a] | 57.7 ± 1.8 [a] |
| 8% composite gel | 187 ± 11 [b] | 56.8 ± 1.3 [a] |
| 10% composite gel | 174 ± 11 [b] | 54.9 ± 2.0 [a] |
| 10% pure WPI gel | 154 ± 16 [b,c] | 60.9 ± 1.4 [a] |

**Table 2.** Mechanical properties of the composite gels. Same letter as superscript indicates that differences are not statistically significant in the same column.

In addition to the study of the mechanical properties of the composite gels, rheological measurements were performed to indirectly observe the microstructure of the WPI and PS gels after heat treatment. As shown in Figure 6, all samples behaved as viscoelastic gels with dominating elastic properties, i.e., the storage modulus G' was higher than the loss modulus G'' (tan $\delta$ <1) in the LVR. Above a certain strain value (i.e., 2-4%), all samples showed a shear thinning behavior probably due to the successive breakdown of the WPI particle gel. $G'_0$, the plateau value of G' in the LVR, was 45.1 ±1.5 kPa, 86.2 ±7.0 kPa and 112.1 ±25.1 kPa for the composite gels made of 6, 8 and 10% WPI, respectively. So, $G'_0$ increased with the increasing protein content, suggesting that more crosslinks were formed when a higher concentration of WPI was used, resulting in a denser and more complex network (Rao, 2007). Alting, Hamer, De Kruif, & Visschers (2003) also observed an increase in the storage modulus plateau value of cold-set gels with increasing whey protein concentration. No significant differences in the extension of the LVR were observed between the three composite gels: the critical strains measured were 2.3 ±1.7 %, 3.1 ±1.8 % and 1.6 ±0.6 % for the composite gels made of 6, 8 and 10% WPI, respectively.

The addition of PS did not influence significantly the storage modulus of the protein gel ($G'_0$ = 107.1 ±3.5 kPa for the pure 10% WPI gel) but slightly extended the LVR (critical strain of 0.5 ±0.1 % for the control gel). This is also in accordance with the microstructure shown in Figure 1d., i.e., starch granules acted as inactive fillers and did not interact with each other or with the protein network. According to these results, gel strength and microstructure were related to starch digestibility. More elastic gels, with a denser microstructure (8 and 10% WPI) protected better PS granules from the enzymatic attack than the less elastic gel (6% WPI), during the intestinal step of the simulated digestion (particle size 5 mm) (Fig. 5). The gastric and intestinal phases both involve the action of proteases that are able to degrade the whey protein network. Throughout the digestion process, the microstructure of the surface of the gel is loosened which in turn accelerate the diffusion of proteases and will eventually lead to

the disintegration of the gel (Luo et al., 2015). Consequently, the progressive softening and breakdown of the network by proteases will expose more PS granules to starch-degrading enzymes as the digestion moves forward, as evidenced in Figure 5. It is then expected that a denser microstructure will have a slower rate of protein hydrolysis which will result in a slower rate of starch hydrolysis. And indeed, the results of this study show that the final amount of glucose released from the matrix, as well as the starch hydrolysis rate during the intestinal step of the digestion, depended on the concentration in WPI of the gels (Fig. 5). Luo et al. (2015) measured a slower proteolysis rate of WPI gels when the protein concentration was increased from 15 to 20 wt% and concluded that WPI gel digestion was determined by the summed effect of enzyme diffusion limitation, hydrolysis rate and microstructure transformation. Also, Macierzanka et al. (2012) showed that particulate gels resisted better the proteolysis than fine stranded gels. However, Opazo-Navarrete, Altenburg, Boom, & Janssen (2018) did not found a correlation between the microstructure, the hardness and the rate of proteolysis in WPI gels.

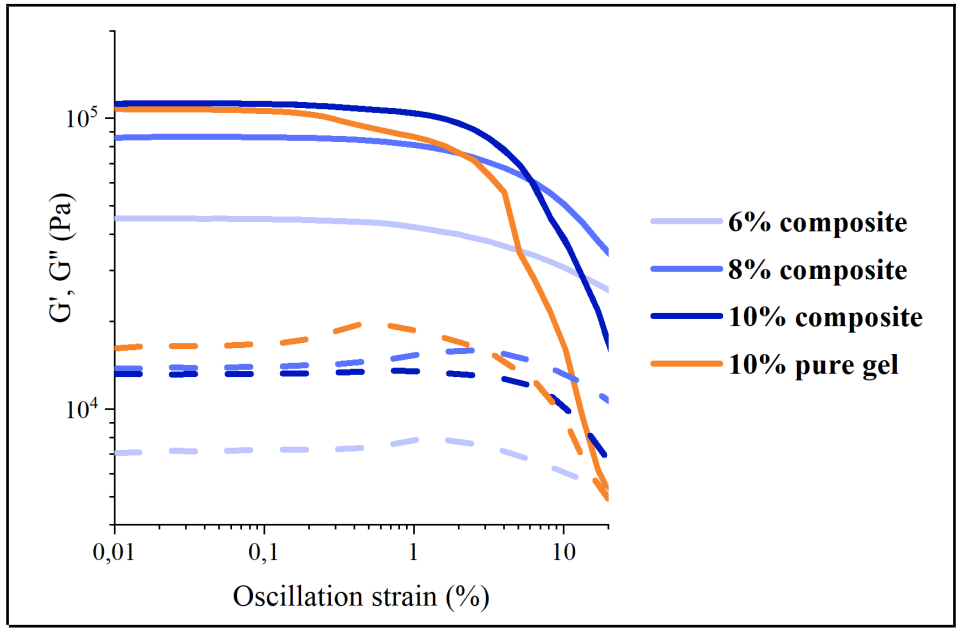

**Figure 6.** Amplitude sweep curves of composite gels after heat treatment. Lines represent the storage modulus G' and dashes represent the loss modulus G''. Error bars are not shown for the sake of clarity.

Structure and material properties have a significant impact on the rate and extent of food breakdown and release of nutrients in the mouth and the stomach (Singh, Ye, & Ferrua, 2015). Rheological and mechanical properties of the gels may be relevant not only to control starch digestibility *in vivo* but also do design specific food textures. Food hardness has a direct influence on the breakdown in the mouth: the harder the food, the smaller the bolus particle size (Chen et al., 2013). For example, heat-set whey protein emulsion gels with increasing hardness led to median particle sizes from 4 to 0.95 mm, respectively, after mastication (Guo, Ye, Lad, Dalgleish, & Singh, 2013). Then, food particle size and hardness also influence gastric emptying. The rate of disintegration in the stomach generally decreases with the increase of food hardness (Singh et al., 2015). According to the results of this study, the negative correlation between digestibility and hardness may restrict the use of whey protein encasing of starch granules to foods with a rather "strong" and "chewy" texture. In addition, the breakdown patterns in the mouth and the stomach of the composite cold-set gels should be carefully considered since particle size was a determinant factor for starch digestibility reduction *in vitro*.

The main factors affecting the digestibility of starch in a whey protein network formed by cold gelation are summarized in Figure 7.

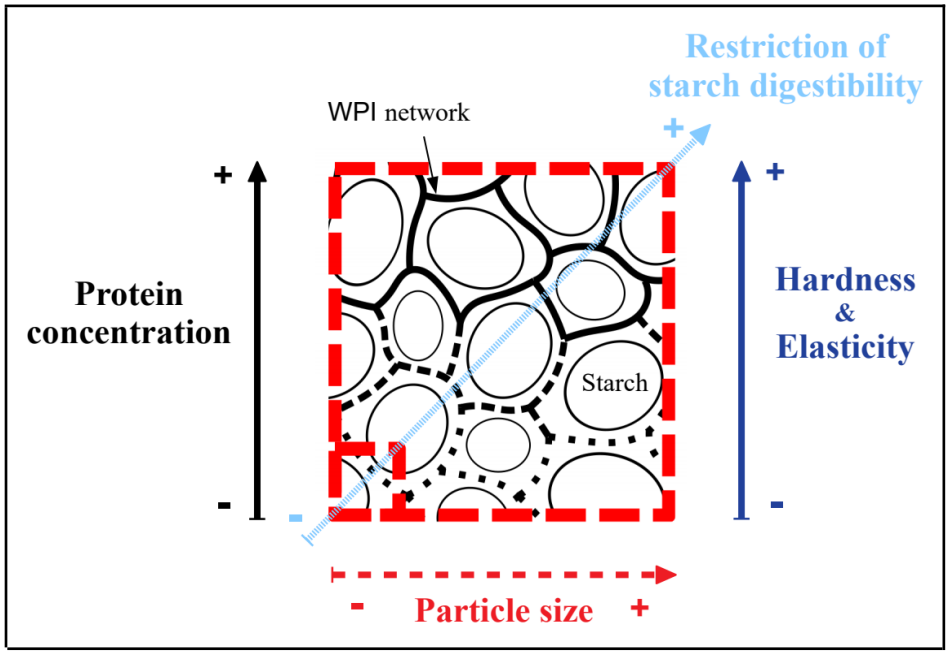


**Figure 7.** Scheme representing parameters influencing starch digestibility in a WPI cold-set gel matrix.

## 4. Conclusions

WPI networks formed by cold gelation restricted the *in vitro* digestibility of PS after heat treatment as measured by glucose release using a three-stage digestion assay. This effect first depended on particle size reduction of the gels. Gels with a particle size of ~ 1 mm protected PS from enzymatic attack until the intestinal step of the simulated digestion, while gels with a particle size ~ 5 mm were a barrier for starch-degrading

enzymes until the end of the digestion protocol. Then, glucose release from the matrix depended on WPI concentration in the gels. At the end of the digestion, PS hydrolysis was reduced by 20.5 and 15.5% for composite gels with 10 and 8% WPI respectively (particle size 5 mm), whereas no significant reduction was observed for the gel with 6% WPI. Moreover, mechanical and rheological properties of the gels were related to starch digestibility. The rate of PS hydrolysis decreased with increasing hardness and elasticity of the gels. Therefore, the microstructure of the protein network also has to be carefully considered to modulate starch digestibility in such composite gels. This work contributes to a better understanding of starch digestion in soft food matrices. The use of whey protein gels appears as an interesting strategy to design low-calorie food products with a slower postprandial release of glucose from gelatinized starch. In future work, the breakdown properties of WPI and PS cold-set gels in the human mouth and stomach will be investigated.

# CHAPTER 3: Impact of heating on the properties of a whey protein cold-set gel

## 1. Introduction

Whey proteins are by-products of cheese manufacture used as functional foods in sports nutrition, as dietary supplements for the elderly and as functional ingredients for the food industry (e.g., in emulsions, foams, gels and fat reduced products) (Smithers, 2015).

The main components of whey proteins in bovine milk are the globular proteins β-lactoglobulin (β-lg) which represents more than 50% of the total proteins, and α-lactalbumin (α-la) ca. 20%. The gelling properties of whey proteins are mainly related to the β-lg (Havea, Singh, & Creamer, 2001).

The native β-lg is made of a sequence of 178 amino acids, including a signal peptide of 16 residues, and contains seven cysteine residues. Two of them are on the signal peptide, four others form disulfide bridges, between $Cys^{82}$ and $Cys^{176}$ (near the C-terminus) and between $Cys^{122}$ and $Cys^{135}$ (in the interior of the molecule), while the last one, $Cys^{137}$, is a free thiol group (The UniProt Consortium, 2019). The secondary structure of β-lg consists of about 8% α-helix, 45% β-sheet and 47% random coil. This structure is organized as strands of anti-parallel β-sheet and forms a hydrophobic barrel (The UniProt Consortium, 2019). At room temperature and neutral pH, native β-lg exists as a dimer of two non-covalently linked monomeric molecules.

Upon heating, dimer dissociation occurs first (between 30 and 55°C), followed by reversible partial unfolding (above 60°C) (Cheison & Kulozik, 2017). In this molten globule state, the free thiol group and part of the hydrophobic groups that were previously buried inside the globular structure are exposed and therefore available for reaction (Bryant & Julian McClements, 1998). Further heating leads to irreversible

aggregation of β-lg, mainly through intermolecular disulfide cross-linking (Hoffmann & Van Mil, 1997). Hydrophobic non-covalent interactions are also involved in heat-induced aggregation of β-lg and seem to contribute to the stabilization of the protein aggregates after cooling (Nguyen, Wong, Guyomarc'h, Havea, & Anema, 2014).

Native α-la consists of 142 amino acids, with a signal peptide of 19 residues and contains eight cysteines, all involved in disulphide bonds (The UniProt Consortium, 2019). The secondary structure of α-la is composed of 26% α-helix, 14% β-sheet and 60% of unordered structures (The UniProt Consortium, 2019). Native α-la exists as Ca-depleted (apo-) or Ca-bound (holo-) forms. The holo form of the protein, which is most often found in bovine milk, has a compact ellipsoidal structure and does not aggregate when heated alone in water at neutral pH (Nielsen, Lund, Davies, Nielsen, & Nielsen, 2018). However, when α-la and β-lg are heated together, the free thiol group on the unfolded β-lg acts as an initiator for thiol-disulphide exchange reactions and α-la also forms irreversible aggregates (homopolymers and heteropolymers with β-lg) (Havea et al., 2001).

Whey proteins are known to form gels by heating dispersions over 70°C and above a critical protein concentration (Aguilera, 1995). Through controlled heat-treatment, stable soluble aggregates of whey protein can be formed. Their morphology and size vary with pH, ionic strength, type of salt and protein concentration (Nicolai & Durand, 2013). At pH 7 and low ionic strength, whey protein heat-induced aggregates are described as flexible strands (Jung, Savin, Pouzot, Schmitt, & Mezzenga, 2008) that subsequently associate into larger randomly branched aggregates (or flocs) when the protein concentration is increased (Ikeda & Morris, 2002). Gelation can then be induced by reducing the electrostatic repulsion between the whey protein aggregates, either by adding a salt like NaCl or $CaCl_2$ (Marangoni, Barbut, McGauley, Marcone, & Narine, 2000) or by decreasing the pH (Alting, De Jongh, Visschers, & Simons, 2002). This

two-step process – heat-induced aggregation followed by association of aggregates at ambient temperature – is known as cold gelation.

Cold gelation induced by $CaCl_2$ leads to the formation of a particulate gel with a fractal dimension of ~ 1.7 to 2.6 depending on the salt concentration (Andoyo, Lestari, Mardawati, & Nurhadi, 2018; Hongsprabhas, 1997, Hongsprabhas, & Barbut, 1997b). The effect of salt type and concentration on the microstructure of the network and on the properties of whey protein gels prepared by cold gelation have been extensively studied (Brodkorb et al., 2016). However, little is known about changes induced by additional heat treatment on cold-set whey protein gels, although heating is common during cooking, industrial food processing and pasteurization. Hongsprabhas & Barbut (1997a) reported that when cold-set whey proteins gels induced by calcium were heated at 80°C for 30 min, the opacity, fracture properties and water holding capacity of the final gels were modified. They suggested that these changes in the characteristics of the gels were related to further aggregation of the proteins during heating, either through hydrophobic interactions or chemical reactions. Similarly, in previous work on composite cold-set gels made of whey proteins and potato starch, we observed that the rheological and mechanical properties of the protein gel were altered by heat treatment above 85°C (Lavoisier & Aguilera, 2019).

The objective of this study was to investigate the impact of heating to 90°C on the microstructure and properties of a model gel of whey protein isolate (WPI) prepared by cold gelation with calcium. This model system was also modified by the addition of free cysteine residues (Cys), in order to better understand the changes occurring at the molecular level during heating of cold-set whey protein gels. The hypothesis of this work was that heating induces a rearrangement of the network structure, driven by an increase in intermolecular interactions (additional disulfide bonds and hydrophobic interactions).

## 2. Material and methods

### 2.1. Materials

BiPro® WPI with a moisture content of 4.6% and a protein content of 95% (d.b.) was purchased from Davisco (Davisco Foods International Inc., Le Sueur, MN, USA). According to the manufacturer, the protein content was divided as follow: 50% of β-lactoglobulin, 20% of α-lactalbumin and 30% of other proteins including bovine serum albumin. L-Cys 30089 BioUltra ≥ 98.5% (RT) was from Sigma-Aldrich (Sigma Chemical Co., St. Louis, MO, USA), All other chemicals were standard analytical grade and Milli-Q® water was used for the preparation of all mixtures.

### 2.2. Sample preparation

WPI gels were prepared by cold gelation induced by calcium chloride ($CaCl_2$) addition. First, a dispersion of 10% (w/w) WPI was prepared by stirring the WPI powder in water for 90 min at 600 rpm (pH of the dispersion = 7). This dispersion was then filtered (Minisart syringe filter, hydrophilic, pore size 0.2 µm from Sartorius Stedim Biotech GmbH, Goettingen, Germany) and heated in a circulating water bath at 80°C for 30 min. The sample was cooled to room temperature under running cold tap water for 5 min and 1 mL of a 100 mM $CaCl_2$ aqueous solution was dropped into 9 mL of the WPI dispersion while stirring at 600 rpm. This mixture was then immediately transferred to glass vials (5 mL) for cryo-SEM studies. To measure the thermal properties as well as in the case of ATR-FTIR and CLSM studies, 50 mg of the sample was sealed in a 100 µL aluminum pan. For rheological measurements, the sample was directly cast in a mold fixed on the lower rheometer plate (25 mm in diameter and 1 mm of height). All samples were finally stored overnight at 4°C.

Free Cys were added at two different steps of the cold gelation: before heat induced aggregation of WPI (i.e., before heating at 80°C for 30 min) or before cold gelation of the WPI aggregates (i.e., before $CaCl_2$ addition). In each case, the concentration of Cys added was 2.6 mM. This concentration was chosen to equal the calculated concentration of β-lactoglobulin molecules in the mixture in the experimental conditions described before.

### 2.3. Thermal properties

Samples gelled in the hermetically sealed pans were heated from 20 to 100°C at 1°C/min with a Mettler Toledo DSC 822 (Mettler-Toledo Inc., Columbus, OH, USA). A pan containing 50 mg of water was used as a reference and the equipment was calibrated with indium. Results were analyzed with the STARe Thermal Analysis Evaluation software, version 14.0 (Mettler-Toledo Inc., Columbus, OH, USA). Each measurement was done in triplicate.

### 2.4. Attenuated Total Reflectance Fourier-transformed infrared spectroscopy (ATR-FTIR)

Heat treatment of the gels was performed with the DSC instrument as described before (cf. Section 2.3). The aluminum lid was carefully removed and gel samples were extracted from the pan and directly measured. ATR-FTIR spectroscopy was performed using a Brucker Tensor II instrument, equipped with a Platinum ATR (Brucker Optik GmbH, Ettlingen, Germany). Data were acquired between 4000 and 400 $cm^{-1}$ with a resolution of 4 $cm^{-1}$ and averaging 32 scans for each spectrum. A background spectrum was scanned at the beginning of the measurements using the same instrumental conditions as for the sample spectra acquisition, as well as a water spectrum and a

control spectrum ("native" WPI in water). Samples were first equilibrated at room temperature for one hour. For liquid samples, one drop of the dispersion was added onto the ATR cell. For gels, samples were gently pressed onto the ATR cell by using the integrated pressure application device with a glass slide. The experiments were performed in duplicate.

The water spectrum was used as baseline and the spectrum of the control sample of "native" WPI in water was subtracted from the samples spectra. The study was focused on the Amide I absorption region (1700 to 1600 $cm^{-1}$) in order to investigate changes in the secondary structure of the whey proteins.

**2.5. Rheological properties**

For all rheological measurements, a TA Instruments Discovery Hybrid Rheometer HR-3 equipped with an advanced Peltier plate and a solvent trap and evaporation blocker (TA Instruments Corp., New Castle, DE, USA) was used. The solvent trap of the 40 mm top parallel plate was filled with distilled water and the gap size was 1 mm. Amplitude sweeps were performed at 20°C at a constant frequency of 1 Hz, between 0.02 and 2000 % strain (γ), measuring 20 points per decade. Sandpaper was used on both plates to avoid sample slipping under increasing strain amplitude. Temperature sweeps were carried out from 20 to 50, 60, 70, 80 or 90°C and from 50, 60, 70, 80 or 90 to 20°C with a heating/cooling rate of 1°C/min, at a constant frequency of 1 Hz and a constant strain of 1.0%, which was in the linear viscoelastic region (LVR) for all samples. An axial force of compression of 0.5 N ±0.1 N was used as conditioning to avoid losing contact between the plates and the sample during the test. After this oscillatory temperature ramp, gels were equilibrated for 15 min at 20°C and subjected to an amplitude sweep test in order to measure the rheological properties of the gels after heat treatment. Each measurement was performed in triplicate. From amplitude sweep curves, the plateau

value of G' ($G'_0$) and tan δ were both evaluated at γ = 0.01%. The critical strain, corresponding to the end of the LVR of the gels was defined as the value of γ for which G' had dropped to 90% of $G'_0$. These parameters were evaluated for both amplitude sweep curves before and after heat treatment.

### 2.6. Particle size

Particle size was determined by dynamic light scattering using a Zetasizer Nano ZS90 (Malvern Panalytical, Malvern, UK). Detection was done at a scattering angle of 90° and at 25°C. The WPI dispersion was diluted with distilled water by a factor of 1:1000. Refractive indices of 1.53 for whey proteins and 1.33 for water were used. The particle size distribution of WPI was bimodal, so the results are presented in the form of a graph showing the intensity (%) as a function of the hydrodynamic diameter (nm). The values reported are an average of 10 determinations.

### 2.7. Isothermal Titration Calorimetry (ITC)

ITC experiments were carried out using a MicroCal PEAQ-ITC (Malvern Panalytical, Malvern, UK) with a 200 µL sample cell, a 40 µL titration syringe, 0.4-2.0 µL injection volumes and 150 s interval between injections. The temperature was set at 25°C and the stirring rate at 750 rpm. Measurements were done in triplicate. A $CaCl_2$ solution (100 mM) was titrated into a Cys solution (5 mM). To correct the data by the heat of dilution, the titrant ($CaCl_2$ solution) was titrated into distilled water and the obtained heats were subtracted from the titration of Cys with $CaCl_2$. Raw ITC data are reported (differential power vs. time) where each spike represents the injection of titrant into the cell, as well as the integrated and normalized heat plotted vs. the molar ratio of $CaCl_2$ to Cys. Data

were fit using the MicroCal PEAQ-ITC instrument control software ("One Set of Sites" binding model).

### 2.8. Atomic Force Microscopy (AFM)

For AFM observations, samples were diluted in water to a final protein concentration of approx. $5.10^{-3}$ µg/mL. Then, 10 µL of the diluted sample was deposited onto the surface of a freshly cleaved mica phlogopite disk. For the observation of the "native" WPI in water, the sample was dried with a gentle blow of argon gas after one minute of incubation. For the observation of the other samples, mica disks were first preheated at 70°C in an oven and samples were then air dried in the same oven at 70°C for 5 min. AFM images were obtained with a Park NX20 instrument (Park Systems Corp., Suwon, South Korea) in tapping mode in air. Standard tapping mode AFM cantilevers with Al reflective coating were used (OPUS 160AC-NA, NanoAndMore GmbH, Wetzlar, Germany). Two replicates were prepared and observed for each experimental condition. Images were flattened and horizontal scars were corrected with the open source software Gwyddion (Nečas & Klapetek, 2012). AFM images of fractal aggregates and clusters were binarized with the open source ImageJ software (Schneider, Rasband, & Eliceiri, 2012) and the $D_f$ of each aggregate was analyzed with the fractal box count tool of the software (box sizes 2,3,4,6,8,12,16,32,64 and black background).

### 2.9. Confocal Laser Scanning Microscopy (CLSM)

As described previously, heat treatment of the gels was performed with the DSC instrument (cf. Section 2.3), the lids of the DSC pans were peeled and gels were carefully removed from the pans. A 10 µL drop of Rhodamine B (diluted in water at 0.001%) was placed in the well of a chambered coverglass and the gel sample was

positioned on top of this staining drop. Gels were observed with a Zeiss LSM 880 inverted confocal laser scanning microscope (Carl Zeiss AG, Oberkochen, Germany) with an excitation wavelength of 543 nm. Fluorescence was measured at 565-600 nm and images were acquired with a water immersion objective C-Apochromat 40x/1.2 W (Carl Zeiss AG, Oberkochen, Germany). Three replicates were prepared and observed for each experimental condition. The open source ImageJ software and the image processing package Fiji were used to visualize and process the images (Schindelin et al., 2012). Image processing was the same for all samples: a "despeckle" filter was used first, then contrast was enhanced (saturated pixels 5%) and finally outliers were removed (radius 2 pixels, threshold 50, bright outliers). Processed images were binarized and areas where clear aggregates were visible were selected. $D_f$ of each selected area was determined with the fractal box count tool of the software (box sizes 2,3,4,6,8,12,16,32,64 and black background).

**2.10. Cryo-SEM**

Gelled samples were heated inside the hermetically sealed glass vials at 90°C for 30 min in a water bath and cooled in iced water for 5 min. Then, the microstructure of the gels before and after heat treatment were investigated with cryo-SEM, according to Ong et al. (2011) with modifications. A Hitachi SU8000 scanning electron microscope, equipped with a cryo-preparation system and a vacuum transfer device, was used (Hitachi Ltd, Tokyo, Japan). A piece of the gel was mounted on a copper holder and immersed into a freshly prepared nitrogen slush for 15 s. The frozen sample was then immediately transferred into the cryo-preparation chamber using the vacuum transfer device. The sample was fractured using a chilled scalpel blade in the chamber which was maintained at -120ºC under a high vacuum condition. The sample was then etched at -90ºC for 30 min. No coating was used. Finally, the sample was transferred under

vacuum onto a nitrogen gas cooled module, maintained at -110ºC and observed at 2.0 kV. Two replicates were prepared and observed for each experimental condition.

## 3. Results and discussion

### 3.1. Heat-induced aggregation of whey proteins

Figure 1 shows the changes in the secondary structure of whey proteins after heating at 80°C for 30 min in water at pH 7 determined by ATR-FTIR spectroscopy. Band intensity decreased at 1658 and 1630 $cm^{-1}$, wavelengths associated with α-helices and intramolecular β-sheets, respectively (Grewal, Huppertz, & Vasiljevic, 2018), and increased at 1615 $cm^{-1}$, a wavelength associated to intermolecular β-sheets (Geara, 1999; Lefèvre & Subirade, 1999; Maltais, Remondetto, & Subirade, 2008). Therefore, the heat treatment resulted in interactions between the whey protein molecules, along with a partial loss of their intramolecular structure. Similar changes in the secondary structure of whey proteins were observed by O'Loughlin, Kelly, Murray, Fitzgerald, & Brodkorb, (2015) in BiPro® WPI dispersions (10% w/v) heated from 70 to 90°C in water at pH 7. They suggested that the intermolecular interactions formed upon heating occurred through hydrophobic bonding at the β-lg dimer surface (I strand; $His^{146}$-$Ser^{150}$).

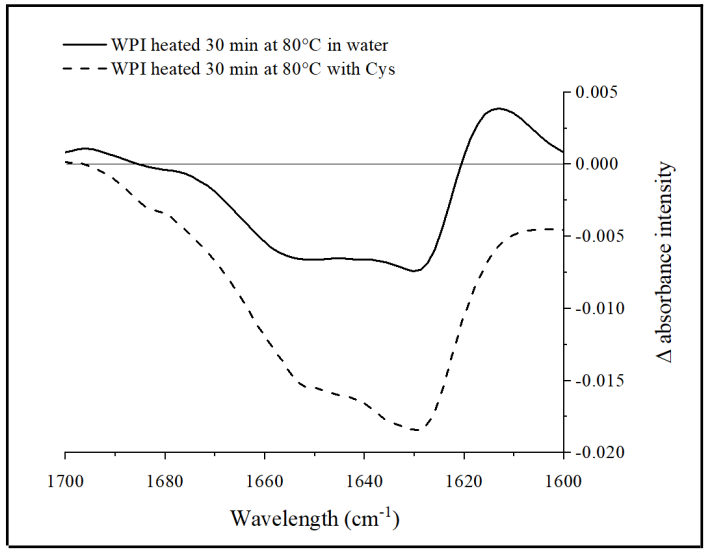


**Figure 1.** ATR-FTIR spectroscopy spectra of WPI heated 30 min at 80°C in water at pH 7 (solid line) and WPI heated 30 min at 80°C in water at pH 7 with Cys (dash line). Both curves are subtracted from the unheated control of WPI.

When Cys was added to the system, a steeper decrease in band intensity at 1658 and 1630 $cm^{-1}$ was observed, with no increase in band intensity at 1615 $cm^{-1}$ (Figure 1). So, ATR-FTIR spectroscopy demonstrated that Cys promoted the unfolding of whey proteins and hindered intermolecular interactions during heating. Cys is a food-grade additive capable of interfering with the thiol-disulfide interchange reaction during heat treatment of globular proteins (Dan & Labuza, 2010). Cys acts mainly as a free thiol group blocking reagent, similar to N-ethylmaleimide (NEM), but Cys may also cleave intramolecular disulfide bonds in proteins (Huggins, Tapley, & Jensen, 1951; Wang & Damodaran, 1990). Therefore, besides preventing the formation of disulfide-linked aggregates, Cys may also increase the unfolding of whey proteins. Indeed, in this study, when Cys was added to the system a greater loss in intramolecular structures was observed. Furthermore, if the free thiol group of β-lg is blocked by Cys, thermal

unfolding will be modified and less hydrophobic sites will be exposed and available to react. Consequently, less intermolecular non-covalent interactions will be possible (Havea, Watkinson, & Kuhn-Sherlock, 2009). This would explain why no increase in the intensity of the band related to intermolecular β-sheets (ca. 1615 $cm^{-1}$) was measured.

AFM was used to observe whey proteins at different stages of the cold gelation process (Figure 2).

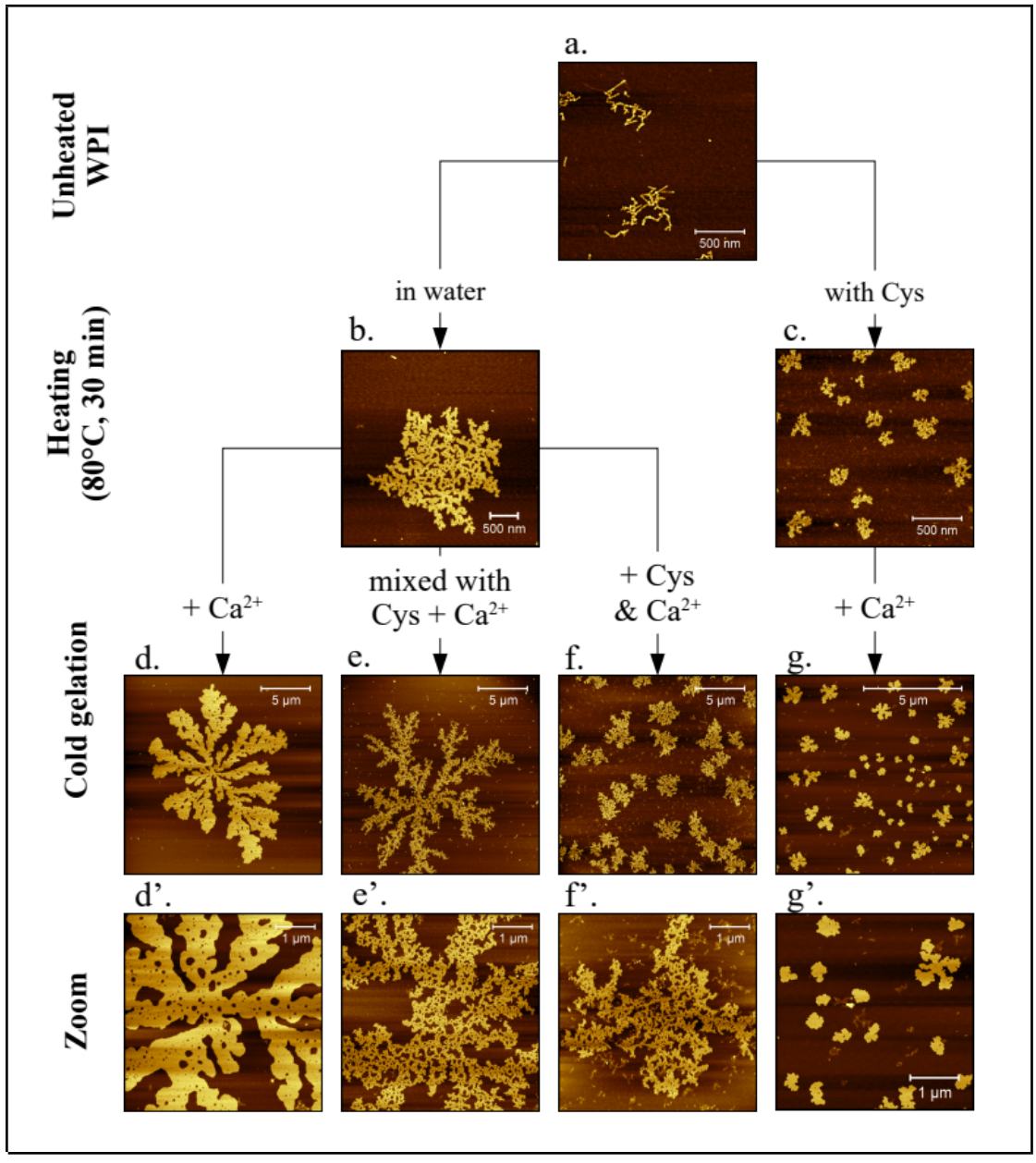


**Figure 2:** Tapping mode AFM height images of (a) unheated WPI in water (pH 7), (b) WPI heated at 80°C for 30 min in water, and (c) WPI heated at 80°C for 30 min in water with free Cys; as well as calcium-induced clusters: (d) calcium added to heat-induced aggregates and zoom (d'); (e) heat-induced aggregates mixed with free Cys before

calcium addition and zoom (e'); (f) calcium and free Cys added together to the heat-induced aggregates and zoom (f'); (g) calcium added to heat-induced aggregates modified by free Cys and zoom (g').

Before heat treatment, whey proteins appeared as stretched single chains between 100 and 250 nm in length and between 1.5 and 3 nm in height (Figure 2a). The protein chains were probably gathered because of sample preparation for AFM (water evaporation by argon flow) but did not seem to directly interact with each other. The size of unheated native β-lg and whey proteins in whey protein concentrate (WPC) measured from the height profiles of AFM images has been reported between 1.5 and 2.5 nm (Elofsson, Dejmek, Paulsson, & Burling, 1997; Ikeda & Morris, 2002; Kehoe, Wang, Morris, & Brodkorb, 2011). It is therefore presumed that the WPI from BiPro® used in this study was already slightly aggregated before any further treatment, which was certainly due to the process of fabrication of the ingredient.

This finding was confirmed by measurements with dynamic light scattering of the particle size of the same unheated WPI, presented in Figure 3. The distribution of the hydrodynamic diameter of the whey proteins was bimodal with a first peak at 21 nm and a wider peak at 164 nm, which matches well with the observations made with AFM (Fig. 2a).

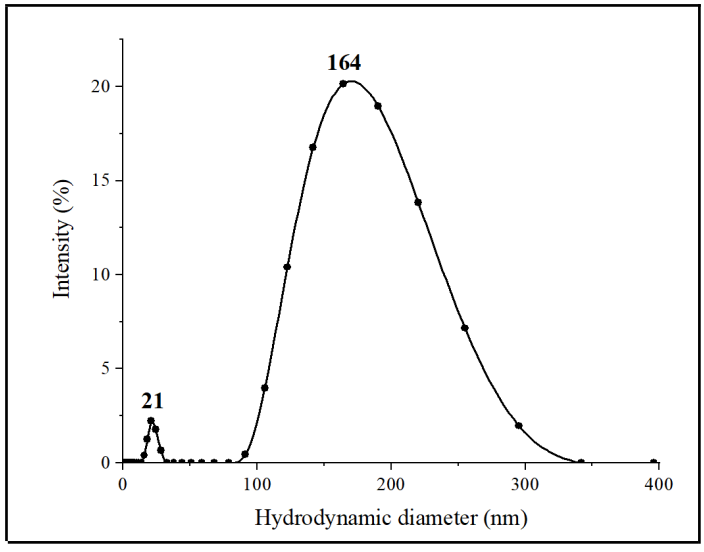


**Figure 3.** Particle size distribution curve of unheated WPI in water at pH 7.

Figure 2b shows the whey protein aggregates formed after heating at 80°C for 30 min in water at pH 7. These aggregates had random shapes and measured ~ 3 μm in diameter. According to cryo-TEM studies, the β-lg pre-aggregates formed at pH 7 and low ionic strength have an elongated shape and measure less than 100 nm in length (Jung et al., 2008; Mahmoudi, Mehalebi, Nicolai, Durand, & Riaublanc, 2007). But further association of these pre-aggregates may happen when protein concentration is increased up to 10% (w/w) (Durand, Gimel, & Nicolai, 2002). Therefore, the aggregates observed here were probably primary objects formed by smaller whey protein pre-aggregates.

In contrast, whey proteins heated with added Cys formed irregular aggregates of ~ 0.3 μm in diameter (Figure 2c). Indeed, when Cys were added to the system, less protein molecules were able to interact with each other to form aggregates. It is well known that added free Cys are able to react with Cys inside the whey proteins chains (Dan & Labuza, 2010). In consequence the free thiol groups of the β-lg (on the signal peptide

and/or $Cys^{137}$), were blocked to form the thiol/disulfide exchange reactions responsible for the heat-induced aggregation of WPI (Hoffmann & Van Mil, 1997; Wijayanti, Bansal, Sharma, & Deeth, 2014; Wijayanti, Oh, Sharma, & Deeth, 2013). However, regardless of the blocked thiol groups, the unfolded proteins may expose other active sites (e.g. hydrophobic regions) and could still form aggregates via non-covalent interactions (Nguyen et al., 2014). It is therefore suggested that the aggregates observed in this case were mainly formed by non-covalent interactions.

These data confirmed that heat-induced aggregation of whey proteins at pH 7 is mainly driven by the formation of intermolecular disulfide bonds, while hydrogen-bonded β-sheets favored by hydrophobic interactions seem to be involved in the stabilization of aggregates upon cooling. The latter is supported by DSC experiments, which clearly showed a reversible formation of β-sheets under repeated cooling and heating cycles (cf. Section 3.3, Fig. 10).

### 3.2. Cold gelation induced by calcium ions

Heat-induced aggregates of whey proteins at room temperature (in water at pH 7) are negatively charged and repel each other. When calcium divalent cations are added to the system, electrostatic repulsion is screened and calcium bridges are formed between aggregates (Bryant & McClements, 2000), promoting the formation of a particle gel network of fractal nature (Marangoni et al., 2000; Walstra, van Vliet and Bremer, 1991).

#### 3.2.1. Clusters

As shown in Figure 2d and 2d', the addition of $CaCl_2$ at 20°C to the dispersion of aggregates (Fig. 2b) resulted in the formation of branched clusters with a mean diameter

of ~11 μm. Calcium ions interacted with the whey protein aggregates and led to the formation of clusters with a fractal structure. Image analysis of the AFM pictures of these clusters yield a two-dimensional $D_f$ of 1.84, which corresponds to the diffusion-limited cluster-cluster aggregation (DLCA) regime (Vreeker, Hoekstra, den Boer, & Agterof, 1992). Different values of $D_f$ have been reported in the literature for WPI cold-set gels with $CaCl_2$ at pH 7. From the analysis of SEM images Kuhn, Cavallieri, & da Cunha (2010) measured a $D_f$ of 1.82 (in 2-D), while Marangoni et al. (2000) used TEM micrographs and obtained a higher $D_f$ of 2.25. However, Hongsprabhas, Barbut, & Marangoni (1999) reported a $D_f = 1.5$ from the analysis of SEM and TEM micrographs. Finally, Wu, Xie, & Morbidelli (2005) measured WPI clusters with a maximum average gyration radius of about 80 μm and a $D_f$ of 1.85 ±0.05 using small-angle light scattering. Besides the differences in the method used to determine $D_f$, the heat treatment as well as the protein and salt concentrations varied among these studies, which make them difficult to compare.

Calcium ions also interacted with the aggregates modified by Cys addition (Fig. 2c), but the size and shape of the clusters formed were different (Figure 2g and 2g'). Two main groups were distinguished: (1) branched clusters, mean size ~1.1 μm; and (2) unbranched clusters, mean size between 0.2 and 0.4 μm. According to Alting et al. (2003), WPI clusters could be partly stabilized by the formation of additional covalent disulfide bonds. Therefore, it seems that the modified aggregates, where thiol groups were blocked, were not able to form these additional stabilizing bonds. Consequently, denser and smaller clusters, more stable thermodynamically than open branched clusters, were formed.

When free Cys were added to the system after heat-induced aggregation of the whey proteins, the addition of $CaCl_2$ resulted in the formation of highly branched clusters, presented in Figure 2e and 2e'. These clusters were heterogeneous in size, the larger ones measured ~17 μm in diameter and the smaller ones ~4 μm. Here, image analysis

yield a Df of 1.75, which also corresponds to the DLCA regime, and confirms that these clusters had a more open structure than the unmodified WPI clusters (Fig 2d and 2d'). Baussay, Le Bon, Nicolai, Durand, & Busnel (2004) observed that the density of β-lg aggregates on small length scales decreased when decreasing ionic strength. Here, free Cys probably positioned themselves close to the surface of the aggregates and increased the steric hindrance around them. Consequently, interactions between the aggregates and the calcium ions were slowed, leading to the formation of loose clusters.

Interestingly though, when free Cys were added at the same time as $CaCl_2$, the formation of clusters was clearly hindered, as shown in Figure 2f and 2f'. Small clusters of ~5 μm in diameter were observed, along with whey protein aggregates (~0.5 μm in diameter) that did not form clusters in spite of the addition of calcium to the system.

To understand this phenomenon better, complex formation between calcium ions and Cys in water at pH 7 was investigated with ITC. Figure 4 shows the results of the titration of a $CaCl_2$ solution into a Cys solution. An endothermic transition with an association constant of ~5500 $M^{-1}$ (ie., 1/KD) and a stoichiometric coefficient (N) around 1 was measured, suggesting that calcium and Cys did form complexes. Since this process was entropically driven, it is proposed that an ionic interaction occurred, excluding water molecules from the surface of Cys. Calcium ions probably interacted with the carboxyl group of Cys (ionized in water at pH 7). Therefore, the ionic strength of the solution was reduced when free Cys and calcium ions were dissolved together. Consequently, the conditions for cluster formation were significantly modified.

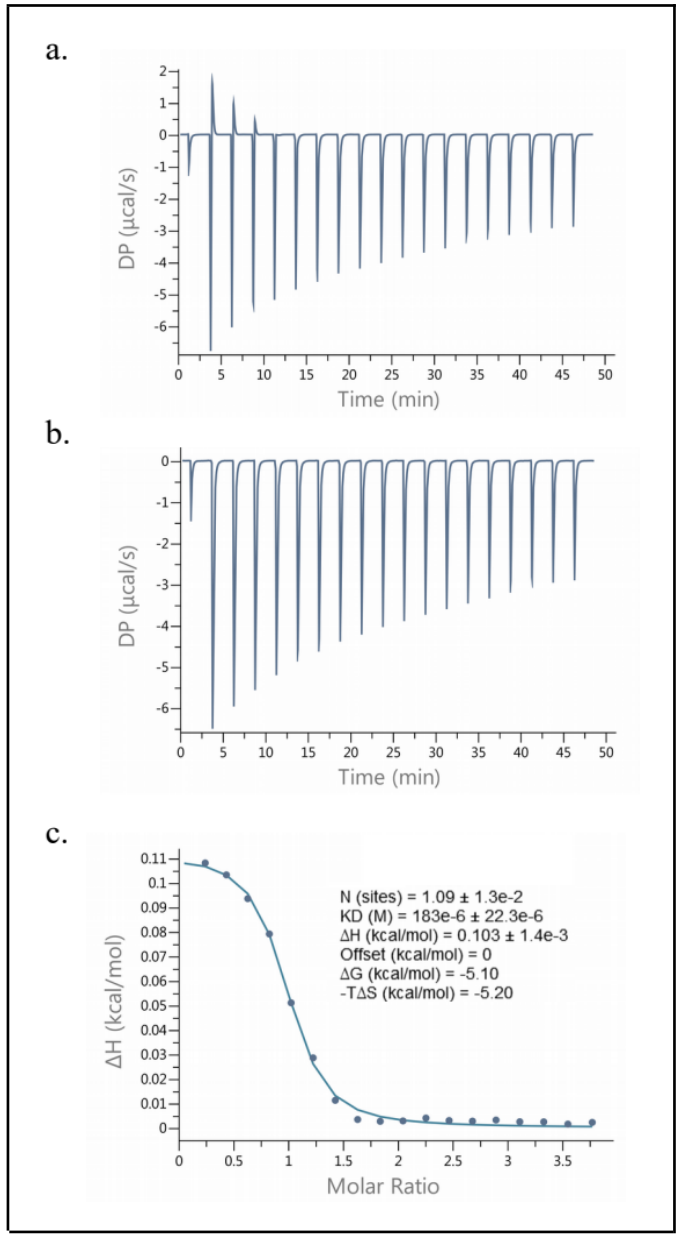


**Figure 4.** Titration of 100 mM $CaCl_2$ into 5 mM Cys; (a) raw ITC data; (b) raw ITC data collected for the titration of 100 mM $CaCl_2$ into distilled water (= heat of dilution); (c) integrated and normalized heat vs. the molar ratio of $CaCl_2$ to Cys, after subtraction of the heat of dilution.

### 3.2.2. Cold-set gels

Amplitude sweep measurements (Figure 5) showed that all samples behaved as viscoelastic gels with dominating elastic properties (tan $\delta < 1$) in the LVR. The plateau value of G' in the LVR, $G'_0$, was around 2 kPa, which corresponds well with the theoretical estimation of the modulus. Indeed, considering a bond energy of calcium ions with carboxyl groups of 77371.21 J/mol, a concentration in β-lg of 4.75% (w/w), an average of 150'000 protein molecules per aggregate (estimated from the size of the aggregates measured on AFM images, cf. Fig. 2b) and an average of 1'500 bonds per aggregate, the estimated total energy density calculated for this system is 1.97 kPa. When calcium and free Cys were added together to the heat-induced aggregates (gel 4), $G'_0$ was significantly reduced to 1.3 ±0.3 kPa. This is consistent with the fact that less calcium ions were available to form salt bridges because of complex formation with Cys (cf. Fig. 4).

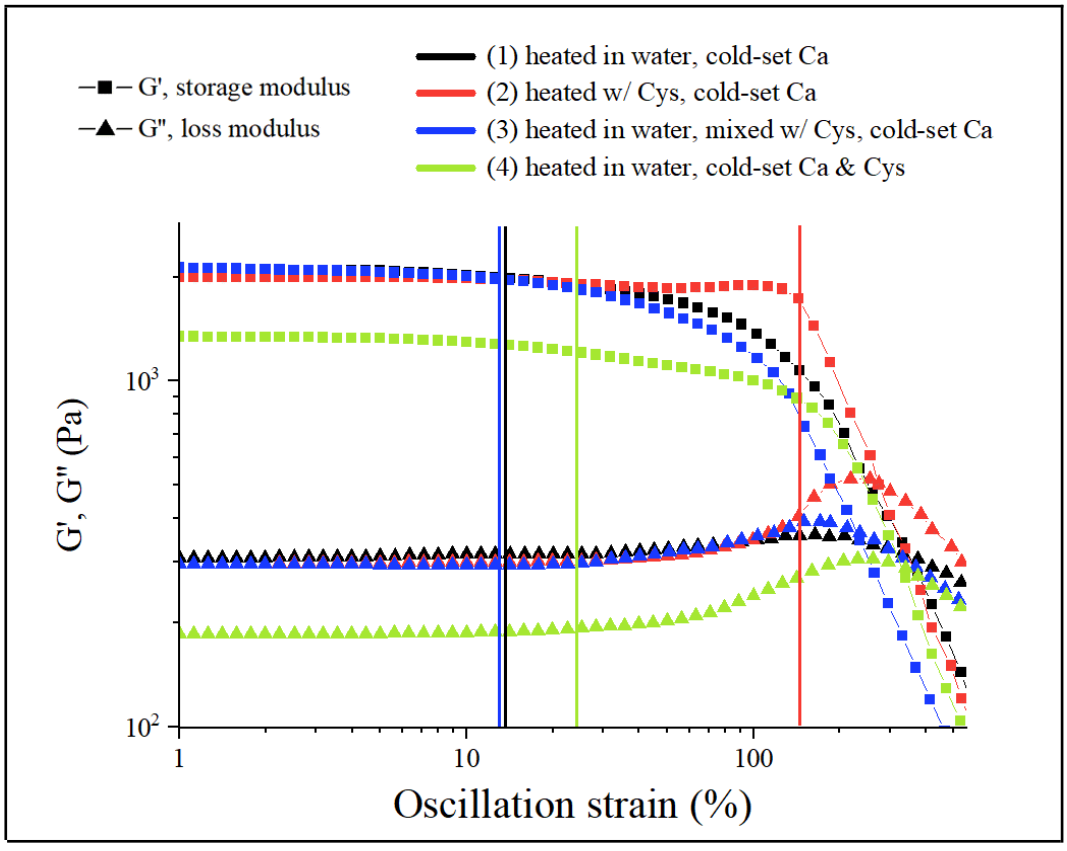


**Figure 5.** Amplitude sweep curves of the four cold-set WPI gels: (1) calcium added to heat-induced aggregates; (2) calcium added to heat-induced aggregates modified by free Cys; (3) heat-induced aggregates mixed with free Cys before calcium addition; (4) calcium and free Cys added together to the heat-induced aggregates.

Under increasing shear amplitude, all samples showed a shear thinning behavior (Rao, 2007), probably due to the successive breakdown of the particle gel. The elastic properties of whey protein networks formed by cold gelation induced by salts generally follow the weak-link regime (Andoyo et al., 2018). In the weak-link regime, the elastic behavior of the gels is dominated by the elastic constant of the interflocs links (ie., the calcium bridges), since the flocs (ie., the heat-induced aggregates) are more rigid than

the interflocs links (Shih, Shih, Kim, Liu, & Aksay, 1990). Here, the applied deformation stretched the salt bridges and calcium molecules were progressively "pulled out". Consequently, the links between the aggregates ruptured successively, until the complete destruction of the network.

Irreversible deformation of samples occurred between 10 and 20% of oscillation strain, except when the heat-induced aggregates were modified by free Cys (gel 2). In this case, the LVR of the gel was significantly increased as the breakdown of the network occurred at 144 ±18% of oscillation strain. A relationship exists between the structural properties of gels and their rheology (Roff & Foegeding, 1996). Different rheological properties were expected for gel 2 since it was formed from dense and small clusters united by non-covalent interactions (cf. AFM pictures, Fig. 2f and 2f'). It may be surmised that the lack of disulfide bonds allowed the proteins in the gel to rearrange when subjected to large deformation, extending the LVR, as proposed by Nguyen et al. (2014).

The observation through CLSM of the WPI network after cold gelation confirmed that significant differences existed between the microstructure of the gels 1 and 2 (Figure 6). Both networks were homogeneous, but gel 1 had a typical mesh size of ~1.4 μm while gel 2 had a significantly smaller mean mesh size of ~0.7 μm. Therefore, the modification of the whey protein aggregates by the free Cys during heating, further resulted in a denser gel network after calcium addition.

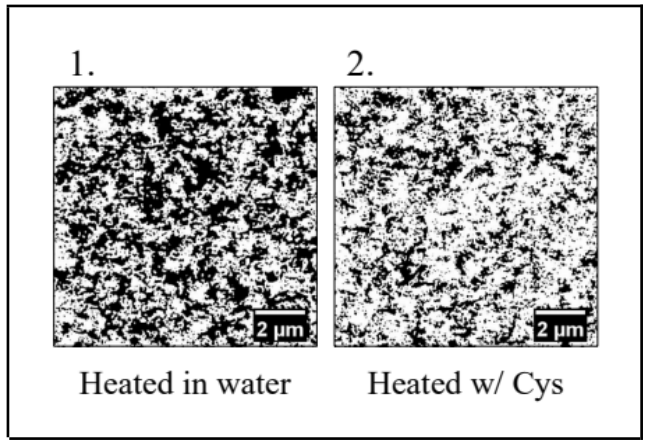


**Figure 6.** CLSM images of the microstructure of the WPI network after cold gelation with calcium ions. (1) calcium added to heat-induced aggregates; (2) calcium added to heat-induced aggregates modified by free Cys.

### 3.2.3. Fractal dimension of the cold-set gel

A $D_f$ of 1.79 was yield by the image analysis of CLSM pictures of the WPI cold-set gel with calcium (1), which is consistent with the Df of the WPI clusters determined by image analysis of AFM pictures (= 1.84).

The $D_f$ of the WPI cold-set gels was also determined by oscillatory rheology. As suggested by Joshi, Beccard, & Vilgis (2018), the rheological behavior of particle gels under deformation can be described by the “Payne effect”; well-known from the elasticity of reinforced elastomers (see e.g. Vilgis, Heinrich, & Klüppel, 2009), which can be quantified by applying the “Kraus model” on amplitude sweep curves. Amplitude sweep curves of the four WPI cold-set gels were therefore fitted with the following function:

$$G' = \frac{1}{1 + K^2 a^{2m}} \quad (1)$$

where G' is the storage modulus, $K$ a constant depending on the system properties and $a$ is the respective deformation amplitude. The exponent m contains $D_f$ as shown in Eq. (2):

$$m = \frac{1}{C - D_f + 2} \quad (2)$$

where $C$ is the connectivity of the network. Here, $C$ was set to 1.3 assuming that the WPI network is completely percolated (Joshi et al., 2018).

Results are shown in Figure 7. The Kraus model suggested a $D_f = 2.42$ for the cold-set WPI gel with calcium (1). Regardless of the method used to calculate $D_f$, the three-dimensional structure of WPI networks formed by calcium-induced cold gelation are generally described in the literature by $D_f$ values around 2.6 (Andoyo et al., 2018). From rheological measurements, Hongsprabhas et al. (1999) and Marangoni et al. (2000) reported a $D_f = 2.54$ for whey protein cold-set gels with $CaCl_2$., using the weak-link model developed by Shih et al. (1990). Kuhn et al. (2010) used the scaling model of Wu et al. (2005) for similar gels and reported a $D_f$ of 2.66. In these studies, $D_f$ was estimated from the values of the initial modulus $G'_0$ (in the linear deformation regime) of the gels measured at different WPI concentrations. In our work, $D_f$ was calculated from the strain dependence of G', considering the transmission of the stress in the network and the change of the internal structure of the gel. However, to understand the dependence of elasticity on the structure of the gels for larger, non-linear deformations, higher strains need to be taken into account, and for whey protein gels the rigid fractal model becomes invalid in the present form.

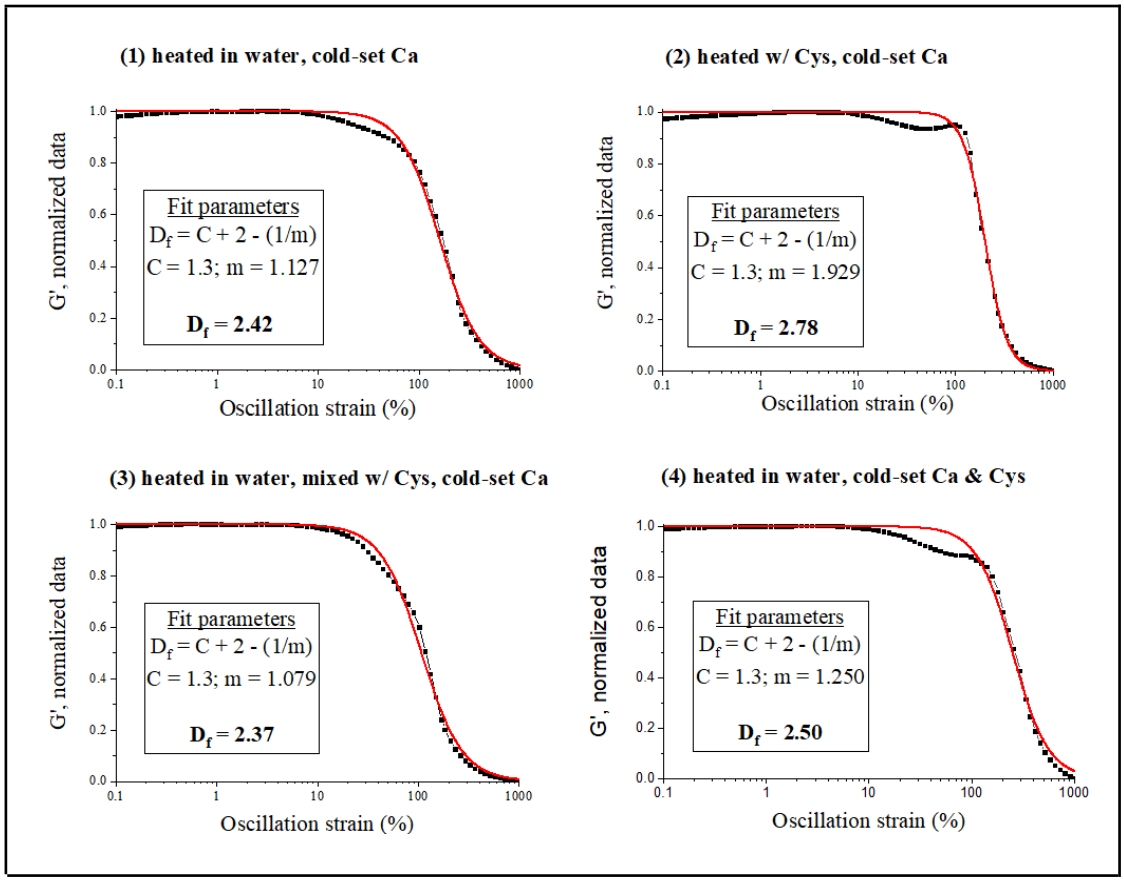


**Figure 7.** Df of the four cold-set WPI gels determined by oscillatory rheology using the "Kraus model". The red line represents the Kraus model on each graph.

An overall shear thinning behavior under increasing shear amplitude could be described by the Payne effect, but additional effects were observed at high amplitudes, as can be seen in Figure 7. Between 10 and 100% of oscillation strain, the Kraus model did not fit well the data. Especially for gel 2 and 4 where G' decreased slowly, reached a plateau and finally dropped rapidly under increasing shear strain. The Kraus model applies for rigid fractals, where particles are non deformable solids. However, whey proteins appear to form "soft" fractals, where the individual aggregates have their own elasticity

and can be deformed, even irreversibly. The use of the Kraus model to estimate the overall fractality of such WPI gels seems therefore limited.

To explain this unusual behavior, the following model is proposed. First, hydrophobic interactions between whey protein molecules are disrupted by shear strain. Then the aggregates deform, probably because of a disentanglement of the polymer chains. Finally, calcium molecules are pulled out, the fractals are separated from each other and the initial structure of the network is merely destroyed. This model is illustrated in Figure 8.

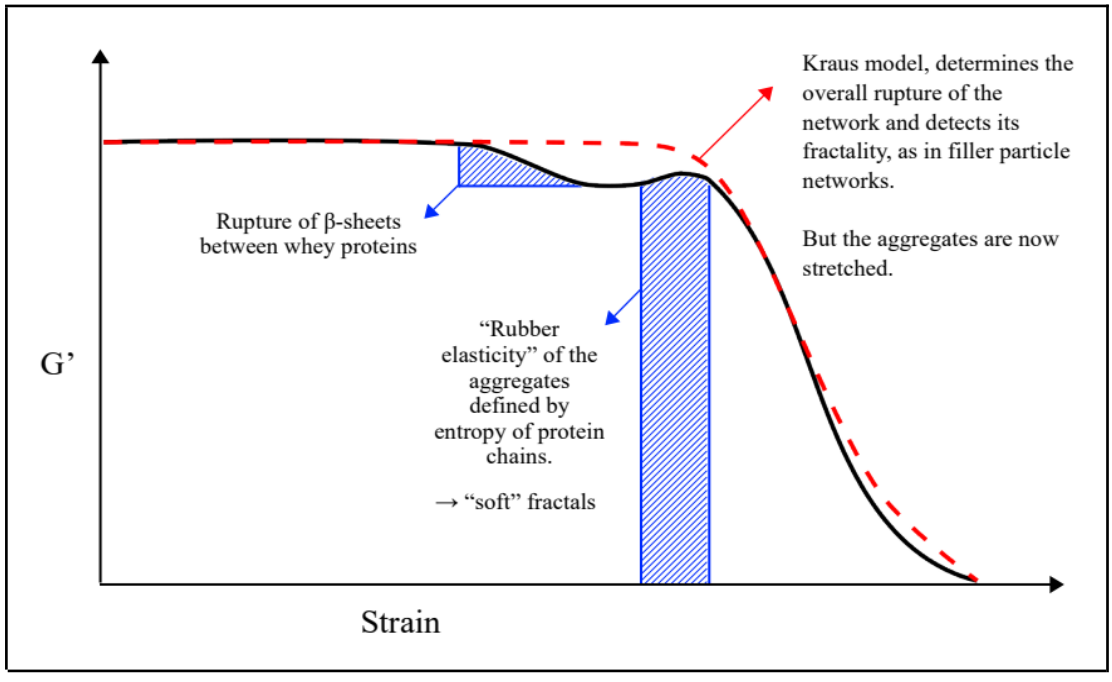


**Figure 8.** Hypothetical model of the successive events leading to the rupture of WPI cold-set gels under increasing strain amplitudes.

Elasticity inside the "soft" fractals depended on the preparation method of the gel. Gel 2 was built from structural units without disulfide bonds, hence, they were able to deform

significantly when subjected to high strain amplitudes. Gels 1, 3 and 4 were formed from the same heat-induced aggregates, but had a different fractal structure (cf. AFM images, Fig. 2d, 2e and 2f respectively) and therefore behaved differently. In gel 4, where less calcium ions were involved in the formation of the network, polymers chains were probably able to rearrange and stretch under high strain amplitudes.

### 3.3. Heating of the cold-set gel

The secondary structure of the whey proteins in gel 1 (i.e., heated in water and cold-set with calcium) was studied before and after heating to 90°C by ATR-FTIR spectroscopy (Figure 9). The secondary structure of the whey proteins was the same in the heat-induced aggregates and in the calcium-induced gels (cf. Fig. 1). Similar molecular structure of the proteins following heat treatment and within the cold-set gels were also observed by FTIR spectroscopy in β-lg gels induced by ferrous ions (Remondetto & Subirade, 2003) and in soy protein isolate gels induced by calcium ions (Maltais et al., 2008). This observation confirms that the heat-induced aggregates are the structural units of gel 1 and its formation is the result of the association of these structural units.

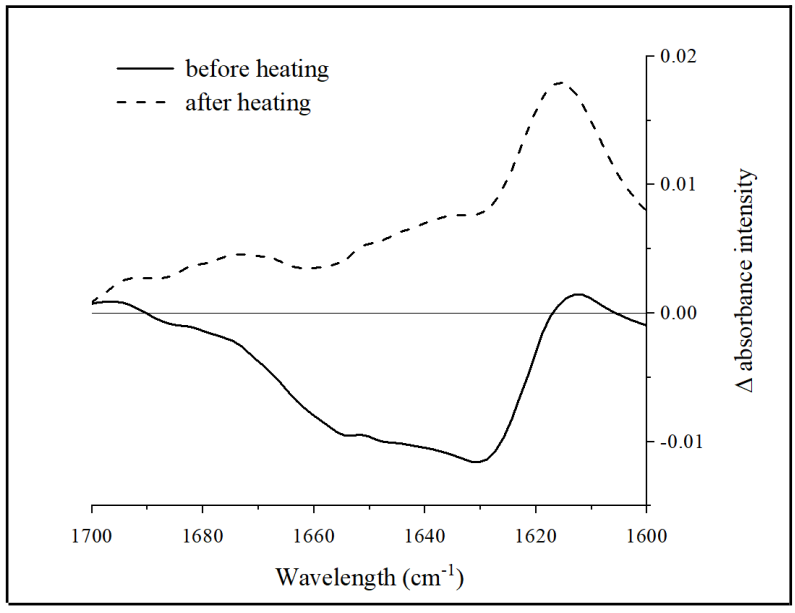


**Figure 9.** ATR-FTIR spectroscopy spectra of the WPI gel cold-set with calcium (gel 1), before (solid line) and after (dash line) heating to 90°C.

However, an increase in band intensity at 1618 $cm^{-1}$ was observed on the spectrum of the cold-set gel heated to 90°C (Fig. 9) meaning that intermolecular interactions, through hydrogen-bonding β-sheets, were enhanced by heating. Furthermore, this spectrum shows an increment in band intensities at ~1640 $cm^{-1}$ and at ~1675 $cm^{-1}$, wavelengths associated to random coils and turns respectively (Geara, 1999) An increase in random coil conformation reflects a gain in conformational entropy and has been related to unfolding and irreversible aggregation of whey proteins (O'Loughlin et al., 2015). This suggests that the heat treatment increased the irreversible unfolding of the whey proteins. The molecular conformation of the heat-induced aggregates, the structural units of the cold-set gel, was therefore modified by heating the gel at 90°C.

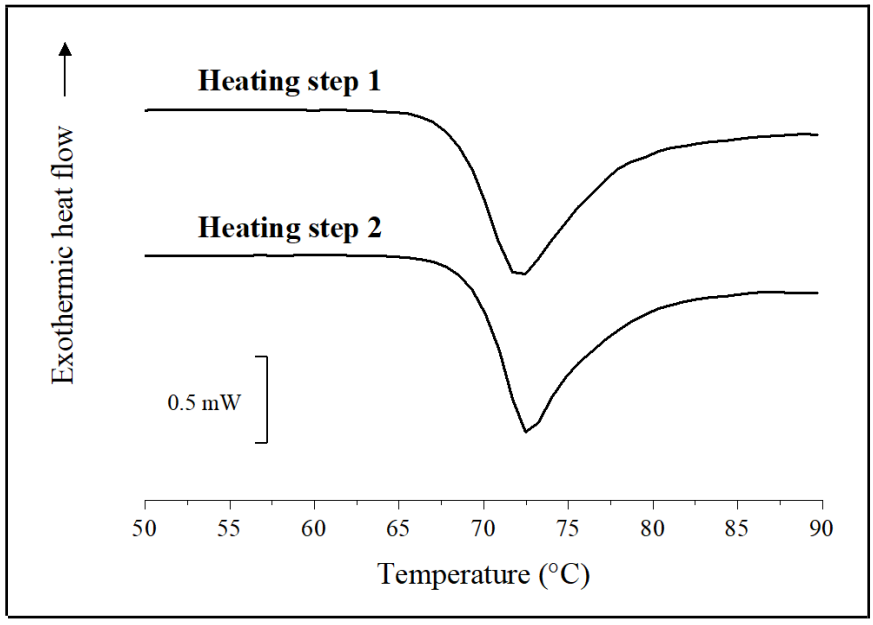


**Figure 10.** DSC thermograms for the WPI gel cold-set with calcium (gel 1), heated two consecutive times from 20 to 90°C at 1°C/min. To facilitate comparison, the DSC scans were displaced vertically to arbitrary amounts.

An endothermic peak at 71.5°C was observed when gel 1 was heated from 20 to 90°C (Figure 10). The same endothermic peak appeared when the sample was subjected to heating/cooling cycles between 20 and 90°C, meaning that this transition was reversible to a second heating cycle. The enthalpy change (ΔH) of the transition was 67.3 ± 2.2 J/g. Considering the results of ATR-FTIR spectroscopy (cf. Fig. 9), this reversible thermal transition is attributed to the unfolding of the intermolecular hydrogen-bonding β-sheets present in the cold-set gel structure. Reverse unfolding of β-sheets in proteins has been observed before by calorimetric studies (Wimley & White, 2004).

Figure 11a presents the effect of heat treatment at different temperatures on the $G'_0$ of the WPI cold-set gel (1) and Figure 11b shows the amplitude sweep curves of the same

gel, before and after heat treatment at 90°C. $G'_0$ increased significantly after heat treatment at T > 50°C and this reinforcement of the gel increased with temperature (Fig. 11a). Such rise in $G'_0$ is probably due to the formation of new hydrophobic interactions and/or disulfide bonds, which are both promoted by temperature (Bryant & McClements, 1998).

After heat treatment at 90°C, the WPI cold-set gel (1) still behaved as a viscoelastic gel with dominating elastic properties (ie., G'' < G') but the rheological properties of the gel were significantly modified by heating (Fig. 11b). In addition to the significant increase of G', from 2.2 ±0.6 to 107.1 ±3.5 kPa, irreversible deformation of the gel occurred at ~0.8% of oscillation strain, against ~15% before heat treatment (Fig.11b). So, the gel network was not only stiffer, but also more brittle. These results are in line with our previous observations on composite cold-set gels of WPI and potato starch: the pure WPI gel (used as control in the study) was harder and more brittle after heating above 85°C (Lavoisier & Aguilera, 2019). It is also in accordance with the results of Hongsprabhas & Barbut (1997a), who reported that heating calcium-induced cold-set WPI gels increased the Young's modulus and the shear stress, but reduced the shear strain. Authors suggested that heating may increase interactions (hydrophobic and disulfide bonds) between the protein aggregates of the gels and modify their microstructure. A similar trend has also been observed when increasing the salt concentration used to induced cold gelation: at fracture, the shear stress increased, whilst the shear strain decreased (Bryant & McClements, 1998).

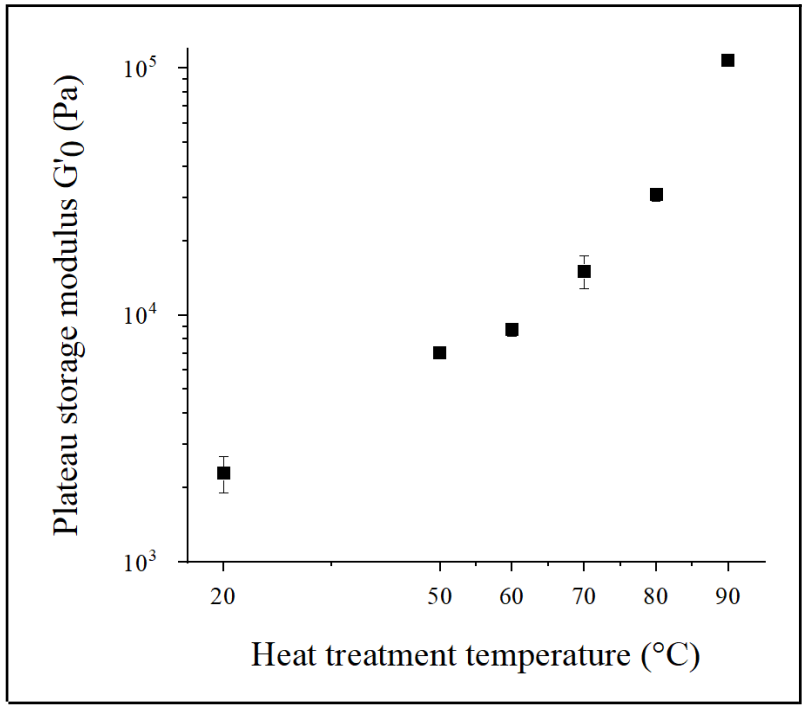


**Figure 11a.** Plateau storage modulus ($G'_0$) of the WPI gel cold-set with calcium (gel 1) at 20°C, after heat treatment from 20 to 50, 60, 70, 80 or 90°C at 1°C/min (temperature sweeps).

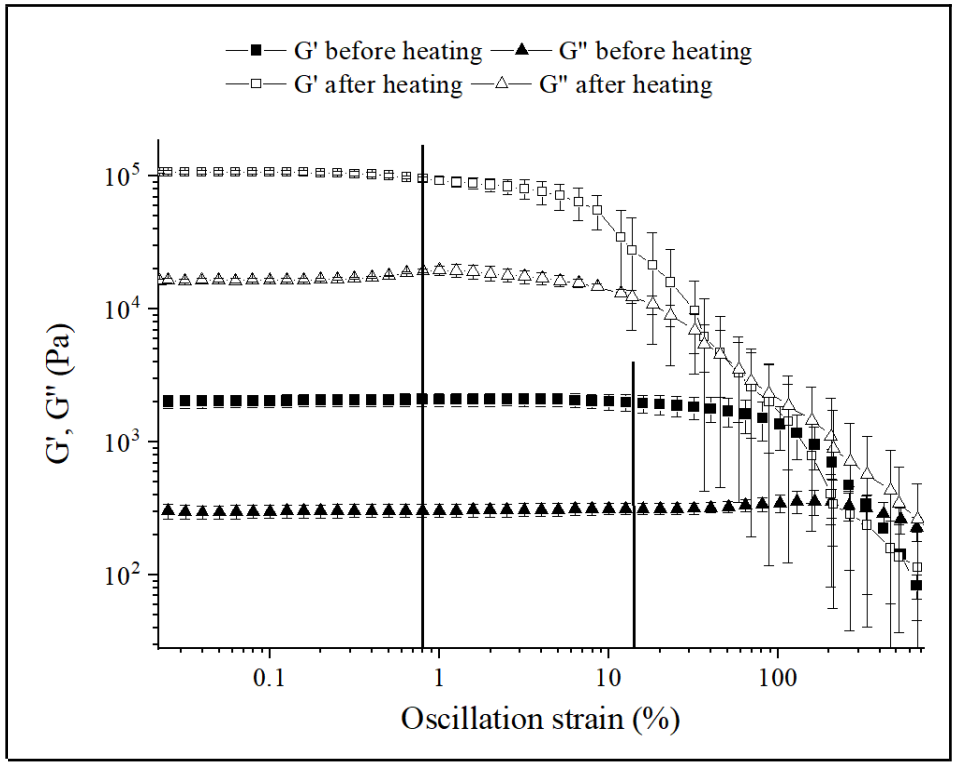


**Figure 11b.** Amplitude sweep curves of the WPI gel cold-set with calcium (gel 1) at 20°, before and after heat treatment at 90°C (temperature sweeps).

Analysis of the microstructure of gel 1, before and after heating, by two techniques (CLSM and cryo-SEM) gives complementary qualitative support to these findings (Figure 12). CLSM images revealed that the microstructure of the gel became coarser after heat treatment, with denser clusters and larger pores (Fig. 12a and 12b). These observations agree with the results of Hongsprabhas & Barbut (1997a) who reported that heating of cold-set WPI gels at 80°C for 30 min caused some of the protein aggregates to collapse together, leading to a lower degree of connectivity among them. Cryo-SEM images should be analyzed with caution since even fast freezing of high-moisture samples may lead to artifacts, i.e., hexagonal-shaped contours formed by segregated material (Efthymiou, Williams, & Mcgrath, 2017). Nevertheless, cryo-SEM

confirmed the formation of a three-dimensional connected protein network after cold gelation, enclosing pores of matching sizes (< 2 μm) as those visualized by CLSM (Fig. 12c). After heat treatment, numerous threads appeared within the pores, suggesting an increase in interactions between the structural units of the gel and an overall modification of the microstructure (Fig. 12d). Some of those threads were stretched and seemed connected on either sides, whereas others looked like a collection of small threads attached to the surface of the particles, resulting in a "hairy" appearance. This structural feature, called "hairiness", has been described before for heat-induced whey protein gels, especially when the NaCl concentration in the system was increased (Langton & Hermansson, 1996).

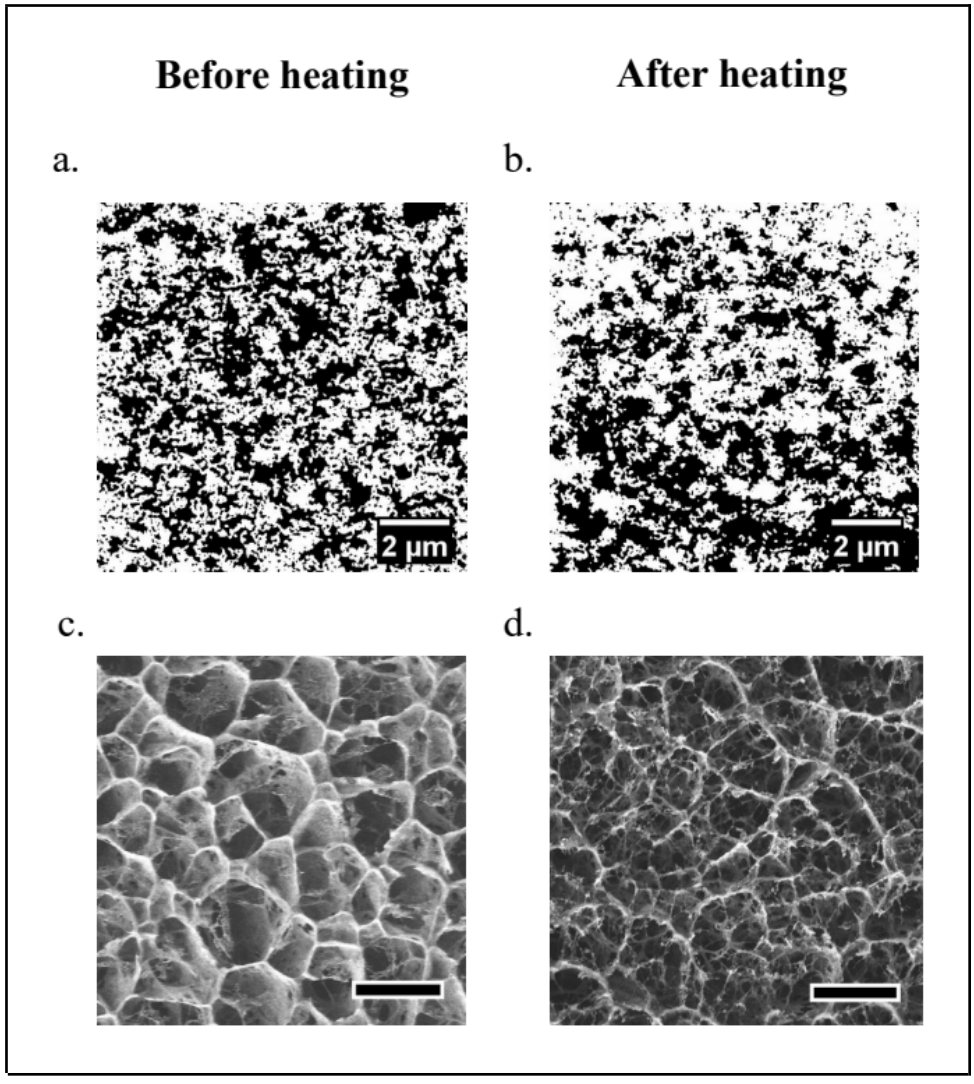


**Figure 12.** Images of the WPI gel cold-set with calcium (gel 1), before and after heating to 90°C. On CLSM images (a, b), the background appears in black and the WPI network in white. On cryo-SEM images (c, d), the markers represent 2 µm.

Changes in the rheological properties of the four WPI cold-set gels during heating from 20 to 90°C and cooling back to 20°C, were followed by measuring G' (Figure 13). G' increased for all samples during the heating segment and continued to rise throughout the cooling step. However, the three gels that were modified by the addition of free Cys reached lower values of G' at the end of the heat treatment. Differences between the gels appeared mainly during the heating phase of the temperature sweep. The final G' value for gel 2 was 42.3 ±8.7 kPa, compared to 93.2 ±10.1 kPa for gel 1. As discussed before, gel 2 had a more packed network structure (cf. Fig. 6), therefore it probably presented less available sites for new molecular interactions during heating/cooling, resulting in a lower G'. Gel 3 reached a similar final G' (36.5 ±9.2 kPa) as gel 2, but in this case G' first decreased slightly up to ~45°C before increasing steadily as it approached 90°C. According to the AFM pictures (cf. Fig. 2e and 2e'), this gel had an open structure, which could explain the decrease in G' at the beginning of the heat treatment. The network was loose enough to allow movement in its structure as the internal energy of the system increased. Then, the added Cys may have hindered the formation of additional disulfide bonds by blocking some of the thiol groups on the particles of whey proteins, which led to a lower G'. Regarding gel 4, G' was 21.0 ±6.6 kPa at the end of the heat treatment, which was the lowest value of all samples. Similar to gel 3, G' decreased slightly when heated to ~45°C, reflecting the relatively loose structure of the initial gel. As commented before, complex formation between free Cys and calcium (cf. Fig. 4) reduced the availability of both to interact with the whey protein particles. So, even if some thiol groups may have been blocked by the free Cys, reduced values of G' are mainly attributed to the lower ionic strength in the system. This suggests that additional calcium bridges may be involved in the reinforcement of the structure of gel 1. Calcium ions in excess, that did not form electrostatic interactions during cold gelation, may participate in the rearrangement of the whey protein network during heating. Furthermore, G' steadily increased in all samples during the cooling phase of the temperature sweep. This important rise in G' is probably related to the

formation of the intermolecular β-sheets observed with ATR-FTIR (cf. Fig. 9) and DSC (cf. Fig. 10).

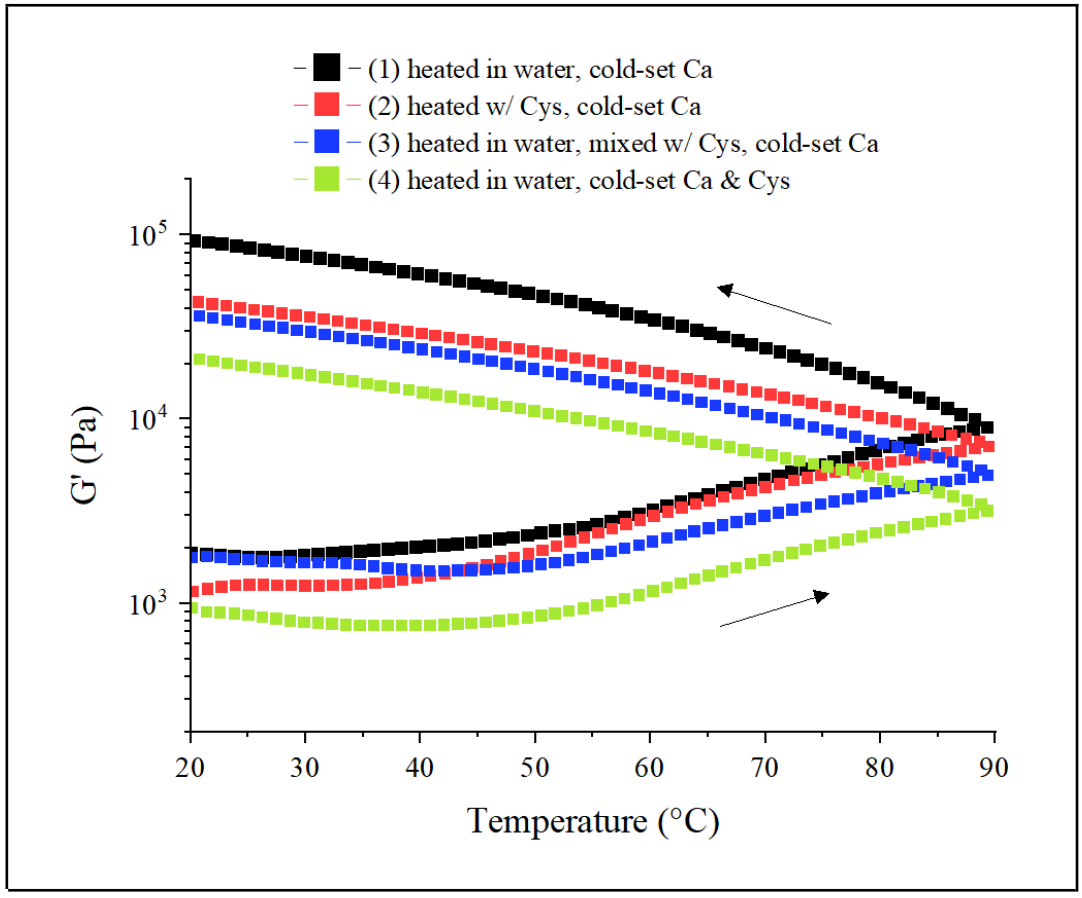


**Figure 13.** Temperature sweep curves of the four WPI cold-set gels: (1) calcium added to heat-induced aggregates; (2) calcium added to heat-induced aggregates modified by free Cys; (3) heat-induced aggregates mixed with free Cys before calcium addition; (4) calcium and free Cys added together to the heat-induced aggregates. G'' and error bars are not indicated for the sake of clarity.

### 3.4. Proposed mechanism of structure reinforcement

According to these results, heating WPI cold-set gels to 90°C leads to an irreversible modification of the protein network structure, illustrated in Figure 14. It is proposed that additional disulfide bonds and calcium bridges form during heating ("strong cross-links"), whereas hydrophobic interactions form during cooling ("weak cross-links"), all contributing to an increase in rigidity of the gel.

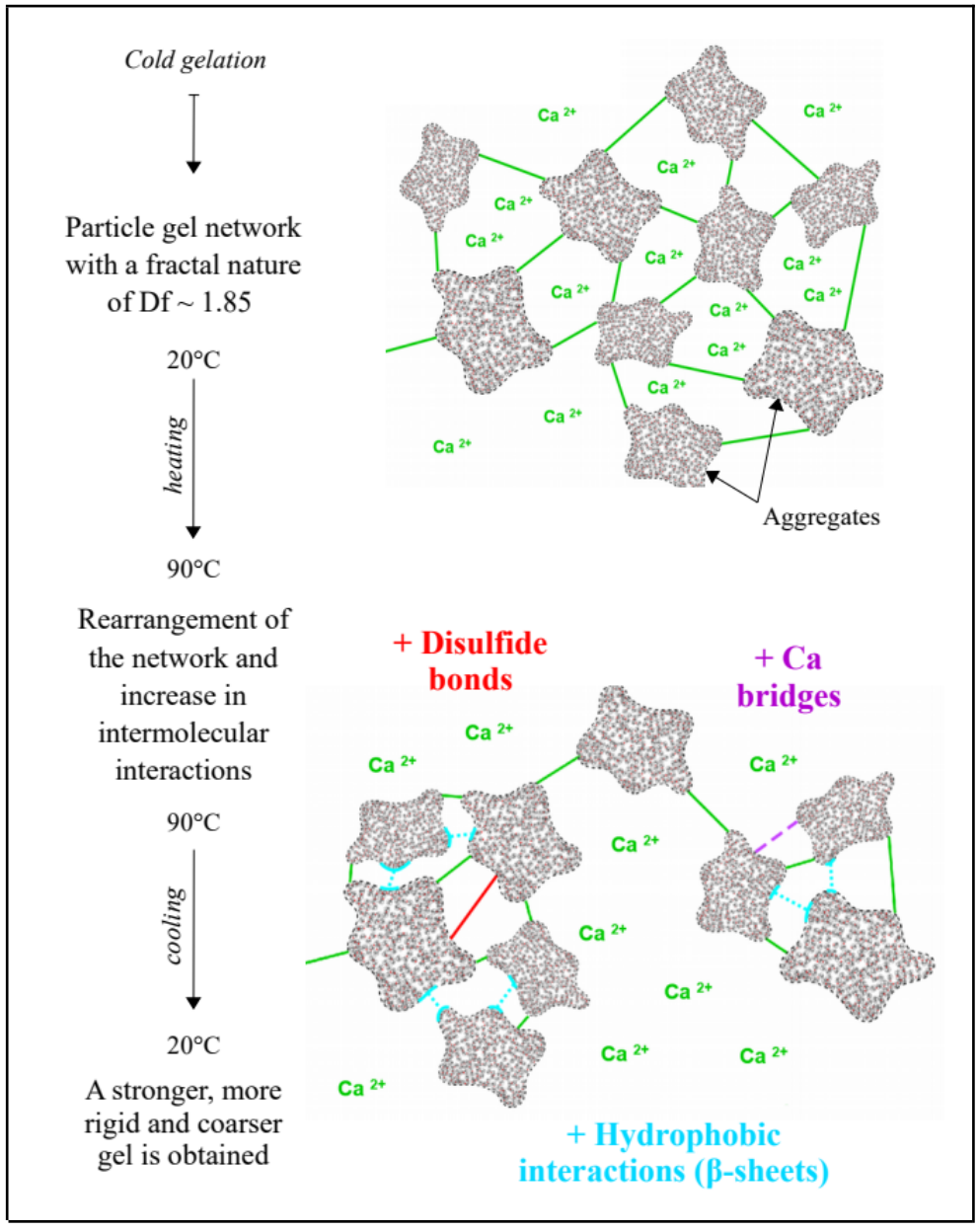


**Figure 14.** Scheme representing the mechanisms involved in the rearrangement of the network structure of the WPI cold-set gels after heating to 90°C.

## 4. Conclusions

Heat-induced aggregation of a WPI dispersion at 80°C and pH 7 is driven by the formation of intermolecular disulfide bonds. These aggregates are also strengthened by intermolecular hydrogen-bonded β-sheets induced by hydrophobic interactions. When calcium ions are added to the system, branched clusters are formed and grow, leading to the creation of a three-dimensional particle gel network of fractal nature. $D_f$ of this network is ~1.85 (2-D), which corresponds to the DLCA regime of the growth model for particles network based on Brownian motion. This phenomenon occurring at room temperature (i.e., 20-25 °C) has been termed cold gelation. Heating the WPI cold-set gels to 90°C results in a rearrangement of the structure of the protein network due to an increase in intermolecular interactions. Additional disulfide bonds and calcium bridges form during heating and reversible H-bonding β-sheets form during further cooling, all contributing to the formation of the final gel network structure. The viscoelastic properties of the WPI cold-set gels are significantly and irreversibly impacted by heating. This should be taken into account when designing soft foods based on cold-set globular protein gels, especially if they undergo thermal treatments or are used in cooking.

# CONCLUSIONS

New strategies are needed to design starchy foods with a slow and steady postprandial release of glucose to help managing disorders of glucose metabolism. But it is a challenging task since starch digestion in food matrices of different compositions and textures is not fully understood yet. This Thesis is a contribution to this effort and its main conclusions are summarized below.

1. Through calcium-induced cold gelation it was possible to encase native PS granules inside a WPI network with a high-water content (> 80%). With this technique, self-standing, soft and elastic composite gels were obtained and PS granules were homogeneously distributed in the microstructure. The addition of PS to the WPI cold-set gel did not modify its mechanical and rheological properties: native PS granules behaved as inactive filler particles dispersed in the viscoelastic protein network.

2. Heat treatment of the composite gels (i.e., heating above 80°C) led to gelatinization of PS inside the WPI network. However, starch gelatinization was restricted by the preformed matrix of WPI. The presence of the protein network around starch granules shortened the gelatinization event, reduced the gelatinization enthalpy and significantly constrained granules swelling.

Upon heating, PS swelling inside the WPI network (i.e., increase in volume and water transfer) influenced the properties of the composite gels. Small amounts of PS weakened the gel, probably because gelatinized granules created flaws in the microstructure. On the contrary, higher amounts of PS led to an actual reinforcement of the gel. In this case, gelatinized granules interacted with each other and an interpenetrating network was formed between PS and WPI.

3. Starch digestibility *in vitro* was also restricted by the preformed matrix of WPI. Gelatinized starch granules were protected from enzymatic attack by the presence of the WPI network.

The effectiveness of this barrier depended on particle size reduction of the gels and on the protein concentration in the gels. The latter was related to the mechanical and rheological properties of the composite gels: starch digestibility decreased while increasing hardness and elasticity of the gels.

WPI networks formed by cold gelation are therefore able to limit the enzymatic attack of starch during digestion, but the microstructure of the protein network must be carefully considered to actually reduce starch digestibility in such composite gels.

4. Heat treatment of the composite gels also modified the properties and the microstructure of the WPI network. WPI cold-set gels were more rigid and brittle after heating to 90°C, reflecting that important changes occurred in the protein network structure. Additional disulfide bonds and calcium bridges formed during heating (i.e., “strong cross-links), whereas hydrophobic interactions formed during cooling (i.e., hydrogen-bonded β-sheets, “weak cross-links”), all contributing to the creation of the final gel network structure.

The viscoelastic properties of the WPI cold-set gels were therefore significantly and irreversibly impacted by heating.

# FUTURE OUTLOOK

In this Thesis, the use of WPI cold-set gels appeared as an interesting strategy to design food products with a slow and steady postprandial release of glucose from potato starch. The latter was used as a model in this study, but concepts could be generalized to other sources of starches. Composite gels of WPI and native starch could be employed as a structural basis for the development of soft foods with low GI and a low calorie content. Such microstructures could be helpful to formulate functional foods for overweight diabetics or the elderly, for example. However, further investigation is needed to understand how to effectively incorporate these starch-trapping protein gels as ingredients in new food products.

First, the breakdown properties of WPI and starch cold-set gels in the human mouth and stomach could be investigated to confirm the findings of the *in vitro* study. Starch digestibility in the gels could also be tested *in vivo* to corroborate a positive effect on GI. It was not possible in this study due to financial limitations. Then, the organoleptic properties of the composite gels after cooking could be evaluated in detail by techniques such as Texture Profile Analysis (TPA) and sensory analysis. The thermal treatment used to process the composite gels could also be optimized. Since heating significantly modifies the properties of the WPI and starch cold-set gels, different thermal treatments could be used to obtain a range of textures and mouthfeel.

**REFERENCES**

Abaee, A., Madadlou, A., & Saboury, A. A. (2017). The formation of non-heat-treated whey protein cold-set hydrogels via non-toxic chemical cross-linking. *Food Hydrocolloids*, *63*, 43–49. https://doi.org/10.1016/j.foodhyd.2016.08.024

Abaee, A., Mohammadian, M., & Jafari, S. M. (2017). Whey and soy protein-based hydrogels and nano-hydrogels as bioactive delivery systems. *Trends in Food Science and Technology*, *70*(October), 69–81. https://doi.org/10.1016/j.tifs.2017.10.011

Aguilera, J. M. (1995). Gelation of whey proteins. *Food Technology*, *49*, 83–89.

Aguilera, J. M. (2018). The food matrix: Implications in processing, nutrition and health. *Critical Reviews in Food Science and Nutrition*, *0*(Sep 10), 1–18. https://doi.org/10.1080/10408398.2018.1502743

Aguilera, J. M., & Baffico, P. (1997). Structure-mechanical properties of heat-induced whey protein/cassava starch gels. *Journal of Food Science*, *62*(5), 1048–1066. https://doi.org/https://doi.org/10.1111/j.1365-2621.1997.tb15035.x

Aguilera, J. M., & Park, D. J. (2016). Texture-modified foods for the elderly: Status, technology and opportunities. *Trends in Food Science and Technology*, *57*, 156–164. https://doi.org/10.1016/j.tifs.2016.10.001

Aguilera, J. M., & Rojas, E. (1996). Rheological, thermal and microstructural properties of whey protein-cassava starch gels. *Journal of Food Science*, *61*(5), 962–966. https://doi.org/10.1111/j.1365-2621.1996.tb10911.x

Aguilera, J. M., & Rojas, G. V. (1997). Determination of kinetics of gelation of whey protein and cassava starch by oscillatory rheometry. *Food Research International*, *30*(5), 349–357. https://doi.org/10.1016/S0963-9969(97)00058-6

Ai, Y., & Jane, J. (2018). Understanding starch structure and functionality. In M. Sjöö & L. Nilsson (Eds.), *Starch in Food: Structure, Function and Applications, Second Edition* (pp. 151–178). Cambridge: Woodhead Publishing. https://doi.org/10.1016/B978-0-08-100868-3.00003-2

Al-Rabadi, G. J. S., Gilbert, R. G., & Gidley, M. J. (2009). Effect of particle size on kinetics of starch digestion in milled barley and sorghum grains by porcine alpha-amylase. *Journal of Cereal Science*, *50*(2), 198–204. https://doi.org/10.1016/j.jcs.2009.05.001

Alam, S. A., Pentikäinen, S., Närväinen, J., Holopainen-Mantila, U., Poutanen, K., & Sozer, N. (2017). Effects of structural and textural properties of brittle cereal foams on

mechanisms of oral breakdown and in vitro starch digestibility. *Food Research International*, *96*, 1–11. https://doi.org/10.1016/j.foodres.2017.03.008

Almario, R. U., Buchan, W. M., Rocke, D. M., & Karakas, S. E. (2017). Glucose-lowering effect of whey protein depends upon clinical characteristics of patients with type 2 diabetes. *BMJ Open Diabetes Research & Care*, *5*(1), e000420. https://doi.org/10.1136/bmjdrc-2017-000420

Alting, A. C., De Jongh, H. H. J., Visschers, R. W., & Simons, J. W. F. A. (2002). Physical and chemical interactions in cold gelation of food proteins. *Journal of Agricultural and Food Chemistry*, *50*(16), 4682–4689. https://doi.org/10.1021/jf011657m

Alting, A. C., Hamer, R. J., De Kruif, C. G., & Visschers, R. W. (2003). Cold-set globular protein gels: Interactions, structure and rheology as a function of protein concentration. *Journal of Agricultural and Food Chemistry*, *51*(10), 3150–3156. https://doi.org/10.1021/jf0209342

Alvani, K., Qi, X., & Tester, R. F. (2012). Gelatinisation properties of native and annealed potato starches. *Starch/Staerke*, *64*(4), 297–303. https://doi.org/10.1002/star.201100130

Alvani, K., Qi, X., Tester, R. F., & Snape, C. E. (2011). Physico-chemical properties of potato starches. *Food Chemistry*, *125*(3), 958–965. https://doi.org/10.1016/j.foodchem.2010.09.088

An, J. S., Bae, I. Y., Han, S. I., Lee, S. J., & Lee, H. G. (2016). In vitro potential of phenolic phytochemicals from black rice on starch digestibility and rheological behaviors. *Journal of Cereal Science*, *70*, 214–220. https://doi.org/10.1016/j.jcs.2016.06.010

Andoyo, R., Lestari, V. D., Mardawati, E., & Nurhadi, B. (2018). Fractal dimension analysis of texture formation of whey protein-based foods. *International Journal of Food Science*, *2018*, 1–17. https://doi.org/10.1155/2018/7673259

Araya, H., Contreras, P., Alviña, M., Vera, G., & Pak, N. (2002). A comparison between an in vitro method to determine carbohydrate digestion rate and the glycemic response in young men. *European Journal of Clinical Nutrition*, *56*, 735–739.

Augustin, L. S. A., Kendall, C. W. C., Jenkins, D. J. A., Willett, W. C., Astrup, A., Barclay, A. W., … Poli, A. (2015). Glycemic index, glycemic load and glycemic response: An international scientific consensus summit from the International Carbohydrate Quality Consortium (ICQC). *Nutrition, Metabolism and Cardiovascular Diseases*, *25*(9), 795–815. https://doi.org/10.1016/j.numecd.2015.05.005

Azzollini, D., Derossi, A., Fogliano, V., Lakemond, C. M. M., & Severini, C. (2018). Effects of formulation and process conditions on microstructure, texture and

digestibility of extruded insect-riched snacks. *Innovative Food Science & Emerging Technologies*, *45*, 344–353. https://doi.org/10.1016/j.ifset.2017.11.017

Bae, I. Y., Jun, Y., Lee, S., & Lee, H. G. (2016). Characterization of apple dietary fibers influencing the in vitro starch digestibility of wheat flour gel. *LWT - Food Science and Technology*, *65*, 158–163. https://doi.org/10.1016/j.lwt.2015.07.071

Bansal, N. (2015). Prediabetes diagnosis and treatment: A review. *World Journal of Diabetes*, *6*(2), 296. https://doi.org/10.4239/wjd.v6.i2.296

Baussay, K., Le Bon, C., Nicolai, T., Durand, D., & Busnel, J. P. (2004). Influence of the ionic strength on the heat-induced aggregation of the globular protein β-lactoglobulin at pH 7. *International Journal of Biological Macromolecules*, *34*(1–2), 21–28. https://doi.org/10.1016/j.ijbiomac.2003.11.003

Bellissimo, N., & Akhavan, T. (2015). Effect of macronutrient composition on short-term food intake and weight loss. *Advances in. Nutrition*, *6*, 3025–3085. https://doi.org/10.3945/an.114.006957

Benelam, B. (2009). Satiation, satiety and their effects on eating behaviour. *Nutrition Bulletin*, *34*(2), 126–173. https://doi.org/10.1111/j.1467-3010.2009.01753.x

Bertoft, E. (2017). Understanding starch structure : Recent progress. *Agronomy, 7*(56),1-29. https://doi.org/10.3390/agronomy7030056

Bhupathiraju, S. N., Tobias, D. K., Malik, V. S., Pan, A., Hruby, A., Manson, J. E., … Hu, F. B. (2014). Glycemic index, glycemic load, and risk of type 2 diabetes : results from 3 large US cohorts and an updated meta-analysis 1 – 3. *American Journal of Clinical Nutrition, 100,* 218–232. https://doi.org/10.3945/ajcn.113.079533.

Bienert, S., Waterhouse, A., De Beer, T. A. P., Tauriello, G., Studer, G., Bordoli, L., & Schwede, T. (2017). The SWISS-MODEL Repository-new features and functionality. *Nucleic Acids Research*, *45*(D1), D313–D319. https://doi.org/10.1093/nar/gkw1132

Bohn, T., Carriere, F., Day, L., Deglaire, A., Egger, L., Freitas, D., … Dupont, D. (2018). Correlation between in vitro and in vivo data on food digestion. What can we predict with static in vitro digestion models ? *Critical Reviews in Food Science and Nutrition*, *58*(13), 2239–2261. https://doi.org/10.1080/10408398.2017.1315362

Boles, A., Kandimalla, R., & Reddy, P. H. (2017). Dynamics of diabetes and obesity: Epidemiological perspective. *Biochimica et Biophysica Acta - Molecular Basis of Disease*, *1863*(5), 1026–1036. https://doi.org/10.1016/j.bbadis.2017.01.016

Bornhorst, G. M., & Singh, R. P. (2013). Kinetics of in vitro bread bolus digestion with varying oral and gastric digestion parameters. *Food Biophysics*, *8*(1), 50–59. https://doi.org/10.1007/s11483-013-9283-6

Brodkorb, A., Croguennec, T., Bouhallab, S., & Kehoein, J. J. (2016). Heat-induced denaturation, aggregation and gelation of whey proteins. In P. McSweeney & J. A. O'Mahony (Eds.), *Advanced Dairy Chemistry, Volume 1B: Proteins: Applied Aspects* (pp. 155–178). New York: Springer.

Bryant, C. M., & McClements, D. J. (2000). Influence of NaCl and CaCl2 on cold-set gelation of heat-denatured whey protein. *Food Chemistry and Toxicology*, *65*(5), 801–804.

Bryant, C. M., & McClements, D. J. (1998). Molecular basis of protein functionality with special consideration of cold-set gels derived from hat-denatured whey. *Trends in Food Science and Technology*, *9*(4), 143–151. https://doi.org/10.1016/S0924-2244(98)00031-4

Bustos, M. C., Vignola, M. B., Pérez, G. T., & León, A. E. (2017). In vitro digestion kinetics and bioaccessibility of starch in cereal food products. *Journal of Cereal Science*, *77*, 243–250. https://doi.org/10.1016/j.jcs.2017.08.018

Cai, C., Cai, J., Zhao, L., & Wei, C. (2014). In situ gelatinization of starch using hot stage microscopy. *Food Science and Biotechnology*, *23*(1), 15–22. https://doi.org/10.1007/s10068-014-0003-x

Campbell, C. L., Wagoner, T. B., & Foegeding, E. A. (2017). Designing foods for satiety: The roles of food structure and oral processing in satiation and satiety. *Food Structure*, *13*, 1–12. https://doi.org/10.1016/j.foostr.2016.08.002

Carrillo-Navas, H., Avila-de la Rosa, G., Gómez-Luría, D., Meraz, M., Alvarez-Ramirez, J., & Vernon-Carter, E. J. (2014). Impact of ghosts on the viscoelastic response of gelatinized corn starch dispersions subjected to small strain deformations. *Carbohydrate Polymers*, *110*, 156–162. https://doi.org/10.1016/j.carbpol.2014.03.088

Carvalho, A. J. F. (2008). Starch: Major sources, properties and applications as thermoplastic materials. In M. Belgacem & A. Gandini (Eds.), *Monomers, Polymers and Composites from Renewable Resources* (pp. 321–342). Amsterdam, Netherlands: Elsevier Science. https://doi.org/10.1016/B978-0-08-045316-3.00015-6

Chassard, C., & Lacroix, C. (2013). Carbohydrates and the human gut microbiota, *16*(4), 453–460. https://doi.org/10.1097/MCO.0b013e3283619e63

Cheison, S. C., & Kulozik, U. (2017). Impact of the environmental conditions and substrate pre-treatment on whey protein hydrolysis: A review. *Critical Reviews in Food Science and Nutrition*, *57*(2), 418–453. https://doi.org/10.1080/10408398.2014.959115

Chen, G., & Sopade, P. (2013). In vitro starch digestion in sweet potato (Ipomoea batatas L.) flours. *International Journal of Food Science and Technology*, *48*(1), 150–156. https://doi.org/10.1111/j.1365-2621.2012.03171.x

Chen, J., Khandelwal, N., Liu, Z., & Funami, T. (2013). Influences of food hardness on the particle size distribution of food boluses. *Archives of Oral Biology*, *58*(3), 293–298. https://doi.org/10.1016/j.archoralbio.2012.10.014

Chen, X., He, X. W., Zhang, B., Fu, X., Jane, J. lin, & Huang, Q. (2017). Effects of adding corn oil and soy protein to corn starch on the physicochemical and digestive properties of the starch. *International Journal of Biological Macromolecules*, *104*, 481–486. https://doi.org/10.1016/j.ijbiomac.2017.06.024

Chung, C., Degner, B., & McClements, D. J. (2013). Creating novel food textures: Modifying rheology of starch granule suspensions by cold-set whey protein gelation. *LWT - Food Science and Technology*, *54*(2), 336–345. https://doi.org/10.1016/j.lwt.2013.07.003

Chung, H.-J., Lim, H. S., & Lim, S.-T. (2006). Effect of partial gelatinization and retrogradation on the enzymatic digestion of waxy rice starch. *Journal of Cereal Science*, *43*(3), 353–359. https://doi.org/10.1016/j.jcs.2005.12.001

Colonna, P., Barry, J. L., Cloarec, D., Bornet, F., Gouilloud, S., & Galmiche, J. P. (1990). Enzymic susceptibility of starch from pasta. *Journal of Cereal Science*, *11*(1), 59–70. https://doi.org/10.1016/S0733-5210(09)80181-1

Cuq, B., Abecassis, J., & Morel, H. (2014). Chapitre 1, la physique et la chimie au service de l'élaboration des pâtes alimentaires. In C. Lavelle (Ed.), *Science culinaire: matière, procédés, dégustation.* (pp. 28–51). Paris: Belin.

Dan, Z., & Labuza, T. P. (2010). Effect of cysteine on lowering protein aggregation and subsequent hardening of whey protein isolate (WPI) protein bars in WPI/buffer model systems. *Journal of Agricultural and Food Chemistry*, *58*(13), 7970–7979. https://doi.org/10.1021/jf100743z

Dartois, A., Singh, J., Kaur, L., & Singh, H. (2010). Influence of guar gum on the in vitro starch digestibility-rheological and microstructural characteristics. *Food Biophysics*, *5*(3), 149–160. https://doi.org/10.1007/s11483-010-9155-2

Delcour, J. a., Bruneel, C., Derde, L. J., Gomand, S. V., Pareyt, B., Putseys, J. a., … Lamberts, L. (2010). Fate of starch in food processing: From raw materials to final food products. *Annual Review of Food Science and Technology - (New in 2010)*, *1*(1), 87–111. https://doi.org/10.1146/annurev.food.102308.124211

Dille, M. J., Draget, K. I., & Hattrem, M. N. (2015). The effect of filler particles on the texture of food gels. In J. Chen & A. Rosenthal (Eds.), *Modifying Food Texture, Volume 1: Novel Ingredients and Processing Techniques* (Vol. 1, pp. 183–200). Cambridge: Woodhead Publishing. https://doi.org/10.1016/B978-1-78242-333-1.00009-7

Do, D. T., Singh, J., Oey, I., & Singh, H. (2018). Biomimetic plant foods: Structural design and functionality. *Trends in Food Science and Technology*, *82*(April), 46–59. https://doi.org/10.1016/j.tifs.2018.09.010

Dona, A. C., Pages, G., Gilbert, R. G., & Kuchel, P. W. (2010). Digestion of starch : In vivo and in vitro kinetic models used to characterise oligosaccharide or glucose release. *Carbohydrate Polymers*, *80*(3), 599–617. https://doi.org/10.1016/j.carbpol.2010.01.002

Durand, D., Gimel, J. C., & Nicolai, T. (2002). Aggregation, gelation and phase separation of heat denatured globular proteins. *Physica A: Statistical Mechanics and Its Applications*, *304*(1–2), 253–265. https://doi.org/10.1016/S0378-4371(01)00514-3

Efthymiou, C., Williams, M. A. K., & Mcgrath, K. M. (2017). Revealing the structure of high-water content biopolymer networks : Diminishing freezing artefacts in cryo-SEM images. *Food Hydrocolloids*, *73*, 203–212. https://doi.org/10.1016/j.foodhyd.2017.06.040

Elofsson, C., Dejmek, P., Paulsson, M., & Burling, H. (1997). Atomic force microscopy studies on whey proteins. *International Dairy Journal*, *7*(12), 813–819. https://doi.org/10.1016/S0958-6946(98)00008-9

Englyst, H. N., Kingman, S. M., & Cummings, J. H. (1992). Classification and measurement of nutritionally important starch fractions. *European Journal of Clinical Nutrition*, *46*(Suppl 2), S33-50.

Englyst, K., Goux, A., Meynier, A., Quigley, M., Englyst, H., Brack, O., & Vinoy, S. (2018). Inter-laboratory validation of the starch digestibility method for determination of rapidly digestible and slowly digestible starch. *Food Chemistry*, *245*(November 2017), 1183–1189. https://doi.org/10.1016/j.foodchem.2017.11.037

Englyst, K. N., Englyst, H. N., Hudson, G. J., Cole, T. J., & Cummings, J. H. (1999). Rapidly available glucose in foods: An in vitro measurement that reflects the glycemic response. *American Journal of Clinical Nutrition*, *69*(3), 448–454. https://doi.org/10.1093/ajcn/69.3.448

Ercan, P., & El, S. N. (2016). Inhibitory effects of chickpea and Tribulus terrestris on lipase, α-amylase and α-glucosidase. *Food Chemistry*, *205*, 163–169. https://doi.org/10.1016/j.foodchem.2016.03.012

Fan, M., Hu, T., Zhao, S., Xiong, S., Xie, J., & Huang, Q. (2017). Gel characteristics and microstructure of fish myofibrillar protein/cassava starch composites. *Food Chemistry*, *218*, 221–230. https://doi.org/10.1016/j.foodchem.2016.09.068

Fardet, A., Hoebler, C., Bouchet, B., Gallant, D. J., & Barry, J. L. (1998). Involvement of the protein network in the in vitro degradation of starch from spaghetti and lasagne: a microscopic and enzymic study. *Reproduction Nutrition Development*, *27*, 133–145. https://doi.org/10.1006/jcrs.1997.0157

Farooq, A. M., Li, C., Chen, S., Fu, X., Zhang, B., & Huang, Q. (2018). Particle size affects structural and in vitro digestion properties of cooked rice flours. *International Journal of Biological Macromolecules*, *118*, 160–167. https://doi.org/10.1016/j.ijbiomac.2018.06.071

Floury, J., Bianchi, T., Thévenot, J., Dupont, D., Jamme, F., Lutton, E., … Le Feunteun, S. (2018). Exploring the breakdown of dairy protein gels during in vitro gastric digestion using time-lapse synchrotron deep-UV fluorescence microscopy. *Food Chemistry*, *239*, 898–910. https://doi.org/10.1016/j.foodchem.2017.07.023

Freitas, D., & Feunteun, S. Le. (2019). Oro-gastro-intestinal digestion of starch in white bread , wheat-based and gluten-free pasta : Unveiling the contribution of human salivary α-amylase. *Food Chemistry*, *274*(September 2018), 566–573. https://doi.org/10.1016/j.foodchem.2018.09.025

Freitas, D., Le Feunteun, S., Panouillé, M., & Souchon, I. (2018). The important role of salivary α-amylase in the gastric digestion of wheat bread starch. *Food & Function*, *9*(1), 200–208. https://doi.org/10.1039/C7FO01484H

Fu, W., & Nakamura, T. (2017). Explaining the texture properties of whey protein isolate/starch co-gels from fracture structures. *Bioscience, Biotechnology and Biochemistry*, *81*(4), 839–847. https://doi.org/10.1080/09168451.2017.1282812

Gallant, D. J., Bouchet, B., & Baldwin, P. M. (1997). Microscopy of starch : evidence of a new level of granule organization, *8617*(97), 177–191.

Gao, J., Lin, S., Jin, X., Wang, Y., Yin, J., & Dong, Z. (2019). In vitro digestion of bread: How is it influenced by the bolus characteristics? *Journal of Texture Studies, (in press)* https://doi.org/10.1111/jtxs.12391

Geara, C. (1999). *Study of the Gelation of Whey Protein Isolate by FTIR Spectroscopy and Rheological Measurements*. McGill University, Montreal, Canada. https://doi.org/10.16953/deusbed.74839

Goñi, I., Garcia-Alonso, A., & Saura-Calixto, F. (1997). A starch hydrolysis procedure to estimate glycemic index. *Nutrition Research*, *17*(3), 427–437. https://doi.org/10.1016/S0271-5317(97)00010-9

Granfeldt, Y., & Björck, I. (1991). Glycemic response to starch in pasta: a study of mechanisms of limited enzyme availability. *Journal of Cereal Science*, *14*(1), 47–61. https://doi.org/10.1016/S0733-5210(09)80017-9

Grewal, M. K., Huppertz, T., & Vasiljevic, T. (2018). FTIR fingerprinting of structural changes of milk proteins induced by heat treatment, deamidation and dephosphorylation. *Food Hydrocolloids*, *80*, 160–167. https://doi.org/10.1016/j.foodhyd.2018.02.010

Guo, Q., Bellissimo, N., & Rousseau, D. (2017). Role of gel structure in controlling in vitro intestinal lipid digestion in whey protein emulsion gels. *Food Hydrocolloids*, *69*, 264–272. https://doi.org/10.1016/j.foodhyd.2017.01.037

Guo, Q., Ye, A., Bellissimo, N., Singh, H., & Rousseau, D. (2017). Modulating fat digestion through food structure design. *Progress in Lipid Research*, *68*(October), 109–118. https://doi.org/10.1016/j.plipres.2017.10.001

Guo, Q., Ye, A., Lad, M., Dalgleish, D., & Singh, H. (2013). The breakdown properties of heat-set whey protein emulsion gels in the human mouth. *Food Hydrocolloids*, *33*(2), 215–224. https://doi.org/10.1016/j.foodhyd.2013.03.008

Guo, Q., Ye, A., Lad, M., Dalgleish, D., & Singh, H. (2014). Effect of gel structure on the gastric digestion of whey protein emulsion gels. *Soft Matter*, *10*, 1214–1223. https://doi.org/10.1039/c4sm00598h

Guo, Q., Ye, A., Lad, M., Dalgleish, D., & Singh, H. (2016). Impact of colloidal structure of gastric digesta on in-vitro intestinal digestion of whey protein emulsion gels. *Food Hydrocolloids*, *54*, 255–265. https://doi.org/10.1016/j.foodhyd.2015.10.006

Ha, E., & Zemel, M. B. (2003). Functional properties of whey, whey components, and essential amino acids: Mechanisms underlying health benefits for active people (Review). *Journal of Nutritional Biochemistry*, *14*(5), 251–258. https://doi.org/10.1016/S0955-2863(03)00030-5

Hamaker, B. R., Zhang, G., & Venkatachalam, M. (2006). Modified carbohydrates with lower glycemic index. In C. K. J. Henry (Ed.), Novel food ingredients for weight control (pp. 198–217). Cambridge: Woodhead Publishing. https://doi.org/10.1533/9781845693114.2.198

Han, H., Hou, J., Yang, N., Zhang, Y., Chen, H., Zhang, Z., … Guo, S. (2019). International Journal of Biological Macromolecules Insight on the changes of cassava and potato starch granules during gelatinization, *126*, 37–43. https://doi.org/10.1016/j.ijbiomac.2018.12.201

Hardy, K. (2015). The importance of dietary carbohydrate in human evolution. *The Quarterly Review of Biology*, *90*(3), 251–268. https://doi.org/10.1086/682587

Havea, P., Singh, H., & Creamer, L. K. (2001). Characterization of heat-induced aggregates of B-lactoglobulin, A-lactalbumin and bovine serum albumin in a whey protein concentrate environment. *Journal of Dairy Research*, *68*(2001), 483–497.

Havea, P., Watkinson, P., & Kuhn-Sherlock, B. (2009). Heat-induced whey protein gels: Protein-protein interactions and functional properties. *Journal of Agricultural and Food Chemistry*, *57*(4), 1506–1512. https://doi.org/10.1021/jf802559z

Heaton, K. W., Marcus, S. N., Emmett, P. M., & Bolton, C. H. (1988). Particle size of wheat, maize, and oat test meals: Effects on plasma glucose and insulin responses and on the rate of starch digestion in vitro. *American Journal of Clinical Nutrition*, *47*(4), 675–682. https://doi.org/10.1093/ajcn/47.4.675

Heneen, W. K., & Brismar, K. (2003). Structure of cooked spaghetti of durum and bread wheats. *Starch/Staerke*, *55*(12), 546–557. https://doi.org/10.1002/star.200300187

Hoebler, C., Karinthi, A., Devaux, M.-F., Guillon, F., Gallant, D. J. G., Bouchet, B., … Barry, J.-L. (1998a). Physical and chemical transformations of cereal food during oral digestion in human subjects. *British Journal of Nutrition*, *80*(05), 429. https://doi.org/10.1017/S0007114598001494

Hoebler, C., Karinthi, A., Devaux, M. F., Guillon, F., Gallant, D. J., Bouchet, B., … Barry, J. L. (1998b). Physical and chemical transformations of cereal food during oral digestion in human subjects. *Br J Nutr*, *80*(5), 429–436. https://doi.org/S0007114598001494 [pii]

Hoffmann, M. A. M., & Van Mil, P. J. J. M. (1997). Heat-induced aggregation of β-lactoglobulin: Role of the free thiol group and disulfide bonds. *Journal of Agricultural and Food Chemistry*, *45*(8), 2942–2948. https://doi.org/10.1021/jf960789q

Holm, J., Lundquist, I., Björck, I., Eliasson, A.-C., & Asp, N.-G. (1988). Degree of starch gelatinization, digestion rate of starch in vitro, and metabolic response in rats. *The American Journal of Clinical Nutrition*, *47*, 1010–1016. https://doi.org/10.1093/ajcn/47.6.1010

Hongsprabhas, P. (1997). *Mechanisms of calcium-induced cold gelation of whey protein isolate*. *The University of Guelph, Ottawa, Canada*.

Hongsprabhas, P., & Barbut, S. (1997a). Ca2+-induced cold gelation of whey protein isolate: Effect of two-stage gelation. *Food Research International*, *30*(7), 523–527. https://doi.org/10.1016/S0963-9969(98)00010-6

Hongsprabhas, P., & Barbut, S. (1997b). Effect of gelation temperature on Ca2+-induced gelation of whey protein isolate. *LWT - Food Science and Technology*, *30*, 45–49. https://doi.org/10.1006/fstl.1996.0132

Hongsprabhas, P., Barbut, S., & Marangoni, A. G. (1999). The structure of cold-set whey protein isolate gels prepared with Ca++. *Lebensmittel-Wissenschaft Und-Technologie*, *32*, 196–202. https://doi.org/10.1006/fstl.1998.0522

Hoover, R. (2001). Composition, molecular structure, and physicochemical properties of tuber and root starches: a review. *Carbohydrate Polymers*, *45*(3), 253–267. https://doi.org/10.1016/S0144-8617(00)00260-5

Huggins, C., Tapley, D. F., & Jensen, E. V. (1951). Sulphydryl-disulphide relationships in the induction of gels in proteins by urea. *Nature*, *167*, 592–593. https://doi.org/10.1038/351111a0

Hur, S. J., Lim, B. O., Decker, E. A., & Mcclements, D. J. (2011). In vitro human digestion models for food applications. *Food Chemistry*, *125*, 1–12. https://doi.org/10.1016/j.foodchem.2010.08.036

Ikeda, S., & Morris, V. J. (2002). Fine-stranded and particulate aggregates of heat-denatured whey proteins visualized by atomic force microscopy. *Biomacromolecules*, *3*(2), 382–389. https://doi.org/10.1021/bm0156429

International Diabetes Federation. (2017). *IDF Diabetes Atlas* (Eighth). Brussels: International Diabetes Federation.

Jane, J. (1993). Mechanism of starch gelatinization in neutral salt solutions. *Starch - Stärke*, *45*(5), 161–166. https://doi.org/https://doi.org/10.1002/star.19930450502

Jane, J., Kasemsuwan, T., Leas, S., Ames, I., A., Zobel, H., Il, D., & Robyt, J., F. (1994). Anthology of starch granule morphology by scanning electron microscopy. *Starch - Stärke 46*(4), 121–129. https://doi.org/10.1002/star.19940460402

Janghorbani, M., Salamat, M. R., Amini, M., & Aminorroaya, A. (2017). Risk of diabetes according to the metabolic health status and degree of obesity. *Diabetes and Metabolic Syndrome: Clinical Research and Reviews*, *11*, S439–S444. https://doi.org/10.1016/j.dsx.2017.03.032

Jekle, M., Mühlberger, K., & Becker, T. (2016). Starch–gluten interactions during gelatinization and its functionality in dough like model systems. *Food Hydrocolloids*, *54*, 196–201. https://doi.org/10.1016/j.foodhyd.2015.10.005

Jenkins, D. J. A., Ghafari, H., Wolever, T. M. S., Taylor, R. H., Jenkins, A. L., Barker, H. M., … Bowling, A. C. (1982). Relationship between rate of digestion of foods and post-prandial glycaemia. *Diabetologia*, *22*, 450–455.

Joshi, B., Beccard, S., & Vilgis, T. A. (2018). Fractals in crystallizing food systems. *Current Opinion in Food Science*, *21*, 39–45. https://doi.org/10.1016/j.cofs.2018.05.009

Jourdren, S., Panouille, M., Saint-Eve, A., Déléris, I., Forest, D., Lejeune, P., & Souchon, I. (2016). Breakdown pathways during oral processing of different breads: impact of crumb and crust structures. *Food & Function*, *7*(3), 1446–1457.

Jung, J. M., Savin, G., Pouzot, M., Schmitt, C., & Mezzenga, R. (2008). Structure of heat-induced β-lactoglobulin aggregates and their complexes with sodium-dodecyl sulfate. *Biomacromolecules*, *9*(9), 2477–2486. https://doi.org/10.1021/bm800502j

Kehoe, J. J., Wang, L., Morris, E. R., & Brodkorb, A. (2011). Formation of non-native β-lactoglobulin during heat-induced denaturation. *Food Biophysics*, *6*(4), 487–496. https://doi.org/10.1007/s11483-011-9230-3

Kim, E. H. J., Petrie, J. R., Motoi, L., Morgenstern, M. P., Sutton, K. H., Mishra, S., & Simmons, L. D. (2008). Effect of structural and physicochemical characteristics of the protein matrix in pasta on in vitro starch digestibility. *Food Biophysics*, *3*(2), 229–234. https://doi.org/10.1007/s11483-008-9066-7

Klucinec, J. D., & Thompson, D. B. (1999). Amylose and amylopectin interact in retrogradation of dispersed high-amylose starches. *Cereal Chemistry, 76*(2), 282-291. https://doi.org/10.1094/CCHEM.1999.76.2.282

Kong, W., Zhang, T., Feng, D., Xue, Y., Wang, Y., Li, Z., … Xue, C. (2016). Effects of modified starches on the gel properties of Alaska Pollock surimi subjected to different temperature treatments. *Food Hydrocolloids*, *56*, 20–28. https://doi.org/10.1016/j.foodhyd.2015.11.023

Kovatchev, B., & Cobelli, C. (2016). Glucose variability: Timing, risk analysis, and relationship to hypoglycemia in diabetes. *Diabetes Care*, *39*(4), 502–510. https://doi.org/10.2337/dc15-2035

Kuhn, K. R., Cavallieri, Â. L. F., & da Cunha, R. L. (2010). Cold-set whey protein gels induced by calcium or sodium salt addition. *International Journal of Food Science and Technology*, *45*(2), 348–357. https://doi.org/10.1111/j.1365-2621.2009.02145.x

Langton, M., & Hermansson, A. (1996). Image analysis of particulate whey protein gels. *Food Hydrocolloids*, *10*(2), 179–191. https://doi.org/10.1016/S0268-005X(96)80033-6

Lavoisier, A., & Aguilera, J. M. (2019). Starch gelatinization inside a whey protein gel formed by cold gelation. *Journal of Food Engineering*, *256*(March), 18–27. https://doi.org/10.1016/j.jfoodeng.2019.03.013

Lefèvre, T., & Subirade, M. (1999). Structural and interaction properties of β-lactoglobulin as studied by FTIR spectroscopy. *International Journal of Food Science and Technology*, *34*(5–6), 419–428. https://doi.org/10.1046/j.1365-2621.1999.00311.x

Lehmann, U., & Robin, F. (2007). Slowly digestible starch – its structure and health implications: a review. *Trends in Food Science & Technology*, *18*(7), 346–355. https://doi.org/10.1016/j.tifs.2007.02.009

Li, J.-Y., & Yeh, A.-I. (2001). Relationships between thermal, rheological characteristics and swelling power for various starches. *Journal of Food Engineering*, *50*(3), 141–148. https://doi.org/10.1016/S0260-8774(00)00236-3

Li, J.-Y., Yeh, A.-I., & Fan, K.-L. (2007). Gelation characteristics and morphology of corn starch/soy protein concentrate composites during heating. *Journal of Food Engineering*, *78*(4), 1240–1247. https://doi.org/10.1016/j.jfoodeng.2005.12.043

Li, Q., Xie, Q., Yu, S., & Gao, Q. (2013). New approach to study starch gelatinization applying a combination of hot-stage light microscopy and differential scanning calorimetry. *Journal of Agricultural and Food Chemistry*, *61*, 1212–1218. https://doi.org/10.1021/jf304201r

Liu, Q., Charlet, G., Yelle, S., & Arul, J. (2002). Phase transition in potato starch–water system I. Starch gelatinization at high moisture level. *Food Research International*, *35*(4), 397–407. https://doi.org/10.1016/S0963-9969(01)00134-X

Liu, T., Hamid, N., Kantono, K., Pereira, L., Farouk, M. M., & Knowles, S. O. (2016). Effects of meat addition on pasta structure, nutrition and in vitro digestibility. *Food Chemistry*, *213*, 108–114. https://doi.org/10.1016/j.foodchem.2016.06.058

Livney, Y. D. (2010). Milk proteins as vehicles for bioactives. *Current Opinion in Colloid & Interface Science*, *15*, 73–83. https://doi.org/10.1016/j.cocis.2009.11.002

López-Barón, N., Gu, Y., Vasanthan, T., & Hoover, R. (2017). Plant proteins mitigate in vitro wheat starch digestibility. *Food Hydrocolloids, 69,* 19-27. https://doi.org/10.1016/j.foodhyd.2017.01.015

Lu, Z. H., Donner, E., Yada, R. Y., & Liu, Q. (2016). Physicochemical properties and in vitro starch digestibility of potato starch/protein blends. *Carbohydrate Polymers*, *154*, 214–222. https://doi.org/10.1016/j.carbpol.2016.08.055

Lucas-González, R., Viuda-Martos, M., Pérez-Alvarez, J. A., & Fernández-López, J. (2018). In vitro digestion models suitable for foods: Opportunities for new fields of application and challenges. *Food Research International*, *107*, 423–436. https://doi.org/10.1016/j.foodres.2018.02.055

Ludwig, D. S. (2002). The glycemic index: Physiological mechanisms relating to obesity, diabetes, and cardiovascular disease. *JAMA*, *287*(18), 2414–2423. https://doi.org/10.1001/jama.287.18.2414

Luo, Q., Boom, R. M., & Janssen, A. E. M. (2015). Digestion of protein and protein gels in simulated gastric environment. *LWT - Food Science and Technology*, *63*(1), 161–168. https://doi.org/10.1016/j.lwt.2015.03.087

Macierzanka, A., Böttger, F., Lansonneur, L., Groizard, R., Jean, A. S., Rigby, N. M., … MacKie, A. R. (2012). The effect of gel structure on the kinetics of simulated gastrointestinal digestion of bovine β-lactoglobulin. *Food Chemistry*, *134*(4), 2156–2163. https://doi.org/10.1016/j.foodchem.2012.04.018

Mackie, A. (2017). Food : more than the sum of its parts. *Current Opinion in Food Science*, *16*, 120–124. https://doi.org/10.1016/j.cofs.2017.07.004

Mahasukhonthachat, K., Sopade, P. A., & Gidley, M. J. (2010). Kinetics of starch digestion in sorghum as affected by particle size. *Journal of Food Engineering*, *96*(1), 18–28. https://doi.org/10.1016/j.jfoodeng.2009.06.051

Mahmood, K., Kamilah, H., Shang, P. L., Sulaiman, S., Ariffin, F., & Alias, A. K. (2017). A review: Interaction of starch/non-starch hydrocolloid blending and the recent food applications. *Food Bioscience*, *19*(March), 110–120. https://doi.org/10.1016/j.fbio.2017.05.006

Mahmoudi, N., Mehalebi, S., Nicolai, T., Durand, D., & Riaublanc, A. (2007). Light-scattering study of the structure of aggregates and gels formed by heat-denatured whey protein isolate and β-lactoglobulin at neutral pH. *Journal of Agricultural and Food Chemistry*, *55*(8), 3104–3111. https://doi.org/10.1021/jf063029g

Maltais, A., Remondetto, G. E., & Subirade, M. (2008). Mechanisms involved in the formation and structure of soya protein cold-set gels: A molecular and supramolecular investigation. *Food Hydrocolloids*, *22*(4), 550–559. https://doi.org/10.1016/j.foodhyd.2007.01.026

Mandalari, G., Merali, Z., Ryden, P., Chessa, S., Bisignano, C., Barreca, D., … Waldron, K. W. (2018). Durum wheat particle size affects starch and protein digestion in vitro. *European Journal of Nutrition*, *57*(1), 319–325. https://doi.org/10.1007/s00394-016-1321-y

Marangoni, A. G., Barbut, S., McGauley, S. E., Marcone, M., & Narine, S. S. (2000). On the structure of particulate gels - The case of salt-induced cold gelation of heat-denatured whey protein isolate. *Food Hydrocolloids*, *14*(1), 61–74. https://doi.org/10.1016/S0268-005X(99)00046-6

Mathieu, V., Monnet, A.-F., Jourdren, S., Panouille, M., Chappard, C., & Souchon, I. (2016). Kinetics of bread crumb hydration as related to porous microstructure. *Food & Function*, *7*(8), 3577–3589. https://doi.org/10.1039/C6FO00522E

Matignon, A., Moulin, G., Barey, P., Desprairies, M., Mauduit, S., Sieffermann, J. M., & Michon, C. (2014). Starch/carrageenan/milk proteins interactions studied using multiple staining and Confocal Laser Scanning Microscopy. *Carbohydrate Polymers*, *99*, 345–355. https://doi.org/10.1016/j.carbpol.2013.09.002

Matignon, A., & Tecante, A. (2017). Starch retrogradation : From starch components to cereal products. *Food Hydrocolloids*, *68*, 43–52. https://doi.org/10.1016/j.foodhyd.2016.10.032

Mignone, L. E., Wu, T., Horowitz, M., & Rayner, C. K. (2015). Whey protein: The "whey" forward for treatment of type 2 diabetes? *World Journal of Diabetes*, *6*(14), 1274–1284. https://doi.org/10.4239/wjd.v6.i14.1274

Minekus, M., Alminger, M., Alvito, P., Ballance, S., Bohn, T., Bourlieu, C., … Brodkorb, A. (2014). A standardised static in vitro digestion method suitable for food – an international consensus. *Food & Function*, *5*(5), 1113–1124. https://doi.org/10.1039/c3fo60702j

Ministerio de Salud de Chile. (2017). *Encuesta Nacional de Salud 2016-2017 Primeros resultados*. Santiago de Chile, Chile. Retrieved from http://web.minsal.cl/wp-content/uploads/2017/11/ENS-2016-17_PRIMEROS-RESULTADOS.pdf

Molina, M. T., Leiva, A., & Bouchon, P. (2016). Examining the effect of freezing on starch gelatinization during heating at high rates using online in situ hot-stage video-microscopy and differential scanning calorimetry. *Food and Bioproducts Processing*, *100*(Part B), 488–495. https://doi.org/10.1016/j.fbp.2016.06.003

Monro, J. A., & Mishra, S. (2010). Glycemic impact as a property of foods is accurately measured by an available carbohydrate method that mimics the glycemic response. *The Journal of Nutrition*, *140*, 1328–1334. https://doi.org/10.3945/jn.110.121210.basis

Mulet-Cabero, A.-I., Rigby, N. M., Brodkorb, A., & Mackie, A. R. (2017). Dairy food structures influence the rates of nutrient digestion through different in vitro gastric behaviour. *Food Hydrocolloids*, *67*, 63–73. https://doi.org/10.1016/j.foodhyd.2016.12.039

Muñoz, L. A., Pedreschi, F., Leiva, A., & Aguilera, J. M. (2015). Loss of birefringence and swelling behavior in native starch granules: Microstructural and thermal properties. *Journal of Food Engineering*, *152*, 65–71. https://doi.org/10.1016/j.jfoodeng.2014.11.017

Nečas, D., & Klapetek, P. (2012). Gwyddion: An open-source software for SPM data analysis. *Central European Journal of Physics*, *10*(1), 181–188. https://doi.org/10.2478/s11534-011-0096-2

Nguyen, G. T., Gidley, M. J., & Sopade, P. A. (2015). Dependence of in-vitro starch and protein digestions on particle size of field peas (Pisum sativum L.). *LWT - Food Science and Technology*, *63*(1), 541–549. https://doi.org/10.1016/j.lwt.2015.03.037

Nguyen, N. H. A., Wong, M., Guyomarc'h, F., Havea, P., & Anema, S. G. (2014). Effects of non-covalent interactions between the milk proteins on the rheological properties of acid gels. *International Dairy Journal*, *37*(2), 57–63. https://doi.org/10.1016/j.idairyj.2014.03.001

Nicolai, T., & Durand, D. (2013). Controlled food protein aggregation for new functionality. *Current Opinion in Colloid and Interface Science*, *18*(4), 249–256. https://doi.org/10.1016/j.cocis.2013.03.001

Nielsen, L. R., Lund, M. N., Davies, M. J., Nielsen, J. H., & Nielsen, S. B. (2018). Effect of free cysteine on the denaturation and aggregation of holo α-lactalbumin. *International Dairy Journal*, *79*, 52–61. https://doi.org/10.1016/j.idairyj.2017.11.014

Nordlund, E., Katina, K., Mykkänen, H., & Poutanen, K. (2016). Distinct characteristics of rye and wheat breads: Impact on their in vitro gastric disintegration and in vivo glucose and insulin responses. *Foods*, *5*(4), 24. https://doi.org/10.3390/foods5020024

O'Loughlin, I. B., Kelly, P. M., Murray, B. A., Fitzgerald, R. J., & Brodkorb, A. (2015). Concentrated whey protein ingredients: A Fourier transformed infrared spectroscopy investigation of thermally induced denaturation. *International Journal of Dairy Technology*, *68*(3), 349–356. https://doi.org/10.1111/1471-0307.12239

Oñate Narciso, J., & Brennan, C. (2018). Whey and pea protein fortification of rice starches: Effects on protein and starch digestibility and starch pasting properties. *Starch - Stärke*, *70*(1700315), 1–6. https://doi.org/10.1002/star.201700315

Ong, L., Dagastine, R. R., Kentish, S. E., & Gras, S. L. (2011). Microstructure of milk gel and cheese curd observed using cryo scanning electron microscopy and confocal microscopy. *LWT - Food Science and Technology*, *44*(5), 1291–1302. https://doi.org/10.1016/j.lwt.2010.12.026

Opazo-Navarrete, M., Altenburg, M. D., Boom, R. M., & Janssen, A. E. M. (2018). The effect of gel microstructure on simulated gastric digestion of protein gels. *Food Biophysics*, *13*(2), 124–138. https://doi.org/10.1007/s11483-018-9518-7

Parada, J., & Aguilera, J. M. (2012). Effect of native crystalline structure of isolated potato starch on gelatinization behavior and consequently on glycemic response. *Food Research International*, *45*(1), 238–243. https://doi.org/10.1016/j.foodres.2011.10.042

Parker, R., & Ring, S. G. (2001). Aspects of the physical chemistry of starch. *Journal of Cereal Science*, *34*(1), 1–17. https://doi.org/10.1006/jcrs.2000.0402

Petitot, M., Abecassis, J., & Micard, V. (2009). Structuring of pasta components during processing: impact on starch and protein digestibility and allergenicity. *Trends in Food Science & Technology*, *20*(11–12), 521–532. https://doi.org/10.1016/j.tifs.2009.06.005

Pogaku, R., Eng Seng, C., Boonbeng, L., & Kallu, U. R. (2007). Whey protein isolate-starch system- A critical review. *International Journal of Food Engineering*, *3*(6), 2007. https://doi.org/10.2202/1556-3758.1164

Primo-Martín, C., van Nieuwenhuijzen, N. H., Hamer, R. J., & van Vliet, T. (2007). Crystallinity changes in wheat starch during the bread-making process: Starch

crystallinity in the bread crust. *Journal of Cereal Science*, *45*(2), 219–226. https://doi.org/10.1016/j.jcs.2006.08.009

Ranawana, V., Henry, C. J. K., & Pratt, M. (2010). Degree of habitual mastication seems to contribute to interindividual variations in the glycemic response to rice but not to spaghetti. *Nutrition Research*, *30*(6), 382–391. https://doi.org/10.1016/j.nutres.2010.06.002

Ranawana, V., Monro, J. A., Mishra, S., & Henry, C. J. K. (2010). Degree of particle size breakdown during mastication may be a possible cause of interindividual glycemic variability. *Nutrition Research*, *30*(4), 246–254. https://doi.org/10.1016/j.nutres.2010.02.004

Rao, M. A. (2007). *Rheology of Fluids and Semisolid Foods Principles and Applications*. (Gustava V. Barbosa-Cánovas, Ed.) (Second Edi). Geneva, NY: Springer.

Ratnayake, W. S., & Jackson, D. S. (2009). Starch gelatinization. *Advances in Food and Nutrition Research*, *55*, 221–268. https://doi.org/10.1016/S1043-4526(08)00405-1

Ratnayake, W. S., Otani, C., & Jackson, D. S. (2009). DSC enthalpic transitions during starch gelatinisation in excess water, dilute sodium chloride and dilute sucrose solutions. *Journal of the Science of Food and Agriculture*, *89*(12), 2156–2164. https://doi.org/10.1002/jsfa.3709

Ravindra, P., Genovese, D. B., Foegeding, E. A., & Rao, M. A. (2004). Rheology of heated mixed whey protein isolate/cross-linked waxy maize starch dispersions. *Food Hydrocolloids*, *18*(5), 775–781. https://doi.org/10.1016/j.foodhyd.2003.12.004

Remondetto, G. E., & Subirade, M. (2003). Molecular mechanisms of Fe2+-induced β-lactoglobulin cold gelation. *Biopolymers*, *69*(4), 461–469. https://doi.org/10.1002/bip.10423

Roff, C. F., & Foegeding, E. A. (1996). Dicationic-induced gelation of pre-denatured whey protein isolate. *Food Hydrocolloids*, *10*(2), 193–198. https://doi.org/10.1016/S0268-005X(96)80034-8

Schiedt, B., Baumann, A., Conde-Petit, B., & Vilgis, T. A. (2013). Short- and long-range interactions governing the viscoelastic properties during wheat dough and model dough development. *Journal of Texture Studies*, *44*(4), 317–332. https://doi.org/10.1111/jtxs.12027

Schindelin, J., Arganda-Carreras, I., & Frise, E. (2012). Fiji: an open-source platform for biological-image analysis. *Nature Methods*, *9*(7), 676–682. https://doi.org/https://doi.org/10.1038/nmeth.2019

Schirmer, M., Jekle, M., & Becker, T. (2015). Starch gelatinization and its complexity for analysis. *Starch - Stärke*, *67*(1–2), 30–41. https://doi.org/10.1002/star.201400071

Schneider, C. A., Rasband, W. S., & Eliceiri, K. W. (2012). NIH Image to ImageJ: 25 years of image analysis. *Nature Methods*, *9*(7), 671–675. https://doi.org/10.1038/nmeth.2089

Seal, C. J., Daly, M. E., Thomas, L. C., Bal, W., Birkett, A. M., Jeffcoat, R., & Mathers, J. C. (2003). Postprandial carbohydrate metabolism in healthy subjects and those with type 2 diabetes fed starches with slow and rapid hydrolysis rates determined in vitro. *British Journal of Nutrition*, *90*, 853–864. https://doi.org/10.1079/BJN2003972

Sęczyk, Ł., Świeca, M., & Gawlik-Dziki, U. (2015). Nutritional and health-promoting properties of bean paste fortified with onion skin in the light of phenolic–food matrix interactions. *Food Funct.*, *6*(11), 3560–3566. https://doi.org/10.1039/C5FO00805K

Semeijn, C., & Buwalda, P. L. (2018). Potato starch. In M. Sjöö & L. Nilsson (Eds.), *Starch in Food: Structure, Function and Applications, Second Edition* (pp. 353–372). Cambridge: Woodhead Publishing. https://doi.org/10.1016/C2015-0-01896-2

Shih, W. H., Shih, W. Y., Kim, S. Il, Liu, J., & Aksay, I. A. (1990). Scaling behavior of the elastic properties of colloidal gels. *Physical Review A*, *42*(8), 4772–4779. https://doi.org/10.1103/PhysRevA.42.4772

Silva, E., Birkenhake, M., Scholten, E., Sagis, L. M. C., & van der Linden, E. (2013). Controlling rheology and structure of sweet potato starch noodles with high broccoli powder content by hydrocolloids. *Food Hydrocolloids*, *30*(1), 42–52. https://doi.org/10.1016/j.foodhyd.2012.05.002

Singh, H., Ye, A., & Ferrua, M. J. (2015). Aspects of food structures in the digestive tract. *Current Opinion in Food Science*, *3*, 85–93. https://doi.org/10.1016/j.cofs.2015.06.007

Singh, J., Dartois, A., & Kaur, L. (2010). Starch digestibility in food matrix: a review. *Trends in Food Science and Technology*, *21*(4), 168–180. https://doi.org/10.1016/j.tifs.2009.12.001

Singh, J., Kaur, L., & Singh, H. (2013). Chapter four – Food microstructure and starch digestion. In *Advances in Food and Nutrition Research* (Vol. 70, pp. 137–179). https://doi.org/10.1016/B978-0-12-416555-7.00004-7

Singh, N., Singh, J., Kaur, L., Singh Sodhi, N., & Singh Gill, B. (2003). Morphological, thermal and rheological properties of starches from different botanical sources. *Food Chemistry*, *81*(2), 219–231. https://doi.org/10.1016/S0308-8146(02)00416-8

Smithers, G. W. (2015). Whey-ing up the options - Yesterday, today and tomorrow. *International Dairy Journal*, *48*, 2–14. https://doi.org/10.1016/j.idairyj.2015.01.011

Szymónska, J., Targosz-Korecka, M., & Krok, F. (2009). Characterization of starch nanoparticles. *Journal of Physics: Conference Series*, *146*(012027). https://doi.org/10.1088/1742-6596/146/1/012027

Tamura, M., Okazaki, Y., Kumagai, C., & Ogawa, Y. (2017). The importance of an oral digestion step in evaluating simulated in vitro digestibility of starch from cooked rice grain. *Food Research International*, *94*, 6–12. https://doi.org/10.1016/j.foodres.2017.01.019

Tang, H., Mitsunaga, T., & Kawamura, Y. (2006). Molecular arrangement in blocklets and starch granule architecture, *63*, 555–560. https://doi.org/10.1016/j.carbpol.2005.10.016

Tavares, G. M., Croguennec, T., & Carvalho, A. F. (2014). Milk proteins as encapsulation devices and delivery vehicles : Applications and trends, *37*. https://doi.org/10.1016/j.tifs.2014.02.008

Tester, R. F., & Sommerville, M. . (2003). The effects of non-starch polysaccharides on the extent of gelatinisation, swelling and α-amylase hydrolysis of maize and wheat starches. *Food Hydrocolloids*, *17*(1), 41–54. https://doi.org/10.1016/S0268-005X(02)00032-2

Tester, R. F., Karkalas, J., & Qi, X. (2004). Starch—composition, fine structure and architecture. *Journal of Cereal Science*, *39*(2), 151–165. https://doi.org/10.1016/j.jcs.2003.12.001

The UniProt Consortium. (2019). UniProt: a worldwide hub of protein knowledge. *Nucleic Acids Research*, *47*(D1), D506–D515. https://doi.org/10.1093/nar/gky1049

Tinus, T., Damour, M., Van Riel, V., & Sopade, P. A. (2012). Particle size-starch-protein digestibility relationships in cowpea (Vigna unguiculata). *Journal of Food Engineering*, *113*(2), 254–264. https://doi.org/10.1016/j.jfoodeng.2012.05.041

Tokita, M. (2016). Transport phenomena in gel. *Gels*, *2*(17), 1–15. https://doi.org/10.3390/gels2020017

Tsubaki, S., & Azuma, J.-I. (2011). Application of microwave technology for utilization of recalcitrant biomass. In S. Grundas (Ed.), *Advances in Induction and Microwave Heating of Mineral and Organic Materials* (pp. 697–722). InTech.

Turgeon, S. L., & Beaulieu, M. (2001). Improvement and modification of whey protein gel texture using polysaccharides. *Food Hydrocolloids*, *15*(4–6), 583–591. https://doi.org/10.1016/S0268-005X(01)00064-9

van den Berg, L., van Vliet, T., van der Linden, E., van Boekel, M., & van de Velde, F. (2007). Breakdown properties and sensory perception of whey proteins/polysaccharide

mixed gels as a function of microstructure. *Food Hydrocolloids*, *21*(5–6), 961–976. https://doi.org/10.1016/j.foodhyd.2006.08.017

Vilgis, T. A., Heinrich, G., & Klüppel, M. (2009). *Reinforcement of polymer nano-composites: Theory, experiments and applications*. Cambridge University Press.

Vreeker, R., Hoekstra, L. L., den Boer, D. C., & Agterof, W. G. M. (1992). Fractal aggregation of whey proteins. *Topics in Catalysis*, *6*(5), 423–435. https://doi.org/10.1016/S0268-005X(09)80028-3

Walstra, P., van Vliet, T., & Bremer, L. G. B. (1991). On the fractal nature of particle gels. In E. Dickinson (Ed.), *Food Polymers, Gels and Colloids* (pp. 369–382). Cambridge: Woodhead Publishing. https://doi.org/10.1533/9781845698331.369

Wang, C. H., & Damodaran, S. (1990). Thermal gelation of globular proteins: Weight-average molecular weight dependence of gel strength. *Journal of Agricultural and Food Chemistry*, *38*(5), 1157–1164. https://doi.org/10.1021/jf00095a001

Wang, S., & Copeland, L. (2013). Molecular disassembly of starch granules during gelatinization and its effect on starch digestibility: a review. *Food & Function*, *4*(11), 1564–1580. https://doi.org/10.1039/c3fo60258c

Wijayanti, H. B., Bansal, N., Sharma, R., & Deeth, H. C. (2014). Effect of sulphydryl reagents on the heat stability of whey protein isolate. *Food Chemistry*, *163*, 129–135. https://doi.org/10.1016/j.foodchem.2014.04.094

Wijayanti, H. B., Oh, H. E., Sharma, R., & Deeth, H. C. (2013). Reduction of aggregation of β-lactoglobulin during heating by dihydrolipoic acid. *Journal of Dairy Research*, *80*(4), 383–389. https://doi.org/10.1017/S0022029913000332

Wimley, W. C., & White, S. H. (2004). Reversible unfolding of β-sheets in membranes: a calorimetric study. *Journal of Molecular Biology*, *342*(3), 703–711. https://doi.org/10.1016/j.jmb.2004.06.093

Woolnough, J. W., Monro, J. A., Brennan, C. S., & Bird, A. R. (2008). Simulating human carbohydrate digestion in vitro: A review of methods and the need for standardisation. *International Journal of Food Science and Technology*, *43*(12), 2245–2256. https://doi.org/10.1111/j.1365-2621.2008.01862.x

World Health Organization. (2006). *Definition and Diagnosis of Diabetes Mellitus and Intermediate Hyperglycemia.* (World Health Organization, Ed.). Geneva, Switzerland: WHO Press.

World Health Organization. (2016). *Global Report on Diabetes*. (World Health Organization, Ed.). Geneva, Switzerland: WHO Press. Retrieved from http://apps.who.int/iris/bitstream/10665/204871/1/9789241565257_eng.pdf

World Health Organization. (2018). *Global Health Estimates 2016: Deaths by Cause, Age, Sex, by Country and by Region*. (World Health Organization, Ed.). Geneva, Switzerland: WHO Press.

Wu, H., Xie, J., & Morbidelli, M. (2005). Kinetics of cold-set diffusion-limited aggregations of denatured whey protein isolate colloids. *Biomacromolecules*, *6*(6), 3189–3197. https://doi.org/10.1021/bm050532d

Xu, X., Huang, X., Visser, R. G. F., & Trindade, L. M. (2017). Engineering potato starch with a higher phosphate content. *PloS ONE, 12*(1), e0169610. https://doi.org/10.1371/journal.pone.0169610

Yang, N., Ashton, J., & Kasapis, S. (2015). The influence of chitosan on the structural properties of whey protein and wheat starch composite systems. *Food Chemistry*, *179*, 60–67. https://doi.org/10.1016/j.foodchem.2015.01.121

Yang, N., Liu, Y., Ashton, J., Gorczyca, E., & Kasapis, S. (2013). Phase behaviour and in vitro hydrolysis of wheat starch in mixture with whey protein. *Food Chemistry*, *137*(1–4), 76–82. https://doi.org/10.1016/j.foodchem.2012.10.004

Yang, N., Luan, J., Ashton, J., Gorczyca, E., & Kasapis, S. (2014). Effect of calcium chloride on the structure and in vitro hydrolysis of heat induced whey protein and wheat starch composite gels. *Food Hydrocolloids*, *42*(P2), 244–250. https://doi.org/10.1016/j.foodhyd.2014.02.022

Ze, X., Duncan, S. H., Louis, P., & Flint, H. J. (2012). Ruminococcus bromii is a keystone species for the degradation of resistant starch in the human colon. *The ISME Journal*, *6*(8), 1535–1543. https://doi.org/10.1038/ismej.2012.4

Zhang, B., Dhital, S., Flanagan, B. M., & Gidley, M. J. (2014). Mechanism for starch granule ghost formation deduced from structural and enzyme digestion properties. *Journal of Agricultural and Food Chemistry, 62*(3), 760–771. https://doi.org/10.1021/jf404697v

Zhang, G., & Hamaker, B. R. (2009). Slowly digestible starch : Concept, mechanism, and proposed extended glycemic index. *Critical Reviews in Food Science and Nutrition*, *49*(10), 852–867. https://doi.org/10.1080/10408390903372466

Zhang, Z., Zhang, R., Chen, L., Tong, Q., & McClements, D. J. (2015). Designing hydrogel particles for controlled or targeted release of lipophilic bioactive agents in the gastrointestinal tract. *European Polymer Journal*, *72*, 698–716. https://doi.org/10.1016/j.eurpolymj.2015.01.013

Zhao, X., Andersson, M., & Andersson, R. (2018). Resistant starch and other dietary fiber components in tubers from a high-amylose potato. *Food Chemistry*, *251*(January), 58–63. https://doi.org/10.1016/j.foodchem.2018.01.028

Zhou, H., Wang, C., Shi, L., Chang, T., Yang, H., & Cui, M. (2014). Effects of salts on physicochemical, microstructural and thermal properties of potato starch. *Food Chemistry*, *156*, 137–143. https://doi.org/10.1016/j.foodchem.2014.02.015

Zhu, F. (2018). Trends in Food Science & Technology Relationships between amylopectin internal molecular structure and physicochemical properties of starch, *78*(May), 234–242. https://doi.org/10.1016/j.tifs.2018.05.024

Zou, W., Sissons, M., Gidley, M. J., Gilbert, R. G., & Warren, F. J. (2015). Combined techniques for characterising pasta structure reveals how the gluten network slows enzymic digestion rate. *Food Chemistry*, *188*, 559–568. https://doi.org/10.1016/j.foodchem.2015.05.032

Zou, W., Sissons, M., Warren, F. J., Gidley, M. J., & Gilbert, R. G. (2016). Compact structure and proteins of pasta retard in vitro digestive evolution of branched starch molecular structure. *Carbohydrate Polymers*, *152*, 441–449. https://doi.org/10.1016/j.carbpol.2016.06.016